Cavallo, John Louis

MICROEMULSIONS AND THEIR RELATION TO SWOLLEN MICELLAR SOLUTIONS

City University of New York PH.D. 1986

PLEASE NOTE:

In all cases this material has been filmed in the best possible way from the available copy. Problems encountered with this document have been identified here with a check mark __✓__.

1. Glossy photographs or pages ✓
2. Colored illustrations, paper or print _____
3. Photographs with dark background ✓
4. Illustrations are poor copy _____
5. Pages with black marks, not original copy _____
6. Print shows through as there is text on both sides of page _____
7. Indistinct, broken or small print on several pages _____
8. Print exceeds margin requirements _____
9. Tightly bound copy with print lost in spine _____
10. Computer printout pages with indistinct print _____
11. Page(s) _____ lacking when material received, and not available from school or author.
12. Page(s) _____ seem to be missing in numbering only as text follows.
13. Two pages numbered _____. Text follows.
14. Curling and wrinkled pages _____
15. Dissertation contains pages with print at a slant, filmed as received _____
16. Other _____

_____

_____

MICROEMULSIONS

AND THEIR RELATION TO

SWOLLEN MICELLAR SOLUTIONS

by

JOHN LOUIS CAVALLO

A dissertation submitted to the Graduate Faculty in
Chemistry in partial fulfillment of the requirements
for the degree of Doctor of Philosophy,
The City University of New York.

1986

This manuscript has been read and accepted for the Graduate Faculty in Chemistry in satisfaction of the dissertation requirement for the degree of Doctor of Philosophy.

04/08/86
date

Chairman of Examining Committee

4/8/86
date

Executive Officer

John Grotzinger

David C. Lorke

Supervisory Committee

The City University of New York

Abstract

MICROEMULSIONS
AND THEIR RELATION TO
SWOLLEN MICELLAR SOLUTIONS

by

John Louis Cavallo

Mentor: Professor Henri L. Rosano

The thermodynamic stability of microemulsion systems and their relation to swollen micellar solutions have been investigated. The results obtained suggest that the apparent path-dependent properties sometimes observed during microemulsion formation may be explained by the small free energy values involved in transforming an emulsion into a microemulsion. These results suggest that the right order of mixing the various components plays a major role in lowering the activation energy barriers these systems must overcome during their formation. Based on these results it is concluded that microemulsions are thermodynamically stable systems.

Emulsions (5 o/w ; 1 w/o) prepared with oil, water and surfactant were titrated to clarity with a cosurfactant. The volume of the continuous phase was varied from 10 to 60 ml. The mole fractions of cosurfactant/surfactant and cosurfactant/continuous phase was determined at various temperatures (15 to 55°C). At 30°C, free energy and enthalpy changes accompanying cosurfactant adsorption during microemulsion formation were found to vary from -19.6 to -6.4 kJ/mole respectively. Entropy of formation changes were found to be positive in 5 cases from 3.5×10^{-2} to 8.3×10^{-2} kJ/K mole and in one case negative -1.8×10^{-2} kJ/K mole. These results indicate that microemulsion formation is a

spontaneous process, however the driving force is small and it may help to explain why the manner of combining the various components may be important in the formation of these systems. O/W emulsions of long chain sulfate/n-hydrocarbon/5% NaCl were titrated to clarity (85% transmittance or better) with long chain dimethylamine oxide. These data confirm that microemulsion formation appears to be dependent on specific interactions among the constituent molecules at the O/W interface.

During the titration of the emulsions with a cosurfactant, just before clearing the system undergoes viscosity changes. The increase and sharp decrease in viscosity are accounted for by the formation and resolution of filament structure into microdroplets. After each addition of cosurfactant, systems prepared with a constant amount of water, oil and surfactant were allowed to equilibrate and phase separation was observed. From these results it is concluded that O/W microemulsions may be described as hydropathic oleomicellar solutions since they correspond to a specific region of a general phase diagram.

The vapor pressure of five O/W microemulsion systems was determined as a function of increasing the volume of hydrocarbon in the dispersed phase using an isoteniscope. The five systems investigated are : 1) n-octane/Na cetyl sulfate (SCS)/5% NaCl + 0.01N NaOH/dodecyldimethylamine oxide (DDAO) and 2) four systems prepared with H_2O/Na dodecyl sulfate (SDS)/n-pentane, n-hexane, n-octane or n-decane/DDAO. At low volume fractions of hydrocarbon, the microemulsion droplets behave like large molecules in solution. The molecular weight and particle size of these aggregates are in agreement with particle size measurements determined by photon correlation spectroscopy. Beyond a certain hydrocarbon volume fraction, the droplets are less stable. The energy of activation corresponding to the breaking of the interfacial sheath was found to be between 35.2 and 20.9 kJ / mole. The results obtained by vapor pressure analysis indicates that two types of microemulsion systems are possible depending on the amount of hydrocarbon in the dispersed phase.

Vapor pressure measurements on microemulsions containing hydrosoluble cationic or anionic polymers in the dispersed phase indicate that these molecules

can in some cases increase microdroplet stability over larger volumes of hydrocarbon. When anionic polymers are added to the dispersed phase, repulsive surfactant/polymer interactions increase microdroplet stability and prevent droplet merging. With the addition of cationic polymers, droplet stability was reduced due to surfactant/polymer association.

Acknowledgements

Impressions people give to others are very often long lasting and are remembered when both time and distance separate them. Anyone who has ever had the opportunity to be acquinted with Professor Henri L. Rosano knows very well that he is by far impressive, not only as an excellent surface chemist but also as a person. I have been one of the fortunate ones to both know Professor Rosano as both a teacher and a person. The many hours we spent discussing everything from my Ph.D. topic to world politics, will certainly be remembered. To myself espically and the other graduate students past or present in his group, Professor Rosano has always set an example for success in life and human character. Not only have I been fortunate enough to have Professor Rosano as my Mentor, I have also had the opportunity to consider him my friend as well. To Professor Rosano I owe a special thanks for making this thesis possible and the time spent in his laboratory an enjoyable experience. Professor Rosano has always demonstrated support, encourgement and confidence in my work and has always had my best interest at heart even though I was always "too slow" for him. Whenever I felt like I was "in the soup", he was always their with an encourging word. After talking with him,the problems never really seemed as bad. Professor Rosano is well deserving of the title "Chief" which he is called by his students in the laboratory. He is someone I will certainly remember through my life.

I would also like to extend personal thanks to Professor John Arents for his comments on my work and assistance he has offered on my papers and to Professor David Locke who always made himself available and found the time to assist me whenever necessary.

I would also like to thank my friends Domingo I. Jon, David L. Chang and Steven Y. Chan for making this time both enjoyable and unforgetable.

THIS WORK IS DEDICATED

TO MY LATE PARENTS

LUCY M. GRANDI

AND

JOHN A. CAVALLO

Table of Contents

Copyright ii
Approval iii
Abstract iv
Acknowledgements vii
Table of Contents ix
List of Figures xii
List of Tables xiv

Chapter 1 Introductory Remarks 1

1.1 Introduction 1
1.2 The Schulman Microemulsion 3
1.2.1 Negative Interfacial Tension 4
1.2.2 Mixed Film Theory 7
1.3 The Flexible Interface 11
1.4 Percolation In Microemulsion Systems 16
1.5 The Thesis Research Statements 18
1.6 References 20

Chapter 2 Microemulsion Systems : Free Energy, Enthalpy and Entropy of Formation 23

2.1 Introduction 23
2.2 Experimental 24
2.2.1 Chemicals 24
2.2.2 Method of Preparation of Transparent Systems 24
2.2.3 Microemulsion Systems Investigated 26
2.2.4 Viscosity and Percent Transmittance 26

2.2.5 Phase Volume and Particle Size Determination 26

2.2.6 Electron Microscopy Sample Preparation 28

2.3 Results 28

2.3.1 Long Chain Dimethylamine Oxide Microemulsions 28

2.3.2 Thermodynamic Properties 30

2.3.3 Viscosity and Percent Transmittance During Microemulsion Formation 35

2.3.4 Phase Volume Changes 35

2.4 Discussion 38

2.4.1 Microemulsion Formation 38

2.4.2 The Role of the Cosurfactant 41

2.4.3 Microemulsions and the Shinoda Phase Diagram 47

2.5 References 57

Chapter 3 Vapor Pressure Measurements of O/W Microemulsion Systems 60

3.1 Introduction 60

3.2 Experimental 64

3.2.1 Chemicals 64

3.2.2 The Systems Investigated 64

3.2.3 The Isoteniscope Method 64

3.2.4 Photon Correlation Spectroscopy 66

3.2.5 Surface Tension Measurements 70

3.2.6 Interfacial Tension Measurements 70

3.2.7 Pressure - Area Measurements 73

3.3 Theory 75

3.3.1 Bending Energy and Microemulsion Formation 75

3.3.2 Phase Separation and Droplet Interaction 78

3.4 Results 81

3.4.1 Ln P vs 1/T 83

3.4.2 Vapor Pressure vs Volume of Oil at Various Temperatures .. 83

3.4.3 Vapor Pressure vs ml of n-Pentane, n-Hexane, n-Decane and two n-Octane Microemulsion Systems at 30°C 87

3.4.4 Molecular Weight Determinations 89

3.4.5 Radii Determinations 91

3.4.6 Activation Energy 93

3.5 Discussion 95

3.5.1 Percolation in Microemulsion Systems 95

3.5.2 Activation Energy Based on Vapor Pressure Measurements .. 98

3.5.3 Heat of Vaporization 99

3.5.4 Interfacial Flexibility 99

3.6 References 104

Chapter 4 The Effect of Hydrosoluble Polymers on the Vapor Pressure of O/W Microemulsion Systems 106

4.1 Introduction 106

4.2 Experimental 107

4.2.1 Chemicals 107

4.2.2 Preparation of Polymer Microemulsion Systems 107

4.3 Results 108

4.3.1 Microemulsion Systems Investigated 108

4.4 Discussion 110

4.4.1 Microemulsion Interaction with Polymer JR 111

4.4.2 Microemulsion Interaction with CMC 111

4.4.3 The Effect of Polymers and Activation Energy 112

4.5 References 116

Chapter 5 Conclusion 117

Appendix A 120

Appendix B 125

List of Figures

CHAPTER 1

FIGURE 1.1 Illustration of the mechanism of film curvature for a microemulsion. 9

CHAPTER 2

FIGURE 2.1 Microemulsion systems containing 2 ml n-hexadecane / 0.5 ml nonylphenol-1.5-EO + 0.5 ml nonylphenol-4- EO / various volumes of water / titrated to clarity with octylphenol-9-EO at 45°C and 55°C. 31

FIGURE 2.2 Change in viscosity and percent transmittance for 2 ml n-decane / 0.5 ml nonylphenol-1.5-EO + 0.5 ml nonylphenol-4-EO / 35 ml water and titrated with nonylphenol-10-EO at 50°C. 36

FIGURE 2.3 Phase volume change and particle size determination for 2 ml n-octane / 0.5 ml nonylphenol-1.5-EO + 0.5 ml nonylphenol-4-EO / 30 ml water and titrated with nonylphenol-10-EO at 22°C. 37

FIGURE 2.4 Photomicrographs of the lower phase region accompaning microemulsion formation. 44

FIGURE 2.5 Particle size distribution in the lower phase. 48

FIGURE 2.6 Schematic illustration of the change in solution behavior of surfactant with hydrophilic-lipophilic balance (HLB) in a water, oil, surfactant system. 53

CHAPTER 3

FIGURE 3.1 Experimental setup used to measure vapor pressure of microemulsion systems. 66

FIGURE 3.2 Block diagram of photon correlation spectroscopic apparatus. 68

FIGURE 3.3 Plot of surface tension vs Log C. 71

FIGURE 3.4 Plot of interfacial tension vs Log C. 72

FIGURE 3.5 Pressure vs area curve. 74

FIGURE 3.6 Change in total free energy vs. radius. 82

FIGURE 3.7 Dependence of the vapor pressure on the temperature. 84

FIGURE 3.8 Variation in the vapor pressure for a microemulsion prepared with 20 ml 5% NaCl + 0.01N NaOH / 1 gm SCS / DDAO and various amounts of n-octane between 15-40°C. 85

FIGURE 3.9 Vapor pressure of four o/w microemulsions prepared with H_2O / various volumes of n-pentane, n-hexane, n-octane and n-decane / 1 gm SDS / DDAO at 30°C. 86

FIGURE 3.10 Titration curve of the volume of DDAO vs volume of saline. 92

FIGURE 3.11 Heat of vaporization vs volume of n-octane. 100

CHAPTER 4

FIGURE 4.1 Change in vapor pressure with addition of polymers. 109

FIGURE 4.2 Microdroplet behavior in A) water and B) water + Polymer JR solution. 113

FIGURE 4.3 Microdroplet behavior in a water + CMC solution. 114

List of Tables

CHAPTER 2

TABLE 2.1 Six microemulsion systems investigated. 27

TABLE 2.2 1 ml hydrocarbon / 20 ml of 5% NaCl + 0.01 N NaOH / 1 gm long chain sodium sulfate / titrated with 30% active long chain dimethylamine oxide (LCDAO). Notation : ml of cosurfactant as 100% active are reported. Percent transmittance @ 520 nm. n = viscosity. * = thick gel. Temperature = 30°C. 29

TABLE 2.3 Free energy, enthalpy and entropy changes corresponding to the adsorption of cosurfactant at the interface for 5 o/w and 1 w/o microemulsion systems. 33

TABLE 2.4 Data on Stearic acid / n-hexadecane/0.375 M KOH microemulsion system titrated with 1-pentanol. 34

CHAPTER 3

TABLE 3.1 The five o/w microemulsions investigated. Sodium dodecyl sulfate (SDS), sodium cetyl sulfate (SCS). 65

TABLE 3.2 Vapor pressure for an o/w microemulsion prepared with 20 ml 5% NaCl + 0.01N NaOH / 1 gm SDS / DDAO and various volumes of n-octane at 30°C. 88

TABLE 3.3 Calculated values for the G.M.W. per mole of droplet for a microemulsion contaning 20 ml 0f 5% NaCl + 0.01N NaOH / 1 gm SCS / 3.7 gm DDAO and various volumes of n-octane between 15-40°C. 90

TABLE 3.4 Radius values for microemulsions prepared with various volumes of n-octane 90

CHAPTER 1

INTRODUCTORY REMARKS

1.1. INTRODUCTION

Emulsions are formed when oil, water and surfactant are mixed together in the proper ratio so that one phase becomes dispersed in the other in the form of large particles.

Emulsions are of two types : oil-in-water (o/w) or water-in-oil (w/o). These systems are stabilized by the presence of amphipatic molecules called surfactants. These molecules have the ability to adsorb at the oil / water interface and reduce the interfacial tension γ_i between the oil and water phases. Due to the size of the particles in the dispersed phase, on the order of 100 nm in diameter, these systems appear milky. If the dispersed phase particles can be diminished in size to where the diameter is less than 1/4 the wavelength of visible light, in certain cases transparent systems are formed which are called microemulsions. To describe these transparent systems, terms such as swollen micellar solution (1), micellar emulsion (2,3), middle phase (4), unstable microemulsion (5) and spontaneous transparent emulsion (1) have been used. Therefore, it is evident that the exact definition of the term microemulsion is still debatable and no one universal definition exists.

Microemulsions are defined in the broadest sense as transparent dispersions of oil, water and surfactants. These systems are of two types ; *oil-in-water* (o/w) where oil is dispersed in a water continuous phase or *water-in-oil* (w/o) where water is dispersed in an oil continuous phase. In this thesis the systems which are defined as microemulsions are transparent dispersions of either o/w or

w/o prepared as suggested by Schulman (6-9) by titrating initial coarse emulsions with a cosurfactant until they spontaneously clear. During the transformation of an emulsion (opaque) into a microemulsion (transparent), the interfacial area greatly increases as the size of the dispersed phase droplets decreases, with little or no mechanical work required. In general, the dispersed phase is made of particles with radii on the order of 10 nm, resulting in the system being transparent.

The question of whether microemulsions are thermodynamically stable or unstable systems has been considered for some time. It was pointed out in 1981 by Rosano (5) that only specific component combinations can produce transparent systems. In addition, it was realized that the order of preparation plays a significent role in the formation of microemulsion systems. For example, emulsions prepared with 2×10^{-3} moles of stearic acid / 2 ml n-hexadecane / 16 ml of 0.375N KOH could be titrated to clarity spontaneously with 1ml of 1-pentanol at 30°C. If however, the same volume of 1-pentanol was first predistributed in various ratios between both the aqueous and oil phases, it is found that the system would not spontaneously clear. From these results it is evident that a specific sequence must be followed in order to produce transparent systems. This fact raises the question of whether microemulsions are : 1) kinetically stable since in certain cases they exhibit path-dependent properties associated with their formation, or 2) thermodynamically stable while these path dependent properties are a reflection of activation energy barriers these systems must overcome during their formation.

Microemulsion systems have been investigated by many scientists for quite some time. In the remainer of this chapter, a general overview will be presented on the major contributions to the field of microemulsion chemistry. It will be shown that many inconsistencies exist as to the basic definition of the

term microemulsion. In view of these results it will be demonstrated that microemulsion systems are thermodynamically stable and should be called swollen micellar solutions.

1.2. The Schulman Microemulsion

Transparent or translucent dispersions of immiscible liquids stabilized by the presence of amphipatic molecules have been known for some time. In 1943 T. P. Hoar and J. H. Schulman (6), noted that : "It is well known that oil / alkali-metal soap (or cationic soap, such as cetyl trimethyl ammonium bromide) / water systems of certain concentration exist as transparent, electrically non-conducting dispersions, in which oil is the continuous phase. Dilution of these systems with excess water inverts them to oil-in-water emulsions, which are milky for low soap / oil ratios and transparent for sufficiently higher soap / oil ratios. The essential conditions for their formation are : 1) a high soap/water ratio and 2) the presence of an alcohol, fatty acid, amine or other non-ionized amphipathic substance in mole fractions approximately equal to that of the soap. When these conditions are met, transparent oil-continuous dispersions were formed and found to be quite stable, showing, however, a slight Tyndall effect. The theoretical size of these droplets were found to be 200 A in diameter, in good accordance with the optical properties of these dispersions. Since these systems are the water-in-oil analog of the hydrophilic "swollen" micelle, they were conveniently termed the "oleopathic hydro - micelle". In a review lecture delivered by Schulman (7) in 1954, he spoke of the work on emulsions being carried out at Cambridge University entitled "Emulsions : Control of Droplet Size and the Phase Continuity in Transparent Oil - Water Dispersions Stabilized By The Addition of Soap and Alcohol." Schulman stated that, "coarse emulsions of nonpolar oils and water stabilized by a soap such as potassium

oleate, may be titrated to transparent fluids by the addition of a short chain alcohol". In 1959 Schulman, Stoeckenius, and Prince (8) called these oil-in-water or water-in-oil optically isotropic systems "microemulsions". The structure of these oil-in-water systems was investigated using a high resolution electron microscope. In order to use this technique to investigate oil-water microemulsion systems, the oil droplets were made resistant to the hot focused electron beam by staining them with osmic tetroxide. The oil droplets seen at high resolution were completely spherical and became more uniform in size as the droplets became smaller. Droplets of 200 A in diameter were clearly observed at magnifications of 40,000 or 80,000. Considerable attention was given to the influence of the chemical potential of both the alcohol and the oil phase molecules upon the formation of microemulsions stabilized with oleate soap and long chain alcohols. It was shown that oil-in-water microemulsions were formed only when the chain length of the alcohol tail was at least as long as the oil phase molecules. This suggested that the oil phase molecules could penetrate the mixed surfactant/cosurfactant film due to strong association among the long alcohol tails and the oil phase molecules. Such penetration would spontaneously increase the pressure π_i of the interfacial film. The mechanism of formation proposed by Schulman (9), was that during the preparation of these systems, surfactant and cosurfactant would form a mixed film at the oil / water interface that would reduce the interfacial tension γ_i below zero, resulting in a metastable negative value, of γ_i. This effect would produce the free energy necessary to increase the interfacial area resulting in spontaneous microemulsification.

1.2.1. NEGATIVE INTERFACIAL TENSION

The concept of negative interfacial tension as advanced by Schulman (8) is

based on the thermodynamic equation which relates the interfacial tension to the oil / water interfacial tension and the spreading pressure of the amphipathic agents present at the interface. The interfacial tension γ_i, in the presence of a mixed film is given by

$$\gamma_i = \gamma_{o/w} - \pi_i \qquad (1.1)$$

where $\gamma_{o/w}$ is the o/w interfacial tension without the film present and π_i is the two-dimensional spreading pressure of the film. According to this equation if $\pi_i > \gamma_{o/w}$ due to the absorption of soap or alcohol molecules at the interface or penetration by oil phase molecules, a negative free energy variation - γ_i dA (dA = the change in interfacial area) would be available to increase the surface area after two or more droplets have coalesced. This was considered to be the condition for the spontaneous formation of microemulsions. Such systems have been characterized by droplet diameters of 80 to 800 A (7,9,16), optical isotropy, faint light scattering and long term stability. If however, $\pi_i < \gamma_i$ only a macroemulsion would form. Droplet diameters of magnitude 10,000 A are usually observed while the system appears milky white, and achieves equilibrium by separating into two phases. Energy input in the form of mechanical work (agitation or homogenization) may temporarily increase the total interfacial area but is not capable *per se* of changing the values of π_i or γ_i. At equilibrium, if the value of γ_i becomes zero, by virtue of uncrowding of the surface molecules and a loss of pressure at the interface, dispersion and not separation will be the final equilibrium condition (5). If the concept of zero interfacial tension is accepted, thermodynamically stable dispersions would result, since no decrease in free energy would accompany droplet coalescence.

Cooke and Schulman (16) later realized that extremely high film pressures were required in order to produce a negative interfacial tension. Using the

duplex film technique Schulman and Montagne (9) have shown that oil molecules have the ability to penetrate films of stearic acid when 2-amino-2-methyl-1-propanol was added to the underlying aqueous subphase. To form a duplex film, a mixture of hydrocarbon and surfactant are spread together on a Langmuir trough, creating two interfaces (i.e., oil/water and oil/air) which behave independently of one another. The direct measurement of the metastable negative interfacial tension at the oil/water interface is impossible to determine since the interface would immediately break up and spontaneously emulsify. However if a countertension is placed on an interfacial measuring device (for example a Wilhelmy plate) to support the interface and prevent surface breakup, π_i can be directly calculated by

$$\gamma_i = \gamma_{o/w} - \pi_i = \gamma_{a/w} - \gamma_{o/a} - \pi_d \qquad (1.2)$$

To produce a negative interfacial tension π_i would have to be greater then 50 dynes/cm if n-hexadecane is used as the oil phase ($\gamma_{o/w}$ = 50 dynes/cm and $\gamma_{o/a}$ = 29 dynes/cm). The measured pressure π_d would than only have to be 43 dyne/cm. Values higher than 43 dyne/cm were found if stearic acid and n-hexadecane were spread on an aqueous phase containing 2-amino-2-methyl-1-propanol at pH = 10.4. This data indicates that oil molecules are able to penetrate mixed interfacial films during microemulsion formation, reducing the interfacial pressure required for microemulsion formation. This technique also gave strong evidence that in some cases, hydrocarbon molecules could be ejected from mixed films of soap and alcohol at the high film pressures necessary to reach negative interfacial tension values.

Prince (17) fully acknowledged the concept of negative interfacial tension suggested by Schulman. However, he also realized that since $\gamma_{o/w}$ was in general high (~ 55 dynes/cm for aliphatic hydrocarbons and ~ 35 dynes/cm for ben-

zene), extremely high surface pressures were required to achieve the negative interfacial tension values necessary for spontaneous microemulsification . He concluded that $\gamma_{o/w}$ in Eq. 1.2 could be replaced by $(\gamma_{o/w})_a$, the reduced oil/water interfacial tension due to a fraction of alcohol disolved in the oil continuous phase. This idea is represented by

$$\gamma_i = (\gamma_{o/w})_a - \pi \qquad (1.3)$$

From this equation, the film pressure required to reduce the interfacial tension to negative values were in effect much lower than previously thought and more easily attainable.

The models presented by Schulman clearly demonstrate the concept of negative interfacial tension. However, they do not seem to be conceptually valid, since $\gamma_i = 0$ alone does not require the dispersed phase to be distributed in spherical droplets as is found in microemulsions (10). It is well known that in oil/water/surfactant systems, cylindrical and lamellar micelles also exist in the equilibrium state. What differentiates these liquid crystalline phases from microemulsions is the type of molecular interactions at the interphase. To insure the formation of dispersed spherical droplets, a low interfacial tension and a high pressure gradient across the flat interphase has been shown to be responsible for interfacial curvature (15). The model proposed by Schulman to explain the pressure gradient is demonstrated by the mixed film theory.

1.2.2. MIXED FILM THEORY.

The essential feature of the mixed film theory is to consider the interfacial film as a liquid, two dimensional third phase in equilibrium with both oil and water. In 1955 Schulman and Bowcott (7) postulated that this film could be represented as a duplex film, i.e., one having different properties on the water

side than on the oil side (15). They pointed out that at the interphase, different surface pressures, π_w and π_o, may exist on either side of the film. To alleviate the surface pressure built up at a flat interphase, curvature of the film would result in the direction of the smaller value of π, until the pressure on both sides of the film become equal. In the case of $\pi_o > \pi_w$, the curvature of the interfacial film will be towards π_w, producing a droplet of encapsulated water characteristic of w/o microemulsions. In the case of $\pi_w > \pi_o$, an encapsulated oil core would result, characteristic of o/w microemulsions. Clearly, the driving force for this behavior is the pressure gradient existing on either side of the interfacial film. This mechanism is illustrated in Fig. 1.1.

Clearly the mixed film theory predicts that surface pressures at the interface depend to a large extent on the interactions between the hydrophobic and hydrophilic portions of the surfactant molecules. If for example, the hydrophobic portion of the surfactant is bulky relative to the hydrophilic group, the hydrophobic portions tend to crowd one another forming a higher surface pressure at the oil side of the film. In this case bending occurs to expand the oil side forming a w/o microemulsion. In the case of surfactants with relatively bulky hydrophilic groups, crowding occurs at the water side of the interphase, producing a curvature towards the oil side of the film, leading to the formation of an o/w microemulsion. A quantitative theory based on lateral stress gradients resulting from the difference in swelling of the heads and tails across the interphase has also been suggested by Robbins (18). The stress gradients were expressed in terms of physically measurable quantities, namely, surfactant molecular volume, interfacial tension and interfacial compressibility. Further, relating the pressure difference across a curved interphase to the activity of water in a w/o microemulsion, Robbins established a criterion for spontaneous water uptake without postulating a negative interfacial tension.

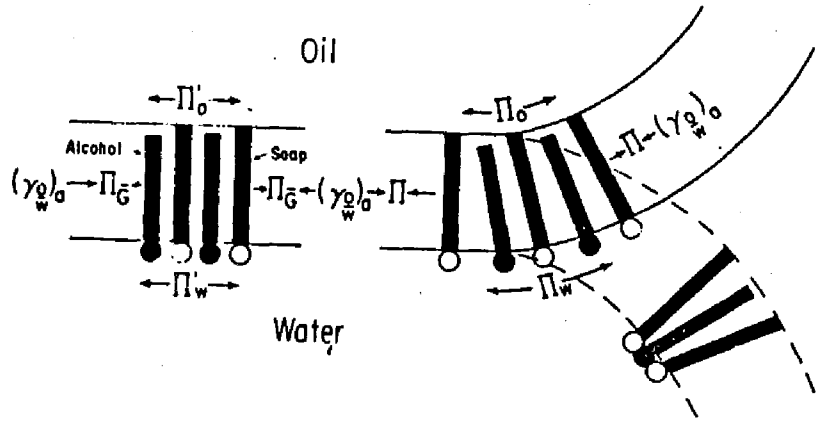

FIGURE 1.1 Diagram illustrating the mechanism of curvature of a microemulsion film. Redrawn from Ref. (24), Fig.4., by courtesy of the Journal of the Society of Cosmetic Chemists.

The two theories proposed by Schulman have experienced successive periods of fashion and rejection. Although the Schulman model represents an adequate qualitative description of the forces occurring at the interface, it neglects any terms which involve entropy effects and curvature energies. Ruckenstein and Chi (22) considered the free energy of microemulsion formation ΔG_m to consist of three contributions : ΔG_1 an interfacial energy term, ΔG_2 an energy of interaction between the droplets term and ΔG_3 an entropy of dispersion term accounting for the dispersion of the dispersed phase into the continuous phase. The interfacial free energy term ΔG_1 was considered to consist of two contributions :

1) the creation of an uncharged surface (given by the product of the area created and the specific free energy of the interface) and,

2) a contribution due to the formation of electric double layers (given by the interfacial area and the specific free energy due to the creation of an electrical double layer).

The double layer contribution was determined using the Debye-Huckel approximation. To calculate ΔG_2, a pairwise additivity of interaction potentials was assumed and for ΔG_3, a lattice model was used to determine the number of configurations of the droplets in the continuous phase. By varying ΔG_m with the radius R, various states could be distinguished which illustrate a transition from kinetically stable (considered by Ruckenstein to be unstable systems) to thermodynamically stable microemulsions depending on the droplet radius. This suggests the existence of an optimum droplet radius in which the free energy of the system is a minimum value. It will be demonstrated that entropy effects alone are not enough to account for microemulsion formation, while a more complete description should include a term describing interfacial flexibility.

Ruckenstein (19) has shown that thermodynamically stable microemulsions can form when the negative free energy change due to the entropy of dispersion of the globules in the continuous phase combined with the "dilution effect" overcomes the positive product of the low interfacial tension and the large interfacial area produced. The dilution effect is defined as the negative free energy change generated as a result of the decreased concentration of the surfactant and cosurfactant in the two bulk phases due to adsorption at the interface. As a result of the dilution effect, the chemical potential of the surfactant and cosurfactant in the two bulk phases are both reduced. Tamlon and Prager (23) then showed that, in the absence of any other interaction effects, the entropy term may impose certain phase transitions ; when the amount of surfactant available is decreased, they predicted that the microemulsion would separate into two phases (oil rich and water rich).

1.3. THE FLEXIBLE INTERFACE

Studies on the interfacial film of birefringent microemulsions close to the isotropic microemulsion droplet region have provided detailed information on the undulations and high flexibility of the interfacial film. De Gennes and Taupin (25) have shown that the interfacial film undulates because of its high flexibility and that the amplitude of the undulations is limited by the interactions between adjacent lamellae. Free energy expressions for these interactions have been determined, which include attractive (van der Waals) and repulsive interaction terms (24,26). For fluid/fluid interfaces, it has been shown that the value of the interfacial energy γ_i dominates system behavior and any effects due to curvature energies represent only minor corrections to the overall system behavior. The curvature energy can be represented as

$$E_c = \frac{1}{2}K\left|\frac{1}{R} - \frac{1}{R_o}\right|^2 \qquad (1.4)$$

where K is the rigidity constant of the film and has the dimensions of energy, R the radius of curvature and R_o the spontaneous radius of curvature, i.e., the radius of curvature that the film would adapt in the absence of any interactions (24,25).

Di Meglio (26) has determined the rigidity constant K for lamellar systems close to the isotropic microemulsion region by the spin labelling technique. This technique consists of studying the electronic paramagnetic resonance of a nitroxyide radical probe. The probe is grafted on the alkyl chain of the surfactant molecule whose alkyl chain length is identical to one of the surfactant molecules at the interface. When one probe per thousand surfactant molecules is used, no perturbation of the interfacial film is observed. The systems investigated were composed of sodium dodecyl sulfate (SDS) / 1-pentanol / cyclohexane / water. The water/surfactant ratio was 2.5 (by weight). These systems were prepared by : 1) varying the swelling ratio (oil/water ratio) while remaining at the linear border of the lamellar phase (to insure that the chemical components of the film remain constant) and 2) by varying the amount of cosurfactant at a fixed swelling ratio. It was found that, as the swelling ratio or cosurfactant concentration is increased, the amplitude of the undulations also increases leading to a decrease in the rigidity of the interfacial film, and to the existence of very curved defects. Since the rigidity constant K was found to decrease upon the addition of cosurfactant, it was concluded that a basic role of the cosurfactant was to reduce the rigidity of the interfacial film, aiding in the resolution of lamellar phase systems into an isotropic microemulsion.

The dynamic role of the cosurfactant in lowering the interfacial tension during the titration of a coarse emulsion into a transparent dispersion has been investigated by Rosano (5). It has been pointed out that during the addition of a cosurfactant to an emulsion of either o/w or w/o, excess cosurfactant accu-

mulates at the oil/water interface during transport, reducing the interfacial tension to well below the positive equilibrium value. The surfactant retards the cosurfactant interfacial transport, while a prolonged low interfacial tension helps in the formation of a large increase in the interfacial area. Eventually, γ_i regains a low positive value responsible for the resolution of the system into microdroplets. When the cosurfactant is a short chain alcohol, not only is the interfacial tension reduced, but a disorder at the interface is also induced (14).

Mitchell and Ninham (20) investigated the importance of the geometric packing of the surfactant film and its relation to microemulsion formation. These authors pointed out that the nature of the aggregates formed depends on the packing ratio given by $V / a_o l_c$ where V is the partial molecular volume, a_o the head group area of the surfactant molecule, and l_c the maximum chain length. Incorporation of a cosurfactant into these surfactant aggregates produces a "wedge effect" which increases the mean volume per surfactant molecule without affecting appreciably a_o or l_c. Consequently, $V / a_o l_c$ would increase with addition of cosurfactant. The packing ratio is effected by many factors which include the ionic strength of the solution, pH, temperature and the hydrophilicity of the head groups. It has been shown that the nature of the microemulsion can be explained in terms of the packing ratio. If $V / a_o l_c$ increases with temperature (resulting in a decrease in a_o) hydrocarbon solubility in nonionic surfactant systems should increase until $V / a_o l_c$ reaches a value of 1 where phase inversion would be expected to occur. At higher temperatures, w/o microemulsions would be expected and the solubility of water would decrease as the temperature rises.

During the International Symposium on Surfactants in Solution (Lund, Sweden, 1982), M. Kahlweit suggested that coordinated studies be carried out between different groups on a particular microemulsion system. This led to

the formation of the European Microemulsion Group. The system chosen for collaborative work within this "Lund Project" was p-octylbenzene sulphonate / 1-butanol / water / toluene or n-decane. To ensure sample uniformity between the groups investigating these systems, a special batch of sodium octylbenzene was prepared by P. Bothorel's group in Bordeaux for the Lund Project.

As part of this group Lindman et al. (27) carried out Fourier-transform n.m.r. self diffusion measurements and multifield C-13 n.m.r. relaxation measurements. These two techniques are both sensitive to the degree of structure in the system but in very different ways. The self-diffusion technique is a convenient method for the detection and measurement of the lateral displacement of matter. It is based on the fact that within a micelle, molecular motion is almost as rapid as in a liquid hydrocarbon and likewise in a reversed micelle, where water molecules and counterions are very mobile. The situation is slightly different for lamellar liquid crystals, where the motion of all the components appears to be very rapid in the direction of the lamellae, while in the perpendicular direction, translational diffusion is found to be slow. It appears to be a general feature of amphiphilic systems that all components move freely within a specific domain. It is characteristic of amphiphilic systems that there is typically a rather sharp spatial separation between hydrophilic and hydrophobic regions. For such systems the passage of a molecule or ion between different regions is an extremely improbable event and thus occurs slowly. Consequently, in studies of self-diffusion over macroscopic distances, diffusion can be rapid or slow depending exclusively on the geometrical properties of the inner structure of the phase. If a phase is water-but not oil continuous, one expects diffusion of hydrophobic components to be rapid and hydrophilic components to be slow. For the case of an oil-but not water continuous structure, the converse situation should apply. Bicontinuous phases

should therefore exhibit rapid diffusion of all the components in all directions. These spectroscopic results indicate that very few microemulsion systems actually exhibit self-diffusion behavior consistent with closed droplet structures as has been suggested to exist by many investigators (3,5-11,14,15). The one exception is the AOT (sodium di-2-ethyl-hexylsulphosuccinate) / water / hydrocarbon system where the closed water-in-oil structure exists over the whole isotropic solution region. C-13 relaxation measurements were performed on the isotropic region of the sodium octylbenzene sulphonate / 1-butanol / toluene / water system. This technique gives quantitive information on the local chain dynamics and packing of the surfactant molecules at the interface. The results show that the motion of the alkyl chains is as rapid as the motion of the liquid hydrocarbon and emphasizes that a substantial fraction of the surfactant molecules are oriented with a marked motional anisotropy. These results also suggest that hydrophobic-hydrophilic interfaces are very flexible and can change direction extensively within a few nanoseconds.

The study was further carried out for the atypical three-component sodium octanoate-octanoic acid-water system (28). This system although not a true microemulsion, was chosen as a model in an attempt to determine the structure of microemulsions. The results indicate that at low water content, there is substantial disorder of the hydrocarbon chains with marked motional restrictions near the polar head group. These results support the idea that well defined complexes are formed for low water content while at higher water content, this simple model with a closed water domain does not apply.

The stability of emulsion and microemulsion systems does not appear to be dependent only on the value of the γ_i, but mainly on the structure of the surfactant film surrounding each droplet (11). For a given oil/surfactant pair, cosurfactant steric requirements determine the volume of the dispersed phase

that can be stabilized. These systems are oil-and cosurfactant-dependent. Both the structure and chain length of the surfactant and cosurfactant have a striking influence on the structure of the microemulsion formed. Surfactant, cosurfactant, the nature of the oil and aqueous phase are four interacting variables that determine the size of the dispersed phase droplet when microemulsions are formed.

1.4. PERCOLATION IN MICROEMULSION SYSTEMS

The concept of percolation transition is often used in interpeting the electrical conductivity observed for w/o microemulsion systems. In systems composed of a random distribution of particles, a percolation transition signifies the formation and existence of an infinite cluster of particles. This transition has been shown to become more and more probable as the dispersed phase volume and temperature are increased (29). Recent measurements have shown that a sharp rise in electrical conductivity results as the system approaches a liquid-gas transition due to the clustering of droplets (30).

Safran (31) has investigated the percolation behavior of spherical particles with short-ranged attractive interactions using Monte Carlo simulations. A model based on short-ranged attractions was motivated by the fact that the neutron-scattering structure factor can be fitted to a model of square well attractions. A Standard Metropolis algorithm was used for systems of 108, 508 and 2048 particles in a cubic box with periodic boundary conditions. The Metropolis Monte Carlo algorithm, developed originally for the equilibrium behavior of a dense gas or liquid, is one example of an important sampling technique and is based on a particular method for generating configurations which satisfy a particular probability density equation.

The Monte Carlo method refers to a general technique of estimating the

value of multidimensional integrals by sampling with the use of random numbers. The Monte Carlo method represents the physical or mathematical system in terms of some *sampling procedure* which satifies the same underlying probability laws as the system being studied. The Monte Carlo algorithm begins with some initial configuration of the particles, and subsequently, a very large number of configurations typical of the equilibrium condition is generated. For a system at equilibrium, the probability of it being in a state with associated energy U is proportional to the Boltzmann factor, i.e., $\exp(-\beta U)$ where $\beta=(k_b T)^{-1}$. In the Monte Carlo procedure the particles are moved according to a criterion which guarantees that a given configuration occurs with probability proportional to $\exp(-\beta U)$ for that configuration. Properties can then be evaluated based on averaging of the appropriate quantity over all the configurations, where equal weights are assigned to all configurations (32).

The results obtained by Monte Carlo simulations on spherical particles indicate that an increased interaction strength ϵ between the particles may either raise or lower the volume fraction ϕ_p required for percolation to occur. It has been reported that when the dispersed phase volume is increased, the percolation threshold is decreased. Safran (33) has shown that for a system to percolate, pairs of particles must have shells that overlap. Thus particles with a greater shell to core ratio have a greater percolation probability for pairwise overlap ; their percolation threshold is lowered. However, it was shown in certain cases, an increase in the interaction strength is analogous to a decrease in the shell-to-core ratio. It has been reported that an increase in ϵ 1) results in the promotion of pairwise overlap, but 2) may render the cluster more compact, thus requiring a greater dispersed phase volume ϕ_p for percolation to occur.

In addition to the effect of temperature via the translational entropy of the globules, thermal fluctuations of the internal dergees of freedom of the globules

exist as well. The entropy of the interface results in globules whose size and shape depart from the ideal spherial shape. The existence of these shapes i.e., the ability of the globules to change its internal structure - differentiates microemulsions from systems such as solid colloids.

The probability that an arbitrary deformation of the globules will occur in thermal equilibrium is proportional to the Boltzmann factor $\exp^{-\Delta F / T}$ where ΔF is the energy cost of the deformation. This energy cost has been determined by Safran (34). It should be noted that these fluctuations are not dynamical fluctuations of individual globules, as has been treated by Ljunggren and Eriksson (35), but rather fluctuations from the ideal monodispersed sphere in an ensemble of droplets. The importance of such a system is the mechanism whereby such ensemble fluctuations occur via collisions in which the globules may exchange surfactant and/or dispersed phase molecules between adjacent ensemble clusters giving rise to a percolation transition.

1.5. THE THESIS RESEARCH STATEMENTS

The question of whether microemulsions are thermodynamically stable or unstable has been investigated for quite some time. Rosano et al. (5) have demonstrated that only specific component combinations can produce microemulsions. In particular, it was found that the right order of mixing the various components (i.e., oil, water, surfactant and cosurfactant) must be followed in order to produce transparent systems. When the order of combining the components was varied, in some cases, these transparent systems were not obtained. This important experiment led these authors to conclude that, microemulsions prepared by titrating coarse emulsions spontaneously to clarity are thermodynamically unstable systems. This conclusion was based on the fact that some microemulsion systems exhibited path-dependent properties asso-

ciated with their formation.

In light of the accepted opinion at the time that microemulsions prepared by titration are thermodynamically unstable systems, the study presented in this thesis was undertaken to present a different view on the stability of microemulsion systems. A series of microemulsions, mainly of the o/w type were selected for investigation. The basic hypothesis was that these systems were considered to be thermodynamically stable. Once this assumption was postulated, the thermodynamic properties associated with microemulsion formation were determined, i.e., the free energy, the enthaply and entropy of formation. Based on these results, it will be demonstrated that the free energy associated with microemulsion formation are small negative values and therefore, the driving force in transforming an emulsion into a microemulsion is a small quantity. The entropy of dispersion involved in microemulsion formation are in agreement with the large increase in interfacial area upon microemulsion formation. The positive values clearly demonstrate the result of the increased interfacial area during the transformation of an emulsion into a microemulsion. From these results it is concluded that when the right order of combining the various components of the system is followed, conditions favorable for dispersion occur. In addition, the right order of mixing the components probably lowers the activation energy barriers these systems must overcome during their formation. These results demonstrate that the path-dependent properties associated with microemulsion formation first reported by Rosano et al. (5) probably reflect higher energy barriers of formation due to the order in which the components are mixed. In view of these results it is concluded that microemulsions prepared by titration appear to be thermodynamically stable systems.

1.6. REFERENCES

1 Shinoda, K., Kunieda, H., Kolloid Z. 42, 381, (1973).

2 Adamson, A., J. Coll. Interface Sci. 29, 261, (1969).

3 Gerbacia, W.E., Rosano, H.L., and Zajac, M., Am. Oil Chemists Soc. J. 53, 101, (1976).

4 Robbins, M. L., "Micellization, Solubilization, and Microemulsions" Vol. 2, edited by K.L. Mittal, Plenum Press, (1977), 713 - 753, also Scriven, L. E., ibid. p. 877 - 893.

5 Rosano, H.L., Lan, T., Weiss, A., Whittam, J.H., and Gerbacia, W.E., J. Phys. Chem. 85, 468-473, (1981).

6 Hoar, T. P., Schulman, J. H. Nature (London) 152, 102, (1943).

7 Bowcott, J. E. L., Schulman, J. H. Z. Elektrochem. 59, 283, (1955).

8 Schulman, J. H., Stoeckenuis, W., Prince, L. M. Kolloid - Z. 169, 170, (1960).

9 Schulman, J. H., Montague, J. B. N.Y. Ann. Acad. Sci. 92, 366, (1961).

10 Gerbacia, W.E., Rosano, H.L., J. Coll. Interface Sci. 44, 242, (1973).

11 Rosano, H.L., U.S. Patent 4,146,499, March 27, (1979).

12 Rehbinder, P.A., Proc. 2nd. Int. Congr. Surface Activity, London, 1, 476, (1957).

13 Ruckenstein, E., J. Coll. Interface Sci., 66, 369, (1978).

14 Schulman, J.H., and McRoberts, T.S., Trans. Faraday Soc. 42B, 165, (1946).

15 Prince, L.M., "Microemulsions" Theory and Practice, Academic Press, New York, (1977), 108.

16 Cooke, C.E., and Schulman, J.H., "Surface Chemistry," p. 231 - 251,

Munksgaard, Copenhagen, (1965).

17 Prince, L.M., J. Coll. Interface Sci. 23, 165, (1967).

18 Robbins, M.L., "Theory of Phase Behavior of Microemulsions", Paper No. 5839, presented at the Improved Oil Recovery Symposium of the Socirty of Petroleum Engineers of AIME, Tulsa, Oklahoma, March 22-24, 1976.

19 Ruckenstein, E., Chem. Phys. Letters, 57, 517, (1978).

20 Mitchell, D.J., and Ninham, B.W., J. Chem. Soc. Faraday Trans II, 77, 601, (1981).

21 Prince, L.M., J. Soc. Cosmetic Chemists 21, 193, (1970).

22 Ruckenstein, E, and Chi, J., J. Chem. Soc., Faraday Trans. II, 71, 1690, (1975).

23 Tolman, Y., and Prager, S., J. Chem. Phys. 69, 2984, (1978).

24 Helfrich, W., Z. Naturforsch C, 28, 693, (1973).

25 De Gennes , P.G., and Taupin, C., J. Phys. Chem. 86, 2294, (1982).

26 di Meglio, J. H., Dvolaitzky, M., Leger, L., Ober, R., Paz, L., and Taupin, C., Presented at the 5th International Conference on Surface and Colloid Sciance, Potsdam, New York, June 25 - 28, 1985.

27 Lindman, B., Ahlnas, T., Soderman, O., and Walderhaug, H., Faraday Discuss. Chem. Soc., 76, (1983).

28 Ahnas, T., Soderman, O., Hjelm, C., and Lindman, B., J. Phys. Chem. 87, 822, (1983).

29 Lagues, M., J. Phys. (Paris) Lett. 40, L331, (1979).

30 Safran, S.A., Turkevich, L.A., Phys. Rev. Lett. 50, 1930, (1983).

31 Safran, S.A., Webman, I., Grest, G.S., Phys. Rev. A, 32, 506, (1985).

32 Castillo, C., Rajagopalan, R., and Hirtzel, C.S., Rev. Chem. Eng. 2, 237,

(1984).

33 Bug, A.L.R., Safran, S.A., and Grest, G.S., Phy. Rev. Letts. 55, 1896, (1985).

34 Safran, S.A., To be published in "Statistical Thermodynamics of Micelles and Microemulsions" (Springer - Verlag), ed. S.H. Chen.

35 Ljunggren, S., Eriksson, J.C., J. Chem. Soc., Faraday Trans. II, 80, 489, (1984).

CHAPTER 2

MICROEMULSION SYSTEMS : FREE ENERGY, ENTHALPY AND ENTROPY OF FORMATION

2.1. INTRODUCTION

The most significant difference between emulsions (opaque) and microemulsions (transparent) lies in the fact that putting work into an emulsion or increasing the surfactant concentration usually improves their stability. This is not the case with microemulsions whose formation appears to be dependent on specific interactions among the constituent molecules. If these interactions are not realized, neither the work imput nor increasing the surfactant concentration will produce a microemulsion. On the other hand, once the conditions are right, spontaneous formation occurs and little mechanical work is required (1).

Recently, evidence has been presented that some microemulsion systems may not be thermodynamically stable (2). This conclusion was based on the differences in the observable results when the order of mixing the components oil, water, and surfactant were changed. It was proposed that there may be two inherently different classes of microemulsion systems. One class consists of thermodynamically stable systems which form spontaneously upon the addition of a cosurfactant, and the other consists of kinetically stable dispersions which can be stable for long periods of time.

In this chapter the mechanism of microemulsion formation will be investigated. Special emphasis will be placed on the thermodynamic properties

associated with their formation. These systems will then be related to specific regions on a simple phase diagram proposed by Shinoda (8).

2.2. EXPERIMENTAL

2.2.1. CHEMICALS

n-Octane, n-decane, n -dodecane, n-tetradecane and n-hexadecane were all 99%+ (gold label) (Aldrich Chemical Co, Milwaukee, WI 53233). Sodium myristyl sulfate (Cyclo Chemicals Corporation, Miami, FL 33166), sodium cetyl sulfate (Henkel Chemical Co., Minn., MN.). Sodium dodecyl sulfate, potassium hydroxide, toluene and 1-pentanol (Fisher Scientific Co., Fair Lawn NJ 07410), were all reagent grade. Octyl and nonylphenolethylene oxide compounds were all 100% active (GAF Corp, New York, NY 10020). Dodecyl, tetradecyl and hexadecyldimethylamine oxide, (Onyx Chemical Co, Jersey City, NJ 07302), were all 30% active. Freshly distilled water was used in all preparations and all glassware was first thoroughly cleaned with a fresh sulfuric acid / potassium dichromate solution.

2.2.2. METHOD OF PREPARATION OF TRANSPARENT SYSTEMS

Microemulsion systems were prepared in water-jacketed beakers maintained at constant temperature, using the titration technique (3). An initial coarse macroemulsion was prepared from an oil / surfactant mixture added to an aqueous phase. The system was then titrated to clarity using a cosurfactant delivered from a microburette. Continuous stirring was maintained throughout the titration process to insure homogeneous mixing. Percent transmittance was measured as the system started to clear using a Bausch & Lomb Spectronic 20 spectrometer at 520 nm.

The two methods of preparation used were :

1) oil / surfactant and water were mixed together in just the right ratio to form the best initial emulsion. The amount of surfactant required was estimated by geometric considerations. The total interfacial area A, (assuming spherical droplets are formed) is given by

$$A = n\sigma = 4\pi r^2 \times a \qquad (2.1)$$

where

n = number of surfactant molecules

σ = cross-sectional area occupied by the surfactant molecules at the o/w interface ($\mathring{A}^2$ /molecule)

r = radius of the dispersed phase droplets (Å)

a = total number of droplets of the dispersed phase

The total volume of the dispersed phase is given by

$$V = \frac{4}{3}\pi r^3 \times a \qquad (2.2)$$

combining equations 2.1 and 2.2, an expression relating the number of molecules of surfactant to the volume of the dispersed phase is given by

$$n = \frac{3V}{r\sigma} \qquad (2.3)$$

The number of grams of surfactant is then given by

$$X = \frac{GMW}{6.02x\ 10^{23}\ \frac{molecules}{mole}} \times n \qquad (2.4)$$

From equation 2.4, the minimum amount of surfactant required to produce the best initial emulsion was determined. This emulsion was then titrated to clarity with a second surfactant (cosurfactant),

2) the cosurfactant is first predistributed in various ratios between oil and aqueous phases before combining them.

When these two methods were used it was found that the manner of combining the components could affect the formation of the dispersion. From these results, it appears that the formation of these spontaneously-forming transparent systems may be, in certain cases, path-dependent (4).

2.2.3. MICROEMULSION SYSTEMS INVESTIGATED

Five o/w and one w/o emulsions were titrated to clarity (transmittance > 90%) with a cosurfactant. Three of the o/w systems investigated were prepared with both nonionic surfactants and cosurfactants ; see Table 2.1.

Oil-in-water microemulsion systems were also prepared with n-octane, n-decane, n-tetradecane and n-hexadecane hydrocarbon oils / 5% NaCl + 0.01N NaON (pH = 11.2) / sodium dodecyl sulfate (SDS) or sodium myristyl sulfate (SMS) or sodium cetyl sulfate (SCS). These systems were titrated to clarity with dodecyl, tetradecyl or hexadecyldimethylamine oxides.

2.2.4. VISCOSITY AND PERCENT TRANSMITTANCE

In a water-jacketed beaker maintained at 30°C, an emulsion consisting of 2.0 ml n-decane / 0.5 ml nonylphenol-1.5-EO + 0.5 ml nonylphenol-4-EO / 35 ml water was titrated to clarity with nonylphenol-10- EO. Upon each addition of nonylphenol-10-EO, percent transmittance and viscosity (Brookfield Synchro-Lectric Model LVT, Stoughton, MA) were determined.

2.2.5. PHASE VOLUME AND PARTICLE SIZE DETERMINATION

Volumes of upper and lower phases were determined for fifteen individual systems prepared with 2.0 ml n-octane / 0.5 ml nonylphenol-1.5-EO + 0.5 ml

TABLE 2.1				
SYSTEMS	CONTINUOUS PHASE	DISPERSED PHASE	SURFACTANT	COSURFACTANT
1	water	2 ml n-octane	0.5 ml C_9phenol-1.5-EO + 0.5 ml C_9phenol-4-EO	C_8phenol-9-EO
2	water	2 ml n-decane	0.5 ml C_9phenol-1.5-EO + 0.5 ml C_9phenol-4-EO	C_9phenol-10-EO
3	water	2 ml n-hexadecane	0.5 ml C_9phenol-1.5-EO + 0.5 ml C_9phenol-4-EO	C_9phenol-9-EO
4	toluene	2 ml water	1.98×10^{-3} M SDS	1-pentanol
5	saline 0.375 N KOH	2.3 ml n-hexadecane	2.3×10^{-3} M stearic acid	1-pentanol
6	5% NaCl saline	1 ml n-decane	1 gm. SDS	DDAO

TABLE 2.1. Microemulsion systems investigated.

nonylphenol-4-EO / 30 ml water. To each system increasing amounts of nonylphenol-9-EO were added. Each of the systems were shaken thoroughly and then stored in graduated cylinders for 30 days at room temperature (22°C). At equilibrium it was found that depending on the amount of nonylphenol-9-EO added, phase separation was observed. A Philips EM 300 electron microscope at 60 kV and a Coulter Sub-Micron Particle Analyzer Model N4, (Coulter Electronics, Inc. Hialeah, FL), were used to determine the structure and mean droplet diameter of the lower water phase as a function of increasing the concentration of octylphenol-10-EO.

2.2.6. ELECTRON MICROSCOPY SAMPLE PREPARATION

Samples investigated by electron microscopy were prepared using the negative staining technique. Formvar-coated grids were prepared with a 0.5% Formvar solution. A drop of the lower phase solution was placed on the Formvar-coated grid and allowed to dry. The excess solution was absorbed with a No. 1 filter paper. A drop of a 5% uranyl acetate solution was then placed on the grid. After 5 seconds, any excess solution was again absorbed with the filter paper. The grid was then allowed again to dry in air for 10 minutes prior to examination with the EM.

2.3. RESULTS

2.3.1. LONG CHAIN DIMETHYLAMINE OXIDE MICROEMULSIONS

Microemulsion systems were prepared with sodium dodecyl sulfate, sodium myristyl sulfate or sodium cetyl sulfate / n-octane, n-decane, n-dodecane, n-tetradecane or n-hexadecane / 20 ml of 5% NaCl + 0.01N NaOH / and titrated with dodecyl or tetradecyl or hexadecyl dimethylamine oxides (see Table 2.2). It was observed that with sodium cetyl sulfate, n-octane produced

TABLE 2.2

Na cetyl sulfate

LCDAO	C8	C10	C12	C14	C16
C16	NC	NC	NC	NC	NC
C14	5.5(90%)*	NC	NC	NC	NC
C12	3.0(88%)	NC	NC	NC	NC

Na myristyl sulfate

LCDAO	C8	C10	C12	C14	C16
C16	NC	NC	NC	NC	NC
C14	6.6(100%)	6.9(95%)	7.8(92%)	7.3(96%)	NC
C12	3.6(96%)	5.4(97%)	NC	NC	NC

Na lauryl sulfate

LCDAO	C8	C10	C12	C14	C16
C16	9.0(100%)	NC	NC	NC	NC
C14	3.3(90%)*	2.1(98%)	3.0(90%)	4.0(88%)	NC
C12	1.8(99%)	3.3(100%)	NC	NC	NC

TABLE 2.2 1 ml. hydrocarbon / 20 ml of 5% NaCl + 0.01 N NaOH / 1 gm long chain sodium sulfate / titrated with 30% active long chain dimethylamine oxide (LCDAO). Notation : ml. of cosurfactant as 100% active are reported. Percent transmittance @ 520 nm, n = Viscosity . * = Thick gel. Temperature = 30°C.

a transparent gel. For sodium myristyl sulfate, transparent systems were more prevalent for all oils used except n-hexadecane. No microemulsions were formed when hexadecyldimethylamine oxide was used as a cosurfactant. With sodium dodecyl sulfate, microemulsion systems were obtained, again no transparent systems were formed when n-hexadecane was used as the oil phase.

2.3.2. THERMODYNAMIC PROPERTIES

Figure 2.1 represents a typical plot of the minimum volume of octylphenol-9-EO and various volumes of aqueous phase, required to titrate an emulsion consisting of 2.0 ml n-hexadecane / 0.5 ml nonylphenol-1.5-EO + 0.5 ml nonylphenol-4-EO spontaneously to clarity at 45° C and at 55 C. For example, at 45° C, if an initial emulsion containing 30 ml of water was titrated, the system remained milky until 1.5 ml of octylphenol-9-EO had been added. Beyond this volume of cosurfactant, the system remained clear. The same process was repeated with various volumes of water (continuous phase) and a straight line was obtained. The values of the slope (ml of octylphenol-9-EO per ml of water) and intercept (ml of octylphenol-9-EO at zero ml water) were determined using a linear regression process. The mole fractions X_c^b of octylphenol-9-EO in the continuous phase and at the interface X_c^i were determined by equations 2.5 and 2.6.

$$X_c^i = \frac{n_i}{n_i + n_s} \tag{2.5}$$

$$X_c^b = \frac{n_b}{n_s + n_a} \tag{2.6}$$

where

n_i = number of mole of cosurfactant at the o/w interface

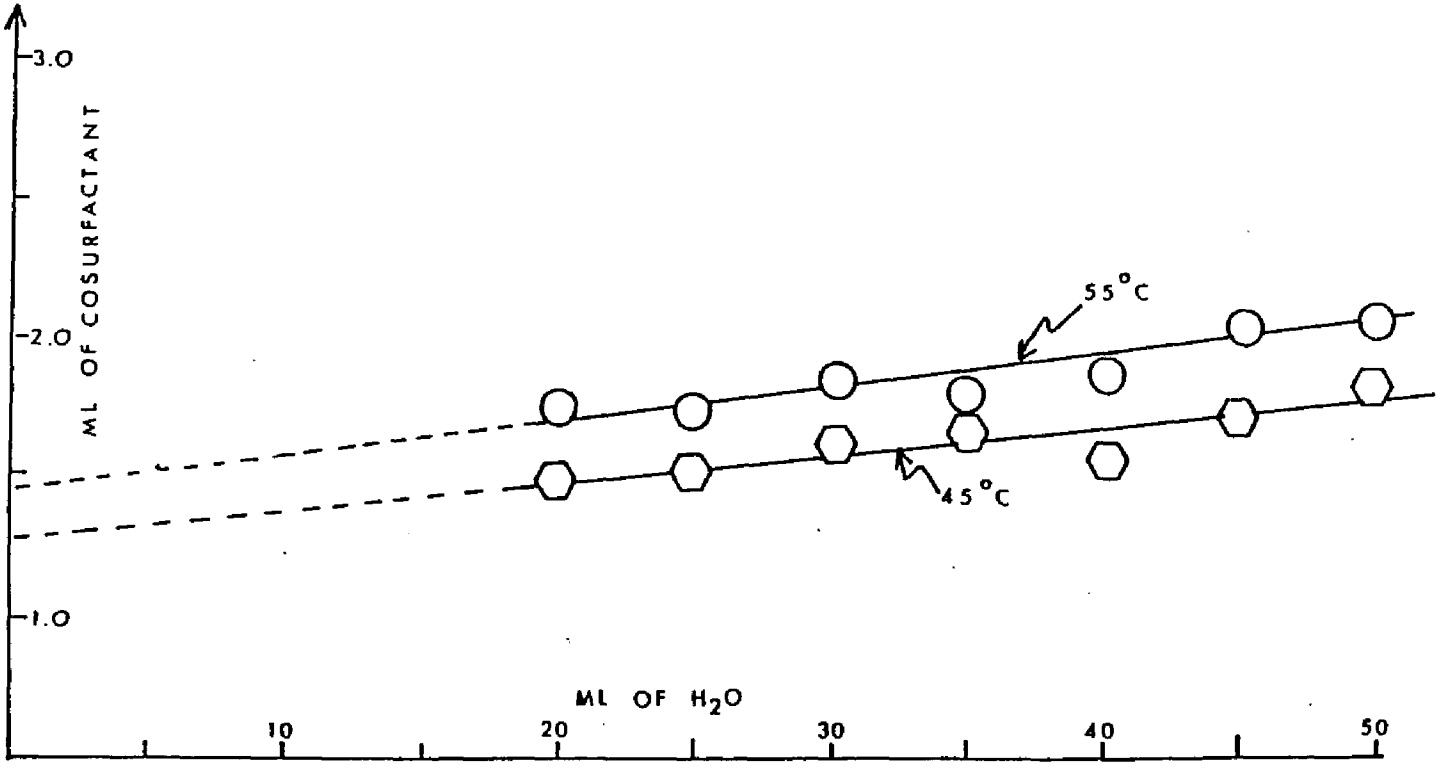

FIGURE 2.1 2ml n-hexadecane / 0.5ml nonylphenol-1.5-EO + 0.5ml nonylphenol-4- EO / variable volume of water / titrated to clarity with octylphenol-9-EO at 45°C and 55°C.

n_s = number of moles of surfactant

n_b = number of moles of cosurfactant in the bulk phase

n_a = number of moles of aqueous phase

It is assumed that all the surfactant molecules are at the o/w interface and there is no surfactant in the bulk phase, therefore, $n_s = 0$. This reduces equation 2.6 to

$$X_c^b = \frac{n_b}{n_a} \tag{2.7}$$

Using the thermodynamic relationship expressed by equation 2.8, for ideal solutions

$$\Delta G = -RT \ln \frac{X_c^i}{X_c^b} \tag{2.8}$$

the free energy change ΔG accompanying the adsorption of octylphenol-9-EO at the interface during the transformation of a primary coarse emulsion into a transparent system was determined. Since the adsorption of cosurfactant results in the transition of an emulsion into a microemulsion, these values actually correspond to the change in free energy accompanying microemulsion formation. The same procedure was repeated at various temperatures. Plotting the change in free energy vs. temperature, the entropy change accompanying cosurfactant adsorption was calculated using

$$\left[\frac{\partial\, \Delta G}{\partial T}\right]_p = -\Delta S \tag{2.9}$$

Table 2.3 shows the calculated values for the free energy, enthalpy and entropy for the six systems investigated at 30° C. All thermodynamic properties were calculated using the computer program shown in Appendix A. Table 2.4

TABLE 2.3			
SYSTEM	ΔG (kJ/mole)	ΔH (kJ/mole)	ΔS (kJ/K mole)
1	-17.4	-6.8	3.5×10^{-2}
2	-18.1	-6.0	4.0×10^{-2}
3	-19.6	-25.0	-1.8×10^{-2}
4	-6.4	18.7	8.2×10^{-2}
5	-14.8	8.7	7.8×10^{-2}
6	-13.9	11.3	8.3×10^{-2}

TABLE 2.3 Free energy, enthalpy and entropy changes corresponding to the adsorption of cosurfactant at the interface for 5 o/w and 1 w/o microemulsion systems.

temp. °C	vol. n-hexadecane,ml	vol. 1-pentanol,ml	vol. 1-pentanol/mL aqueous phase x 10^2	moles of 1-pentanol/ mole K sterate	X_a^i	X_a^b X 10^3	G, kJ/mol
25	2.30	1.0401	1.4150	4.1709	0.8066	2.8819	-13.978
30	1.15	0.9010	1.1375	4.0607	0.8024	1.8882	-15.264
30	2.30	0.8947	1.3058	3.587	0.7820	2.1678	-14.854
35	2.30	1.1353	1.1561	4.524	0.8199	1.9192	-15.532
40	2.30	1.188	0.9771	4.7638	0.8265	1.6242	-16.240
43	2.30	0.8815	1.7259	3.5346	0.7795	1.8652	-14.749
45	2.30	1.2675	1.1647	5.08356	0.8356	1.8535	-16.178
50	2.30	1.4989	1.7259	6.0104	0.8574	1.8506	-16.509

TABLE 2.4 Tabulated data for system 4 of Table 2.1.

shows the tabulated results obtained by titrating system 4 to clarity with 1-pentanol at various temperatures. It is interesting to note that in one experiment where the volume of n-hexadecane was reduced from 2.3 to 1.15 cc, it was found that the volume of 1-pentanol required to produce an abrupt rise in transmittance was very similar in both cases.

2.3.3. VISCOSITY AND PERCENT TRANSMITTANCE DURING MICROEMULSION FORMATION

Relative viscosity and percent transmittance for a system prepared with 2.0 ml n-decane / 0.5 ml nonylphenol-1.5-EO + 0.5 ml nonylphenol-4-EO and 35 ml water were measured upon addition of nonylphenol-10-EO, shown in Fig. 2.2. Upon addition of 2.5 ml of cosurfactant the viscosity increased to 40 cps and filaments were first observed while the system was being stirred. A maximum viscosity of 110 cps was reached when 3.10 ml of cosurfactant was added. Filaments were still observable up to 4.2 ml of nonylphenol-10-EO. The viscosity of the system then decreased upon further addition of nonylphenol-10-EO and the system cleared at 4.85 ml. Upon further addition of nonylphenol-10-EO, the system remained clear (95% transmittance) but the viscosity again increased.

2.3.4. PHASE VOLUME CHANGES

Fig. 2.3 shows the change in phase volume for fifteen individual systems prepared with 2 ml n-octane / 0.5 ml nonylphenol-1.5-EO + 0.5 ml nonylphenol-4-EO / 30 ml water and various amounts of octylphenol-9-EO. Initially, the systems started out as two phases, both the upper and lower phases being clear. By adding octylphenol-9-EO, the upper phase started to become milky and increased in volume. When 1 ml of this cosurfactant was

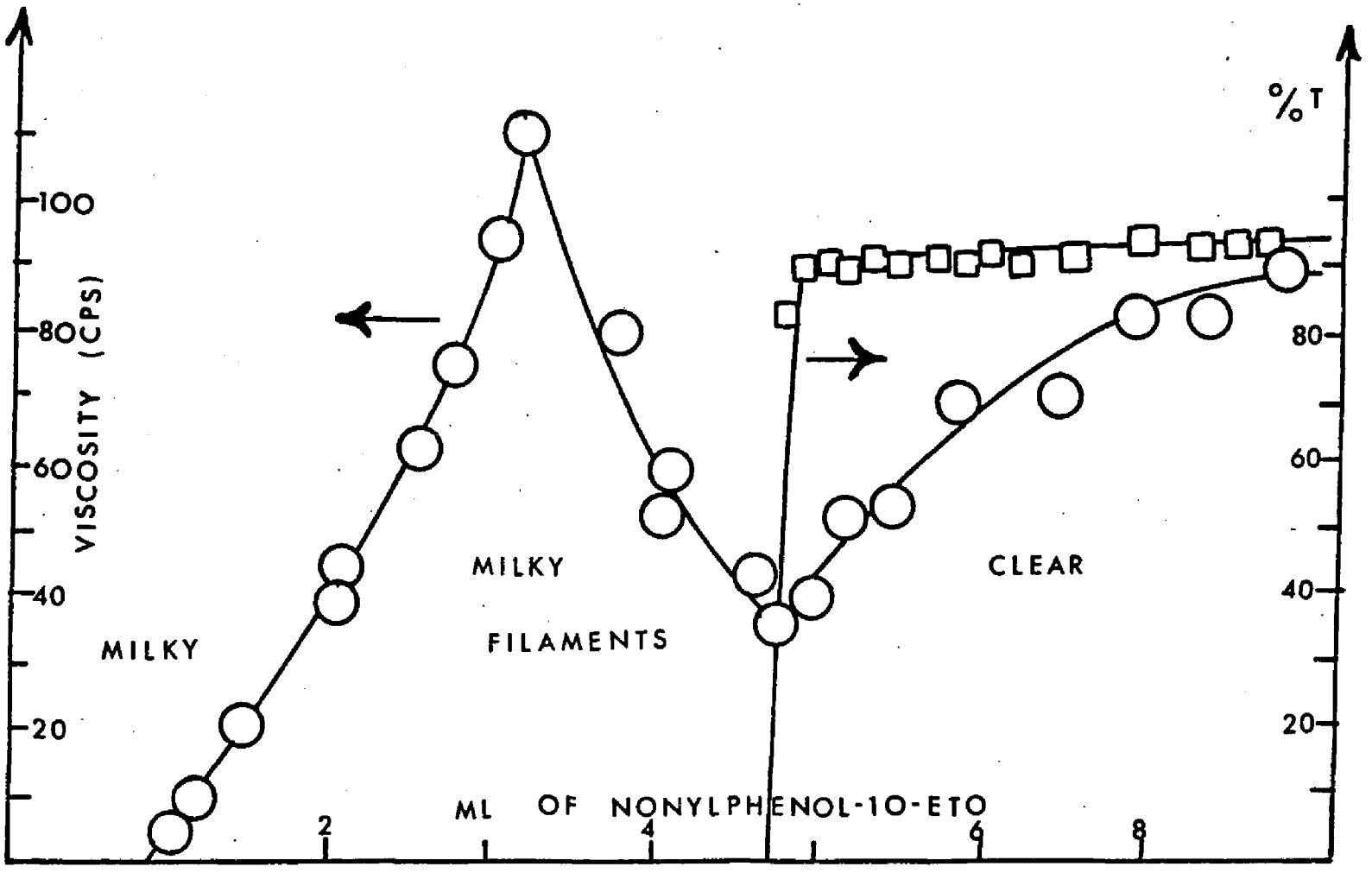

FIGURE 2.2 Change in viscosity and percent transmittance for 2ml n-decane / 0.5ml nonylphenol-1.5-EO + 0.5ml nonylphenol-4-EO / 35ml water and titrated with nonylphenol-10-EO at 30°C.

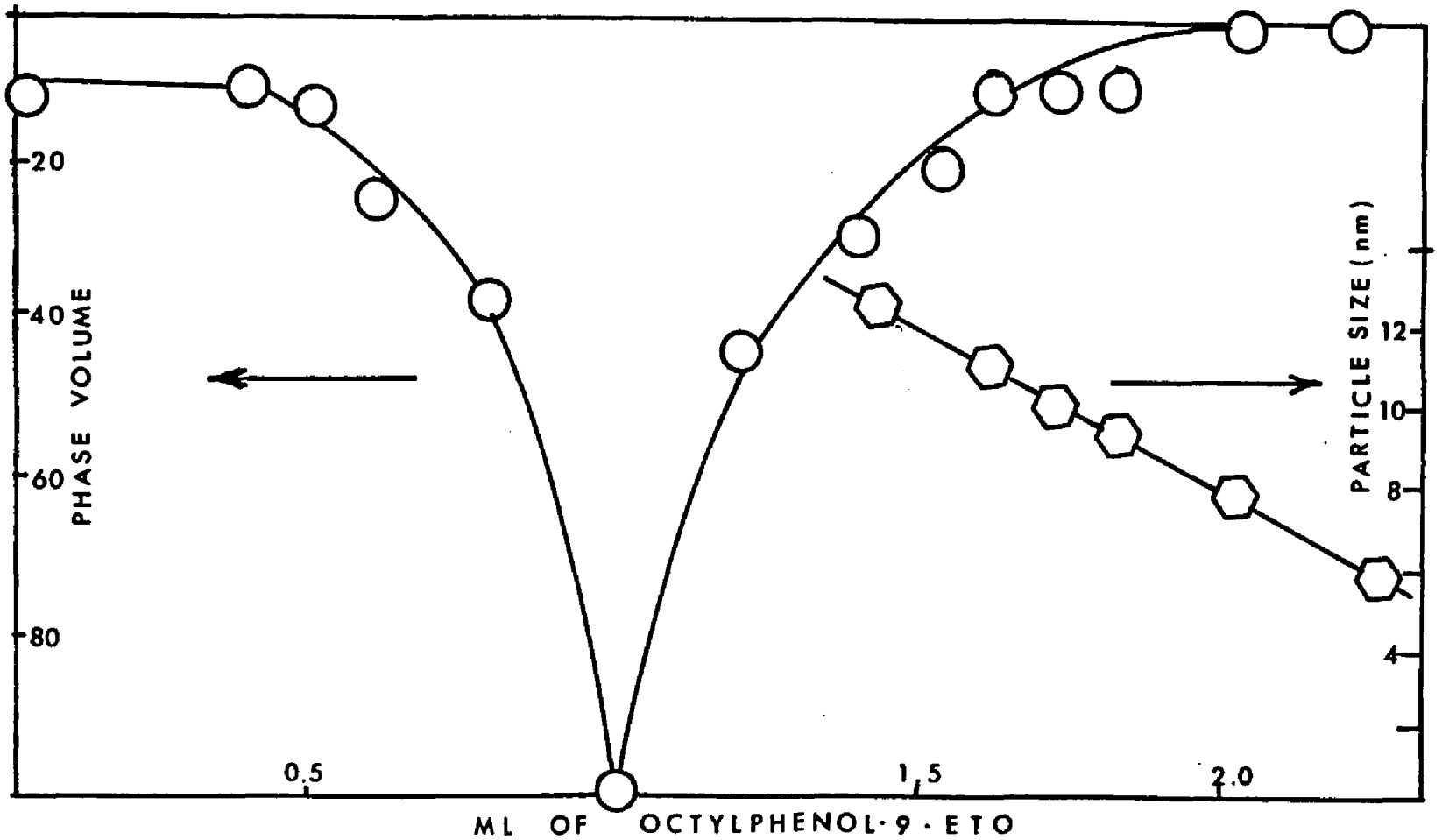

FIGURE 2.3 Phase volume change and particle size determination for 2ml n-octane / 0.5ml nonylphenol-1.5-EO + 0.5ml nonylphenol-4-EO / 30ml water and titrated with nonylphenol-10-EO at 22°C.

added, a one phase system was obtained. Addiion of still more cosurfactant caused the upper phase to start to decrease in volume as the lower phase began to clear (i.e., resolution into a microemulsion). The particle size of the lower phase region for each system was determined. It was found that the particle size decreased as the concentration of octylphenol-9-EO was increased.

2.4. DISCUSSION

2.4.1. MICROEMULSION FORMATION

Rosano et al. (4) have shown that the formation of transparent systems is affected by many factors, including 1) the type and composition of the surfactant and cosurfactant, 2) the dispersed phase volume, and 3) the structure of the oil. For a system prepared with 2.0×10^{-3} moles stearic acid, 2.0 ml of oil and 16 ml of 0.375 N KOH, it was found that out of fifty-two alcohols, only five produced transparent o/w systems (transmittance $> 79\%$). These results illustrate that only specific component combinations can produce microemulsions. As seen in Table 2.2, emulsions prepared with various long chain sodium sulfates, saline and oil, only specific combinations will produce transparent systems when titrated with a long chain dimethlyamine oxide as a cosurfactant.

For the six systems in Tables 2.1, investigated, it was found that the free energy values are all negative, indicating that the transformation of an emulsion into a microemulsion is a spontaneous process. However, the driving force for these processes is small which may explain why the method of preparation sometimes affects their formation. Since the free energy values are small, the correct order of preparation probably lowers the activation energy barriers these systems must overcome during their formation. Experimentally, the first consideration in the preparation of these transparent systems seems to be that

enough primary surfactant has to be present to cover the interfacial area and that the primary emulsion be as finely dispersed as possible. The method of preparation used must produce the best kinetic conditions favorable for the dispersion of the dispersed phase into a microemulsion (5).

Microemulsion formation involves : 1) a large increase in the interfacial area (for example, it was determined based on geometric considerations that a droplet of radius 120 nm will disperse into 1728 microdroplets of radius 10 nm, a 12-fold increase in the interfacial area), and 2) the formation of a mixed surfactant / cosurfactant film at the oil / water interface responsible for a very low transitory interfacial tension. It is reasonable to assume that droplet dispersion would increase the total entropy of the system while the formation of a mixed surfactant / cosurfactant film at the droplet interface would have a negative effect on the systems total entropy. For the systems investigated, the entropy values were found to be positive with one exception (SYSTEM 3). In view of the results obtained, it is concluded that microemulsions are thermodynamically stable systems. The occasional path-dependent properties sometimes observed can thus be explained in terms of the energies the particular system must overcome during formation.

During the transformation of an initial coarse emulsion into a microemulsion, under dynamic conditions, changes in the system viscosity seem to be a basic characteristic leading to microemulsion formation. This effect is observed in particular for systems prepared with both nonionic surfactants and cosurfactants. Figure 2.2 illustrates the change in viscosity and percent transmittance for a system prepared according to SYSTEM 3 and titrated to clarity with nonylphenol-10-EO. Initially, a coarse milky emulsion of low viscosity is formed. By adding cosurfactant, the viscosity increases and reaches a maximum value (15). Within this region the system remains milky

and filament structures are observed throughout. By adding more cosurfactant, the viscosity decreases to a minimum value, at which point the system spontaneously clears (95% transmittance). It is interesting to note that once the system becomes transparent, further addition of cosurfactant does not decrease the transmittance. Rosano et al. (4) have shown that the percent transmittance of microemulsions prepared with stearic acid / n-hexadecane / 0.375 N KOH titrated to clarity with 4-methylcyclohexanol, decreases once the capacity for cosurfactant of the aqueous phase and the interface is exceeded. Since both sites are saturated, the excess cosurfactant penetrates the interfacial film and dissolves in the oil phase. For o/w systems this means an increase in droplet size and a concomitant decrease in transmittance. For nonionic surfactant systems (SYSTEMS 1, 2 and 3), once maximum transparency is reached, the excess cosurfactant increases the system bulk viscosity probably because of further cosurfactant adsorption on the droplet surfaces and/or formation of micelles in the bulk phase.

Emulsions made of 1.95% sodium dodecylsulfate / 3.75% 1- butanol / 46.3% toluene and varying weight percentages of a stock 48% sodium chloride solution were prepared (6). Below 4.7% sodium chloride, a 2-phase system was formed with an upper clear oil phase and a lower milky aqueous phase, displaying oil-in-water emulsion characteristics. Above 6.4% sodium chloride, a water-in-oil emulsion dispersion started to form, indicated by the milky upper oil phase and clear lower aqueous phase. In the region between 4.7 and 6.4% sodium chloride, a 3-phase system with a clear upper oil phase, a clear lower aqueous phase and a middle surfactant phase was obtained. Within the three-phase region, filament structures were observed if the system was gently shaken. The formation of the filament structures seems to be due to the ultra low values of the γ_i within this region. When the overall change in the inter-

facial tension of the upper and lower phases was plotted against sodium chloride concentration, it was found that the value of γ_i between the o/w microemulsion and the excess oil phase decreased simultaneously as γ_i between the microemulsion and the excess water phase increased. The value of the interfacial tension was at a minimum within the 3-phase region (23, 24). It seems that achieving low γ_i values is a necessary step in microemulsion formation. Once the value is sufficiently low ($< 10^{-3}$ dynes/cm) spontaneous dispersion occurs with little or no mechanical work required. However, the resolution of the system into stable microdroplets seems to be accompanied by an increase in γ_i to a small positive value. It also is worth noting that phase separation rates also varied as a function of salt concentration. Fastest separation was reported for the system in which the middle phase contained equal volumes of oil and water. It has been suggested by Robbins (7) that spontaneous microemulsification occurs in the middle of the three-phase region and as a result, the middle phase is transparent or transluscent.

2.4.2. THE ROLE OF THE COSURFACTANT

Addition of a cosurfactant seems to be a basic requirement to microemulsion formation. During the preparation of microemulsions under dynamic conditions, (the titration method) two basic questions should be addressed : 1) what is the role of the cosurfactant in microemulsion formation and 2) are these systems undergoing phase volume changes as a function of increasing the cosurfactant concentration ? Recently, spectroscopic evidence (22) has indicated that the role of the cosurfactant is to reduce the rigidity of the interfacial film, allowing for the transition from a well-organized lamellar phase toward an isotropic microemulsion. For microemulsions prepared with stearic acid / n-hexadecane / 0.375 M KOH and 1-pentanol, it is evident that the ratio of the number of moles of 1-pentanol to stearic acid at the interface varies from 3.6:1

to 6:1 as shown in Table 2.3 (30). From film penetration monolayer experiments it is well known that the presence of alcohols in the film produces an expanded monolayer (31). The presence of alcohols at the interface results in a liquefaction of the interface while reducing the interfacial rigidity. In many cases investigated, transitions from emulsion to microemulsion are also accompanied by phase changes as the system resolves itself into microdroplets. Fig. 2.3 illustrates the phase volume behavior for SYSTEM 2 as the concentration of octylphenol-10-EO is increased. Upon the addition of octylphenol-10-EO, the upper phase starts to become milky and increases in volume. Once a total of 1 ml is added, a one-phase system is obtained. Within this region the system is milky, birefringent, and filament structures are prevalent throughout the system. As the cosurfactant concentration is further increased, the upper phase volume starts to decrease simultaneously as the lower phase begins to clear. When just the right amount of cosurfactant is added, a 1-phase transparent o/w system is obtained.

The results obtained indicate that as the cosurfactant concentration is increased, a phase inversion process is a necessary requirement for the resolution of an emulsion prepared with nonionic surfactants into a microemulsion. Upon the addition of a cosurfactant to an initial emulsion, the droplets in the lower phase start to elongate and reach a maximum length (formation of filament-like structures) at the point of phase inversion. Using electron microscopy, the lower phase region approaching the point of phase inversion was investigated. This technique allows the structure of the lower phase to be determined as a function of cosurfactant concentration.

For the staining of fats or proteins in biological tissues, osmic tetroxide is used among other heavy metal oxide complexes as a staining agent (29). The tissue is then bedded in a polymer such as methacrylate or alkyl esters of this

compound, which does not change volume appreciably on polymerization. The entire system is then microtomed into sections 300-900 A. in thickness and the structure is investigated by electron microscopy. It was considered that this technique could be used to investigate o/w microemulsion systems. It was found that o/w microemulsions could be successfully stained if the oil or surfactant contained a number of double bonds in conjugated form, which were reactive towards the metal oxides. For the microemulsions investigated by electron microscopy, both the surfactant and cosurfactant contain a ring with conjugated double bonds available for complexation with the metal oxides used for staining. The bonds of the surfactant and cosurfactant can therefore interact with uranyl acetate structuring the surfactant and cosurfactant molecules intermolecularly in a type of uranyl acetate polymer. Fig. 2.4 a, b, c, shows three photo-micrographs taken of the lower phase of Fig. 2.3 as the concentration of octylphenol-10-EO was increased from 0.6 to 0.9cc. Fig. 2.4a shows a picture of the lower phase structure for a system containing 0.6cc of octylphenol-10-EO. It is observed that throughout this phase, small structures are present. As the concentration of octylphenol-10-EO is increased to 0.8cc, the droplet size increases and jagged filament structures are formed, as seen in Fig. 2.4b. The increase in droplet size is due to the uptake of oil by the water phase since the system is becoming more hydrophilic upon increasing the cosurfactant concentration. When the structure of the lower phase is examined for 0.9cc of octylphenol-10-EO, a randomized filament network is observed. Distinct filament structures are no longer visible, giving rise to a bicontinuous structure in the region of phase inversion. At this point it should be mentioned that if equal volumes of oil and water are used, this phase inversion would actually correspond to a three-phase system. Beyond the phase inversion point, the particle size of the lower phase was found to decrease

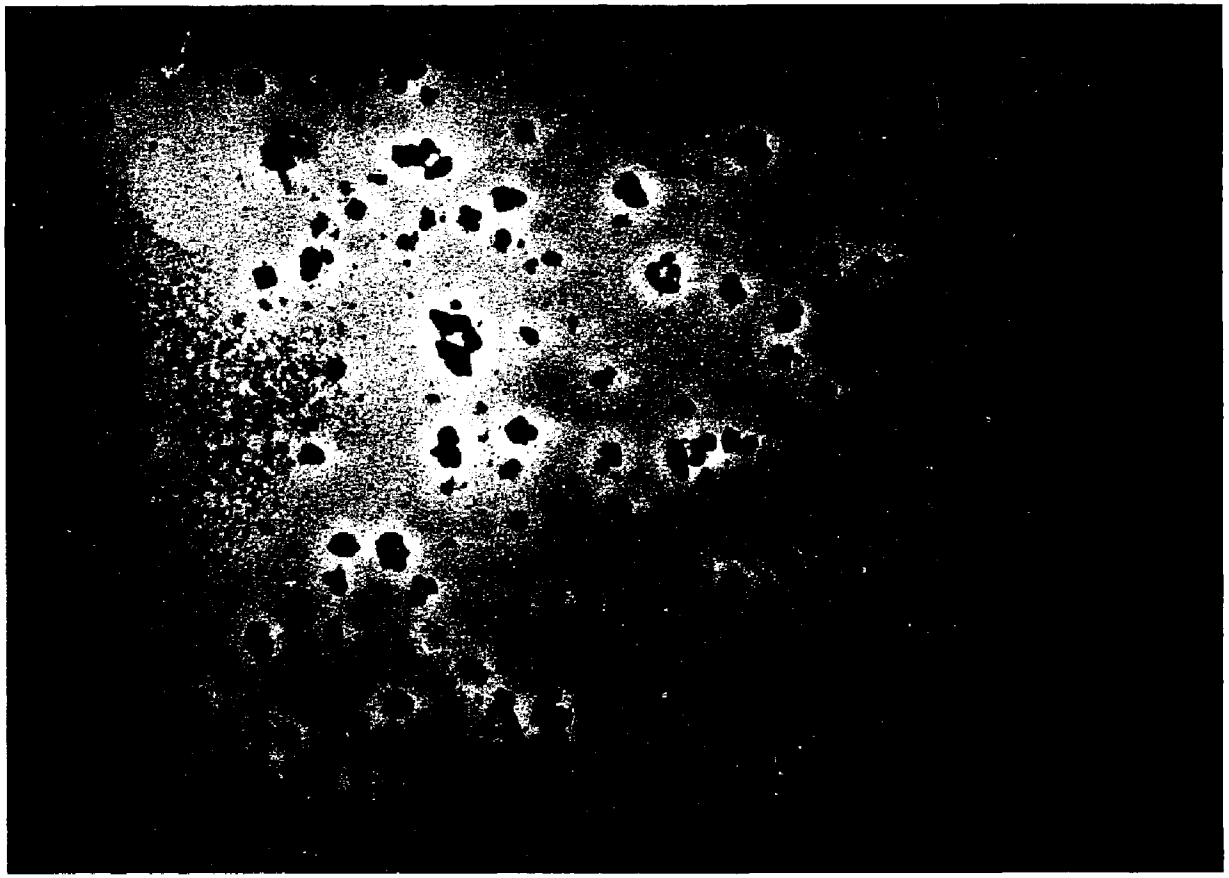

FIGURE 2.4a Photomicrograph of lower aqueous phase for a system containing 0.5 cc octylphenol-9-EO.

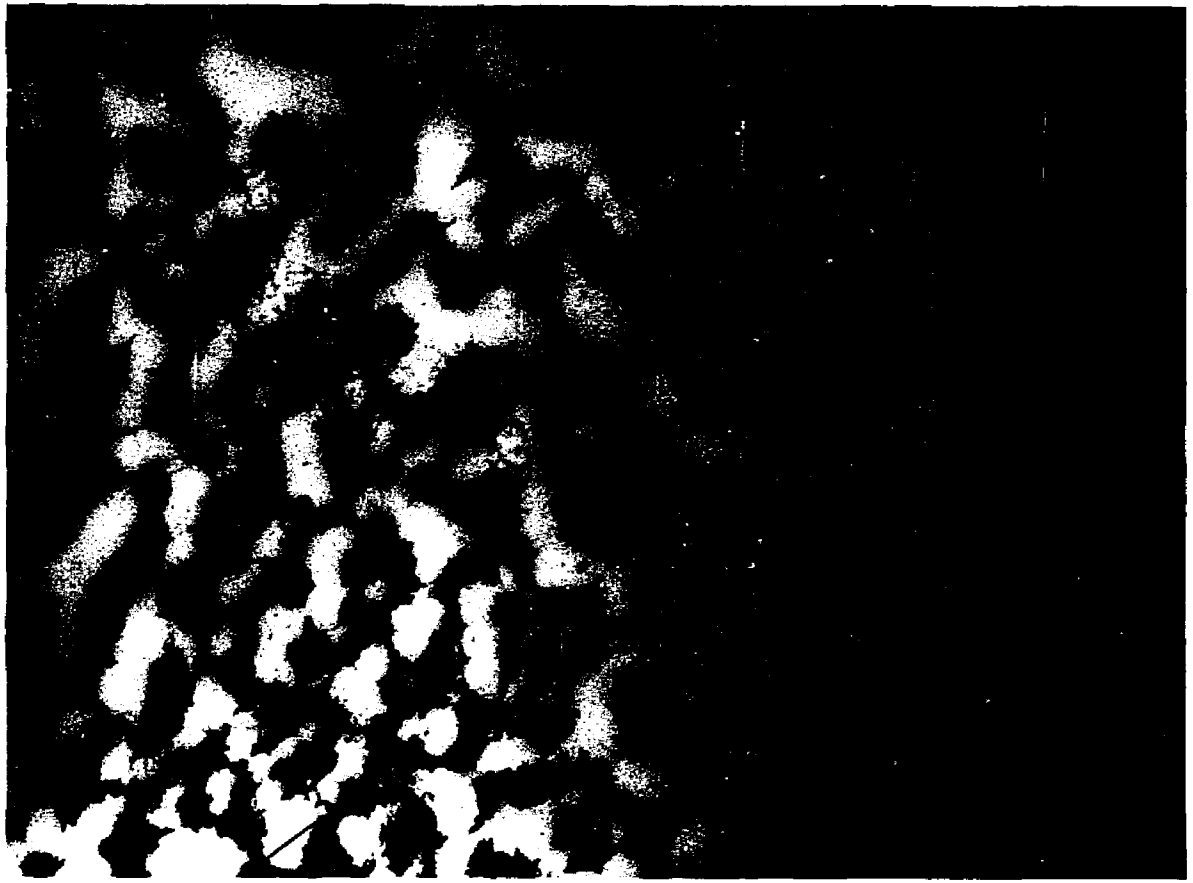

FIGURE 2.4b Photomicrograph of system containing 0.8 cc octylphenol-9-EO.

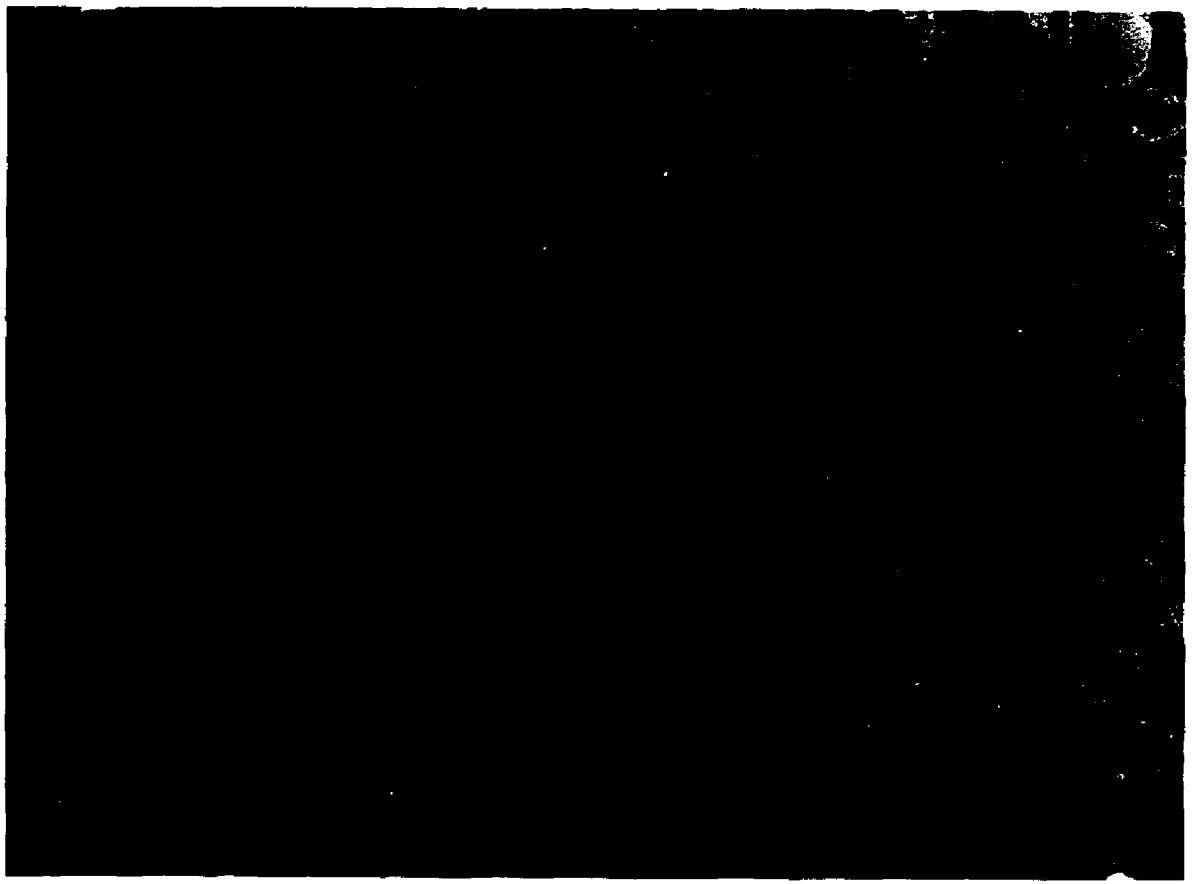

FIGURE 2.4c Photomicrograph of system containing for 0.9 cc octylphenol-9-EO.

as shown in Fig. 2.3, supporting the idea that as the cosurfactant concentration is increased, filament structures start to break into smaller fragments until finally microdroplets are formed (17,22). This effect was observed to be a fundamental characteristic of systems prepared with nonionic surfactants. The particle size distribution data plotted in Fig. 2.3 is shown in Fig. 2.5a, b, c, d, and e. Figure 2.5b is an example of the correlation function used to determine the particle size of Fig. 2.4a.

2.4.3. MICROEMULSIONS AND THE SHINODA PHASE DIAGRAM

The phase diagram shown in Fig. 2.3 represents a special case of a general phase diagram suggested by Shinoda (20) illustrating the change of solution behavior of a surfactant with the hydrophilic-lipophilic balance (HLB). For a system prepared with equal volumes of oil and water plus a lipophilic surfactant (or surfactant mixture), Fig. 2.6 shows that at equilibrium a 2-phase system is obtained with a clear lower aqueous phase and a milky upper oil phase. When the system becomes more hydrophilic, a three-phase system is formed, with upper and lower phases clear and a middle surfactant phase. On further increasing the hydrophilicity, again a 2-phase system is formed, with a milky lower aqueous phase and clear upper oil phase. The same basic trend in solution behavior is observed for nonionic surfactants if the temperature is increased, resulting in a decrease in the HLB value. For ionic surfactants, if instead of increasing the temperature, the salt concentration is increased (decreasing the HLB) the solution behavior will also show 2-to 3-to 2-phase behavior as previously mentioned (6, 24).

This schematic diagram can be related to Fig. 2.3. In the initial preparation of our o/w emulsion systems, only 2 ml of oil was used with a larger volume of water. Therefore, half of the diagram in Fig. 2.6 should be considered (represented by the dotted line). For a primary emulsion prepared

RESULTS

SAMPLE ID = 0093
TEMPERATURE = 20 DEG C
VISCOSITY = .0195 POISE
REFRACTIVE INDEX= 1.337

MEAN DIAMETER= 13.4 NM
95% LIMITS = 13.3 TO 13.5 NM

STANDARD DEVIATION = 3.0 NM
GOODNESS OF FIT = 1.3
DIFFUSION COEFFICIENT = 1.64 E-7 CM**2/SEC

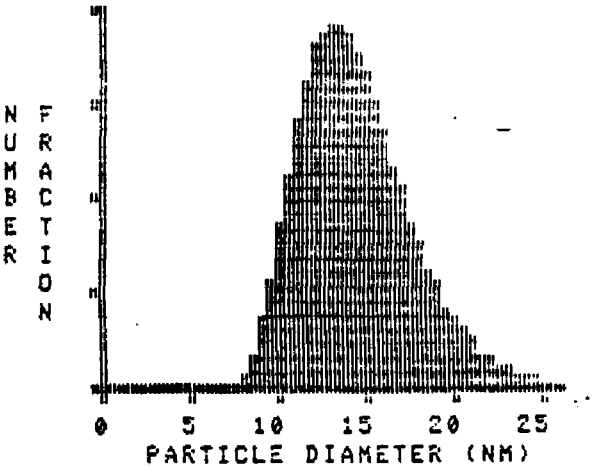

PARTICLE DIAMETER
NUMERIC DISTRIBUTION

10% OF SAMPLE) 17.3 NM

25% OF SAMPLE) 15.1 NM

50% OF SAMPLE) 13.1 NM

75% OF SAMPLE) 11.6 NM

90% OF SAMPLE) 10.7 NM

RAW DATA

SAMPLE ID = 0093

A = 1.49 E+1
B = -1.23 E-1
C = 2.57 E-4
MU2 = 2.24 E+6
GAMMA = 5.78 E+3
MU2/GAMMA SQ= 6.71 E-2
32 CHANNELS
SAMPLE TIME = 10.7 MICRO-SEC
PRE-SCALE = 8
RUN TIME = 20 SECONDS
END OF RUN = 1844 SECONDS

FIGURE 2.5a **Particle size distribution data of the lower phase for a system prepared with 2 cc n-octane / 0.5 cc nonylphenol-1.5-EO + 0.5 cc nonylphenol-4-EO / 30 cc water and 1.2 cc of octylphenol-9-EO.**

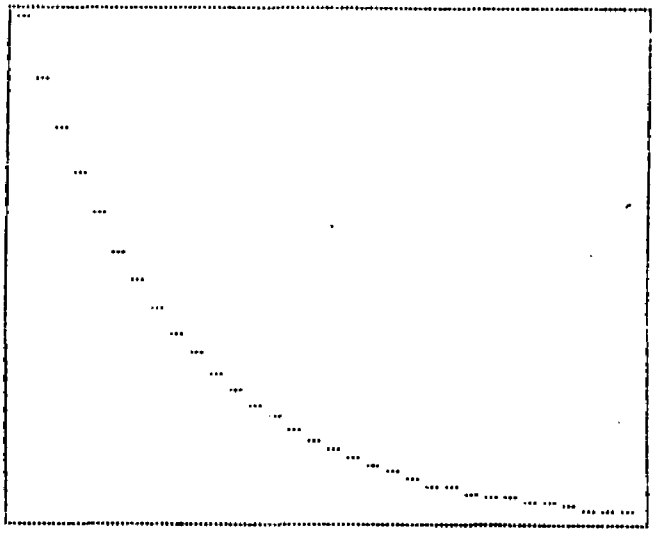

1	23626540	23315590	23047441	22808904	22600094
6	22413606	22252651	22107946	21979984	21867164
11	21768084	21679864	21602479	21532560	21470622
16	21416497	21369004	21324465	21286200	21251918
21	21221387	21193261	21171223	21150446	21132180
26	21115685	21101596	21089291	21078822	21069191
31	21060401	21052415	20975115	20974421	20974134
36	20972218	20972008	20972961	20973922	20975318
41	1869159	6222732			

FIGURE 2.5b Typical correlation function used to determine the particle size.

RESULTS

SAMPLE ID = 0095
TEMPERATURE = 20 DEG C
VISCOSITY = .0164 POISE
REFRACTIVE INDEX= 1.338

MEAN DIAMETER= 11.4 NM
95% LIMITS = 11.3 TO 11.4 NM

STANDARD DEVIATION = 2.1 NM
GOODNESS OF FIT = 1.1
DIFFUSION COEFFICIENT = 2.29 E-7 CM**2/SEC

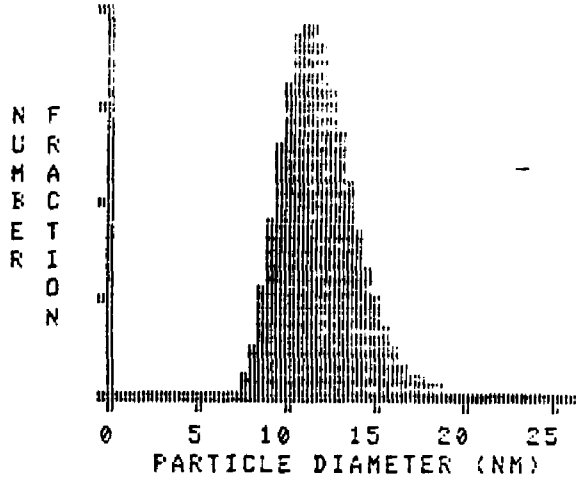

PARTICLE DIAMETER
NUMERIC DISTRIBUTION

10% OF SAMPLE) 14.0 NM
25% OF SAMPLE) 12.6 NM
50% OF SAMPLE) 11.2 NM
75% OF SAMPLE) 10.2 NM
90% OF SAMPLE) 9.6 NM

RAW DATA

SAMPLE ID = 0095

A = 1.50 E+1
B = -1.29 E-1
C = 1.76 E-4
MU2 = 2.75 E+6
GAMMA = 8.10 E+3
MU2/GAMMA SQ= 4.19 E-2
32 CHANNELS
SAMPLE TIME = 8.0 MICRO-SEC
PRE-SCALE = 4
RUN TIME = 20 SECONDS
END OF RUN = 2545 SECONDS

FIGURE 2.5c Particle size distribution data for 1.4 cc octylphenol-9-EO.

RESULTS TEMP

SAMPLE ID = 0031
TEMPERATURE = 20 DEG C
VISCOSITY = .0153 POISE
REFRACTIVE INDEX= 1.341

MEAN DIAMETER= 8.2 NM
95% LIMITS = 8.2 TO 8.3 NM

STANDARD DEVIATION = 2.1 NM
GOODNESS OF FIT = 1.0
DIFFUSION COEFFICIENT = 3.39 E-7 CM**2/SEC

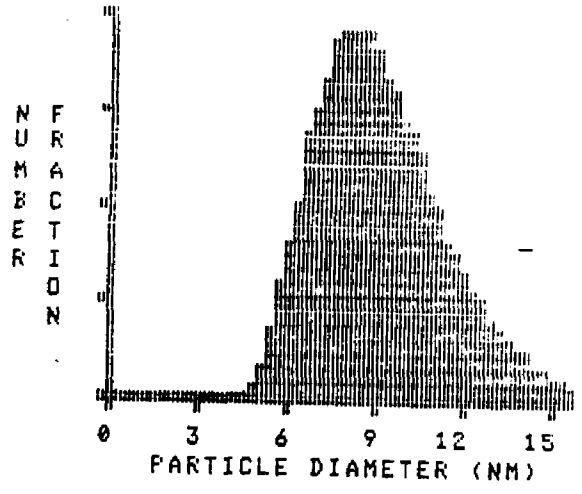

TEMP

PARTICLE DIAMETER
NUMERIC DISTRIBUTION

10% OF SAMPLE > 11.0 NM
25% OF SAMPLE > 9.4 NM
50% OF SAMPLE > 8.0 NM
75% OF SAMPLE > 6.9 NM
90% OF SAMPLE > 6.3 NM

RAW DATA TEMP

SAMPLE ID = 0031

A = 1.54 E+1
B = -1.22 E-1
C = 3.55 E-4
MU2 = 1.36 E+7
GAMMA = 1.20 E+4
MU2/GAMMA SQ= 9.45 E-2
32 CHANNELS
SAMPLE TIME = 5.1 MICRO-SEC
PRE-SCALE = 1
RUN TIME = 20 SECONDS
END OF RUN = 475 SECONDS

FIGURE 2.5d Particle size distribution data for 2.0 cc octylphenol-9-EO.

RESULTS

SAMPLE ID = 0025
TEMPERATURE = 20 DEG C
VISCOSITY = .0175 POISE
REFRACTIVE INDEX= 1.342

MEAN DIAMETER= 7.6 NM
95% LIMITS = 7.6 TO 7.7 NM

STANDARD DEVIATION = 2.0 NM
GOODNESS OF FIT = 1.3
DIFFUSION COEFFICIENT = 3.19 E-7 CM**2/SEC

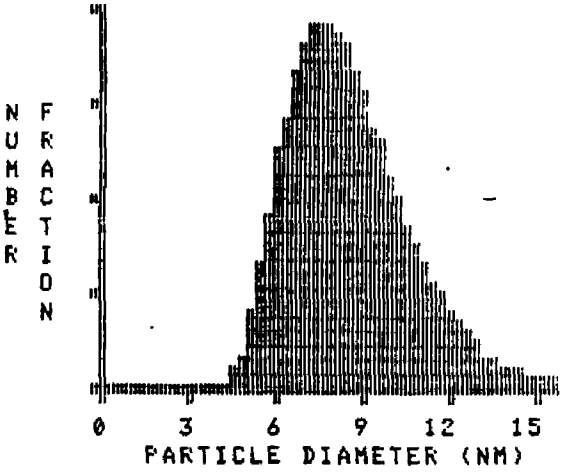

PARTICLE DIAMETER
NUMERIC DISTRIBUTION

10% OF SAMPLE) 10.3 NM
25% OF SAMPLE) 8.8 NM
50% OF SAMPLE) 7.4 NM
75% OF SAMPLE) 6.4 NM
90% OF SAMPLE) 5.8 NM

RAW DATA

SAMPLE ID = 0025

A = 1.54 E+1
B = -1.22 E-1
C = 3.86 E-4
MU2 = 1.32 E+7
GAMMA = 1.13 E+4
MU2/GAMMA SQ= 1.02 E-1
32 CHANNELS
SAMPLE TIME = 5.4 MICRO-SEC
PRE-SCALE = 1
RUN TIME = 20 SECONDS
END OF RUN = 1083 SECONDS

FIGURE 2.5e Particle size distribution data for 2.5 cc octylphenol-9-EO.

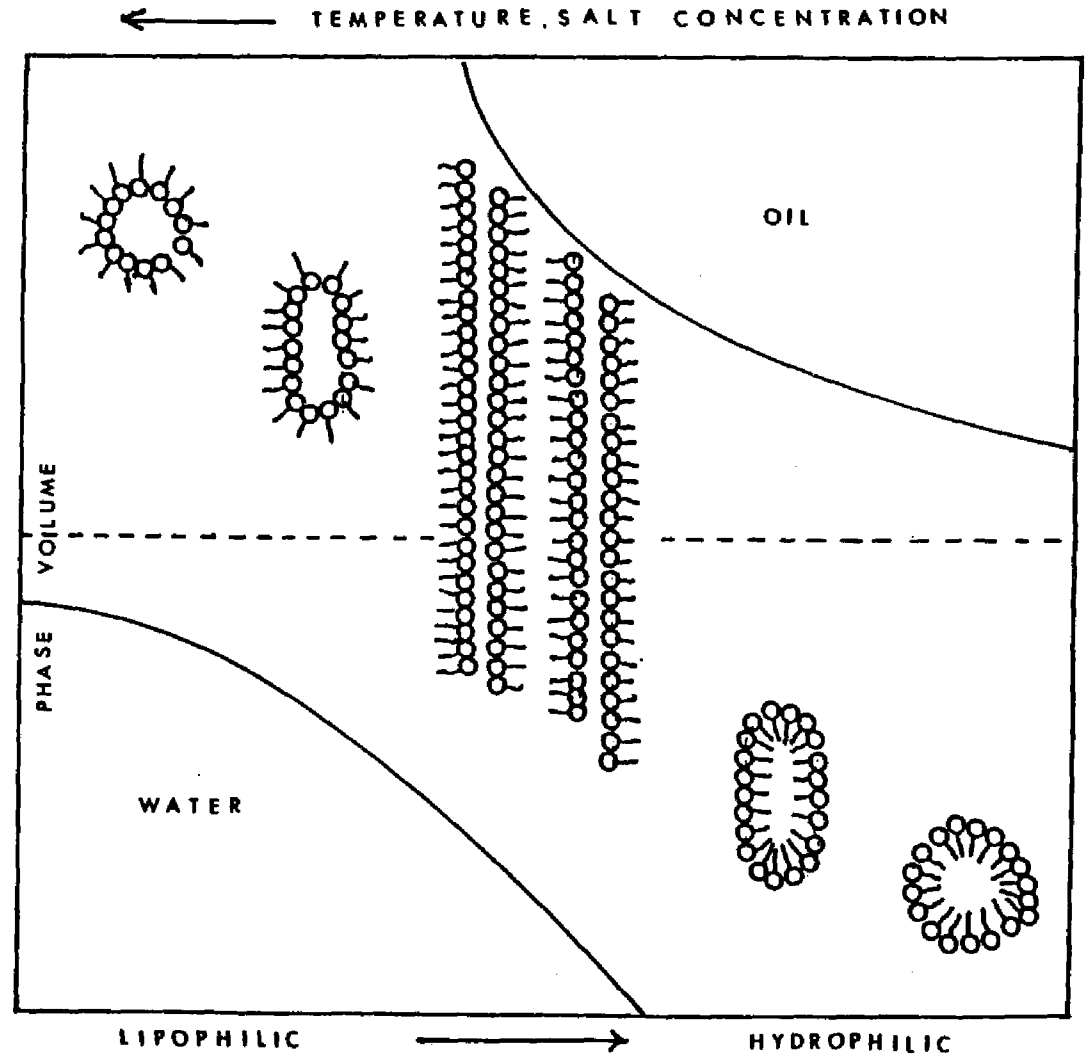

FIGURE 2.6 Schematic illustration of the change in solution behavior of surfactant with hydrophilic-lipophilic balance (HLB) in a water/oil/surfactant system.

with a small o/w volume ratio, and a lipophilic surfactant (or surfactant mixture), upon titrating the system with a hydrophilic cosurfactant the HLB value increases. Increasing the HLB value results in the upper phase volume increasing, until a 1 -phase system is formed (filament structures are observed). Upon further increasing the systems HLB, a 1-phase transparent o/w microemulsion is obtained. Therefore, it is concluded that microemulsions of the o/w type correspond to systems in the lower right side of Fig. 2.6 while microemulsions of the w/o type correspond to systems in the upper left region. It is concluded that a more appropriate term to describe transparent o/w systems would be to consider them as swollen micellar solutions. In the case of transparent w/o systems, they should be described as inverted micellar solutions as is illustrated in Fig. 2.6.

Using Fourier transform proton and carbon-13-pulsed-gradient-spin-echo (PGSE) NMR techniques, Lindman, Stilbs, and Moseley (9) have investigated seven microemulsion systems by determining the multicomponent self-diffusion coefficient for systems prepared with oil / water and surfactant and a cosurfactant of either short or long chain alcohols. They reported that, for the ionic surfactant / short chain alcohol / hydrocarbon / water-type system, 1) no distinct separation into hydrophobic and hydrophilic domains was observed ; 2) these systems show no extended aggregates ; and 3) the internal interfaces were determined to be flexible and highly disorganized, an idea already suggested by de Meglio (16). Microemulsions formed with nonionic surfactants of the polyethyleneoxide type, hydrocarbon and water, are probably similar in structure to those formed with short-chain alcohols. Microemulsions prepared with long-chain alcohols are somewhat different in structure and form distinct droplets of water in a hydrophobic medium. However, in some cases a bicontinuous structure may also occur. In a review article, de Gennes and Taupin

(14) have also concluded that a flexible interface is an absolute requirement to maintain some microemulsion-type systems, an idea already advanced by Schulman (25). Kahlweit (18) et al. have studied the phase behavior of ternary systems (H_2O / oil / nonionic surfactant) and quaternary systems (H_2O / oil-nonionic surfactant / electrolyte). In the case of ternary systems the temperature was varied, while for quaternary systems the salt concentration was varied. Their results verified that maximum mutual solubility between oils and surfactants may be explained in terms of "simple" phase behavior with respect to the existence of a tricritical point in ternary systems. Chatenay et al. (17) have found that for polyphasic systems away from the three-phase domain, the interaction between the droplets is hard sphere-like, while in the middle of the three-phase region, the structure is bicontinuous as evidenced from conductivity measurements. These studies therefore indicate that not all interfaces fall into the same classical picture of well-organized oil or water droplets with distinct boundaries. What is seen is that internal interfaces have either a quite limited spatial extension or are very dynamic and flexible in nature, breaking up and reforming at a very high rate, or both. These data suggest the possibility of two distinct types of microemulsion systems depending on the interactions associated with the dispersed phase droplets.

Other structural models have been proposed to describe the structure and formation of microemulsions. Taupin and co-workers (10) have presented a model of hard oil and water globules with a relatively sharp transition between them ; Scriven (11) one of a complex periodic three dimensional networks of both oil and water continuity ; and Talman and Prager (12), one of hard randomly arranged polyhedra ; while Friberg (13) proposed a random structure with varying curvatures. Robbins (19) has shown that for a w/o microemulsion system, the activity of the water in the droplet core must be reduced for

the water to flow into the droplets. This effect was readily verified by water vapor pressure measurements. Based on vapor pressure analysis of o/w microemulsions, two distinct regions of transparency seem to exist (26). The droplet structures are that of encapsulated noninteracting droplets for low volumes of hydrocarbon, while a dynamic equilibrium between the breaking and reformation of droplet interfaces has been found to exist for higher volumes. Similar behavior has also been suggested by Weatherford (27) for w/o systems.

In the following chapter, the vapor pressure of o/w microemulsion systems will be investigated as a function of increasing the dispersed phase volume. Vapor pressure analysis will be used to investigate the possibility of droplet interactions in o/w microemulsion systems as the dispersed phase volume is increased.

2.5. REFERENCES

1 Tadros, Th. F., Structure / Performance Relationships in Surfactants, M.J. Rosen, Ed., 253rd ACS Symposium Series ACS, Washington, D.C. (1984) p.154. and Interface Sci., Vol. II, edited by M. Kerker, 245, Academic Press Inc. (1976).

2 Gerbacia, W. E., Rosano, H. L., J. Coll. Interface Sci. 44, 242, (1973).

3 Rosano, H. L., J. Soc. Cosmetic Chem., 25, 609, (1974).

4 Rosano H. L., Lan, T., Weiss, A., Gerbacia, W. E. F. and Whittam, J. H. J. Coll. Interface Sci. 72, 233, (1979).

5 Rosano, H. L., U.S. Patent 4,146,499 March 27, 1979.

6 Rosano, H. L., Jon, D., Whitttam, J. H., J. Am. Oil Chem. Soc., 59, 360, (1982).

7 Robbins, M., Private Communication.

8 Shinoda, K., Prog. Coll. & Poly. Sci., 68, 1, (1983).

9 Lindman, B., Stilbs, P., and Moseley, M., J. Coll. Interface Sci. 83, 569, (1981).

10 Lagues, M ., Ober,R., and Taupin, C, J. Phys. Lett. 39, 487, (1978).

11 Scriven, L. E., in "Micellization, Solubilization and Microemulsions", K.L. Mittal, Ed., Vol. 2, 877. Plenum Press , New York, (1977).

12 Talmon, Y., and Prager, S., J. Chem. Phys. 69, 517, (1978).

13 Friberg, S., Lapezynska, I., and Gillberg, G., J. Coll. Interface Sci. 56, 19, (1976).

14 de Gennes, P.G., Taupin, C., J. Chem. Phys. 86, 2294, (1982).

15 Rosano, H. L. Weiss, A., Gerbacia, W. E. in Proceedings of the VIIth. International Congress on Surface Active Substances, Moscow. Sept. 12-16,

1976, Vol. 1, 453 (1977).

16 di Meglio, J.M., Dvolaitzky, M., Ober, R., Taupin, C., J. Phys. Lett. 44, L229, (1983).

17 Chatenay, D., Guering, P., Urback, W., Cazabet, A. M., Langevin, P., Meuiner, J., Leger, L., Lindman, B., Paper submitted for the proceedings of the 5th International Conference on Surface and Colloid Science (Potsdam, June 25-28,1985).

18 Kahlweit, M.,Lessner, E, and Strey, R. J. Phys. Chem. 87, 5032, (1983).

19 Robbins, M. L., Preprints, 48th National Colloid Symposium, 174, (1974).

20 Shinoda, K., Kunieda, H., Arai, T, and Saijo, H., J. Phys. Chem. 88, 5126, (1984).

21 di Meglio, J.M., Paz, L., Dvolaitzky, M., and Taupin, C., J.Phys. Chem. 88, 6036, (1984).

22 di Meglio, J.M., Dvolaitzky, M., and Taupin, C. Paper submitted for the proceedings of the 5th International Conference on Surface and Colloid Science (Potsdam, June 25-28,1985).

23 Bellocq, A. M., Bourbon, D., and Lemmcean, B., J. Coll. Interface Sci. 79, 419, (1981).

24 Healy, R. N., Reed, R. L., and Stenmark, D. G. S.P.E. J. 16, 147, (1976).

25 Stoeckenius, W., Schulman, J.H., Prince, L.M., Kolloid Z. 169, 170, (1960).

26 Cavallo, J. L., Rosano, H.L., Submitted for publication in the J. Phys. Chem.

27 Weatherford, W. D. J. Dispersion Sci. Technol. 6, 467, (1985).

28 Hoar, T. P., Schulman, J. H., Nature (London), 152, 102, (1943).

29 Stoeckenius, W., Schulman, J.H., and Prince, L. M., Kolliod Z. 169, 170, (1960).

30 Rosano, H.L., Lyons, G.B., J. Phys. Chem. 89, 363, (1985).

31 Schulman, J.H., McRoberts, M., Trans. Faraday Soc. 42, 165, (1946).

CHAPTER 3

VAPOR PRESSURE MEASUREMENTS OF O/W MICROEMULSION SYSTEMS

3.1. INTRODUCTION

In the previous chapter the mechanism of microemulsion formation was demonstrated. It was shown that emulsions could be spontaneously titrated to clarity with an appropriate cosurfactant. Individual systems were prepared containing a constant amount of n-octane, nonylphenol-1.5 + 4-EO (a lipophilic surfactant mixture), water and increasing amounts of nonylphenol-10-EO (a hydrophilic cosurfactant). These systems were allowed to equilibrate for 60 days at 22°C during which time phase separation occurred (1). Upon the addition of cosurfactant, a 2-phase system is formed (milky upper oil phase and a clear lower aqueous phase). Increasing the cosurfactant concentration resulted in the upper phase volume increasing and the formation of a lamellar phase containing filament-like structures. Upon further addition of cosurfactant, the volume of the upper phase starts to decrease resulting in the formation of a 1-phase transparent o/w microemulsion. Under dynamic conditions (i.e., when the emulsion is being titrated to clarity in a water-jacketed beaker), the phase volume changes described are never observed. While the system is being continuously stirred, what is observed is that an opaque emulsion becomes spontaneously clear (2). These results indicate that emulsions prepared with a lipophilic surfactant mixture can be transformed into microemulsions when titrated with a hydrophilic cosurfactant i.e., by changing the hydrophilic-lipophilic balance (HLB). In the case of w/o microemulsions,

the same type of behavior is observed if the initial emulsion is prepared with a hydrophilic surfactant and titrated with a lipophilic cosurfactant. These microemulsions were then related to a phase diagram proposed by Shinoda (3) which shows the surfactant behavior in a 1:1 oil-water mixture as a function of temperature, salt concentration and HLB. It was concluded that microemulsions of the o/w or w/o type correspond to specific regions of this diagram and that these systems become transparent as the lamellar phase filament structures become resolved into microparticles.

It is evident that only specific component combinations can produce a microemulsion. In addition, the components must be put together in just the right order. When this procedure is followed, thermodynamically stable microemulsions form spontaneously (2). Surfactant type, cosurfactant type and the nature of the oil phase are three interacting variables that determine the size of the dispersed phase particles when microemulsions are formed.

In order to determine the structure of the dispersed phase, the colligative properties of microemulsion systems have been investigated and various structural models have been proposed (4-9). For the dispersed phase Schulman (2) has suggested that the best description is one of droplets surrounded by a mixed surfactant film. However, recent evidence now suggests that a more dynamic situation seems to exist for microemulsion systems. Weatherford (14) has shown using vapor pressure analysis that for a w/o diesel fuel system prepared with a surfactant mixture of oleyldiethanolamide, diethanolamine and diethanolammoniumoleate, two regimes of differing phase behavior exist as the water content is varied. These results suggest a transition from an inverted micellar solution, at low water concentrations, to a microemulsion, at a higher water content. It was suggested that a dynamic equilibrium exists between the breaking and reforming of the droplets when the water content is high.

This transition has also been investigated by Eicke (20) for the AOT/isooctane/water system. Based on photon correlation spectroscopy, it was demonstrated that when the ratio of surfactant to cosurfactant is below 3.7, these systems behave as inverted micellar solutions. In this case the water core is highly structured within the aggregates by hydrogen bonds. For larger volumes of water, a well-defined water core is surrounded by a surfactant monolayer. These systems behave as either micro or macroemulsions depending on the volume of water. Droplet interactions have also been investigated by Cazabat (16) using electrical conductivity, electrically induced birefringence, and self-diffusion measurements on fluorescent probes. The systems investigated were ternary w/o microemulsions prepared with water / benzene / decyldimethyl ammonium chloride and quaternary w/o microemulsions containing sodium dodecyl sulfate (SDS) / toluene / water and 1-butanol or 1-pentanol. These results indicate that at low water concentrations, the dispersed phase is composed of identical spherical isolated droplets, while at higher concentrations, the structure of the dispersed phase depends on the interactions between the droplets, which are in some cases attractive, resulting in an overlap of droplet interfaces.

In this chapter the vapor pressures of five o/w microemulsion systems are investigated in order to develop a physical model applicable to our transparent systems. The existence of a vapor pressure and its increase with temperature are consequences of the Maxwell-Boltzmann energy distribution. Even at low temperatures a fraction of the molecules in a liquid have, because of the energy distribution, energies in excess of the cohesive energy of the liquid. This fraction increases rapidly with an increase in temperature. This implies that a liquid with a larger cohesive energy (a large molar heat of vaporization) will have a smaller vapor pressure than one with a small cohesive energy. The

systems investigated were prepared with a constant amount of water, sodium cetyl sulfate (SCS) or sodium dodecyl sulfate (SDS), dodecyldimethylamine oxide (DDAO) and various volumes of n-pentane, n-hexane, n-octane or n-decane. The results obtained indicate that depending on the volume of n-octane in the dispersed phase, two distinct microemulsion regions exist. For low volumes of n-octane the system was found to be composed of isolated noninteracting droplets, while for higher volumes, evidence of a merging dynamic system of overlapping droplet interfaces were found. It is hypothesized that since microemulsions consist of the stable dispersion of one phase (oil for o/w microemulsions) in a continuous phase, the vapor pressure behavior of these systems should be similar to those of regular colloidal solutions, whereby the vapor pressure of the system is less than that of the continuous phase. Based on the vapor pressure data, microemulsion droplet molecular weight, radius, heat of vaporization and activation energy values were determined.

Using the titration technique (1,10) the stoichiometry of SCS/DDAO at the droplet interface was determined in the two microemulsion regions by titrating o/w emulsions prepared with a constant amount of n-octane and SCS to clarity with DDAO while varying the aqueous phase volume. This plot represents the minimum volume of DDAO required to transform an emulsion into a microemulsion. From the slope and extrapolated intercept values, the mole fraction of DDAO in the bulk and at the droplet interface was determined. From these values the free energy associated with microemulsion formation and the entropy of mixing were then calculated for microemulsions containing 0.5 and 1.4 cc of n-octane.

3.2. EXPERIMENTAL

3.2.1. Chemicals

n-Pentane and n-hexane (Eastman Kodak Co.) ; n-octane and n-decane (99%+ gold label) and sodium dodecyl sulfate (SDS) (Aldrich Chemical Co.) ; sodium cetyl sulfate (SCS) (Henkel Chemical Co., Minn., MN.) ; and dodecyldimethylamine Oxide (DDAO) 30% active (Onyx Chemical Co.). Potassium hydroxide and sodium chloride (Fisher Scientific Co.) were both reagent grade. Freshly distilled water was used in all solution preparations.

3.2.2. The Systems Investigated

Five o/w microemulsion systems were prepared using the titration technique (2,7,10). Initial coarse emulsions were prepared by mixing together various amounts of oil, water and surfactant in a water-jacketed beaker maintained at 25°C. The emulsions were titrated to clarity (transmittance $> 85\%$) with DDAO. A teflon magnetic stirring bar was used to insure complete mixing. The systems investigated are seen in Table 3.1. Systems 1 - 4 were prepared with 20 cc H_2O and system 5 was prepared with 20 cc of 5% Nacl + 0.01N NaOH (pH = 11.2).

3.2.3. The Isoteniscope Method

Vapor pressure measurements were determined with an isoteniscope attached to a water jacketed condenser. In the cases where volatile oils were used, a refrigerated water bath maintained the condenser at 5°C to insure complete condensation of the oils. A vacuum pump attached to a dry ice trap was used to reduce the pressure within the system. A schematic illustration of the experimental setup is shown in Fig. 3.1.

TABLE 3.1			
SYSTEMS	OIL	SURFACTANT (1gm)	DDAO (ml active)
1	n-pentane	SDS	1.2
2	n-hexane	SDS	1.8
3	n-octane	SDS	2.4
4	n-decane	SDS	3.7
5	n-octane	SCS	3.7

TABLE 3.1 Five o/w microemulsions systems investigated. Notation : Na dodecyl sulfate (SDS), Na cetyl sulfate (SCS) and ml of 30% active dodecyldimethylamine oxide (DDAO) used.

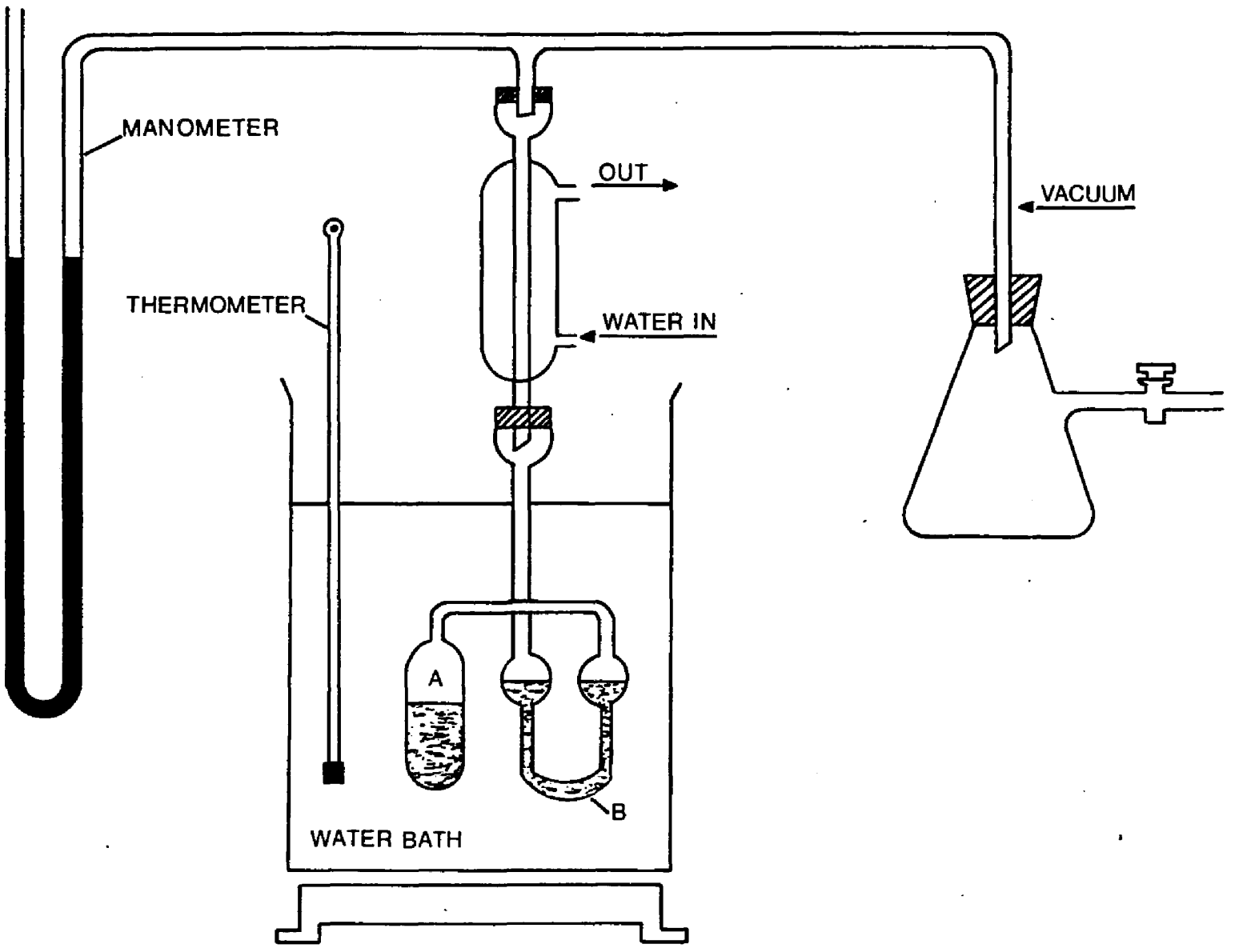

FIGURE 3.1 Diagram illustrating the experimental setup used to determine vapor pressure.

The microemulsions investigated were placed in the isoteniscope and submerged in a water bath. A teflon magnetic stirring bar was used to maintain gentle stirring. The systems were allowed to boil for 10 minutes to evacuate any excess air that may be present. The bath was slowly cooled with ice chips until an equilibrium between the liquid and vapor was obtained. The pressure within the system along with the temperature of the water bath were then recorded. The pressure was then reduced and the same procedure was repeated. Using the Clausius - Clapeyron equation

$$\ln\frac{p}{p_o}=-\frac{\Delta H_v}{R}\left|\frac{1}{T}-\frac{1}{T_o}\right| \tag{3.1}$$

where

p and p_o are the vapor pressures at T and T_o

ΔH_v the heat of vaporization

R the gas constant

the vapor pressure p and heat of vaporization was determined. In this case, p_o = 1 atm was used as a reference; then the normal boiling point of the liquid was given by T_o.

3.2.4. PHOTON CORRELATION SPECTROSCOPY

Microemulsion droplet size were determined by photon correlation spectroscopy (PCS). The apparatus used is described in Ref. (13) and a schematic diagram is shown in Fig. 3.2. Light from an argon ion laser at 488 nm was focused on the sample in a glass cuvette maintained at constant temperature (20°C) by a Lauda water circulator. The intensity of the scattered light was detected at 90 degrees to the incident beam with a Hamamatsu (Middlesex, NJ) photomultiplier tube.

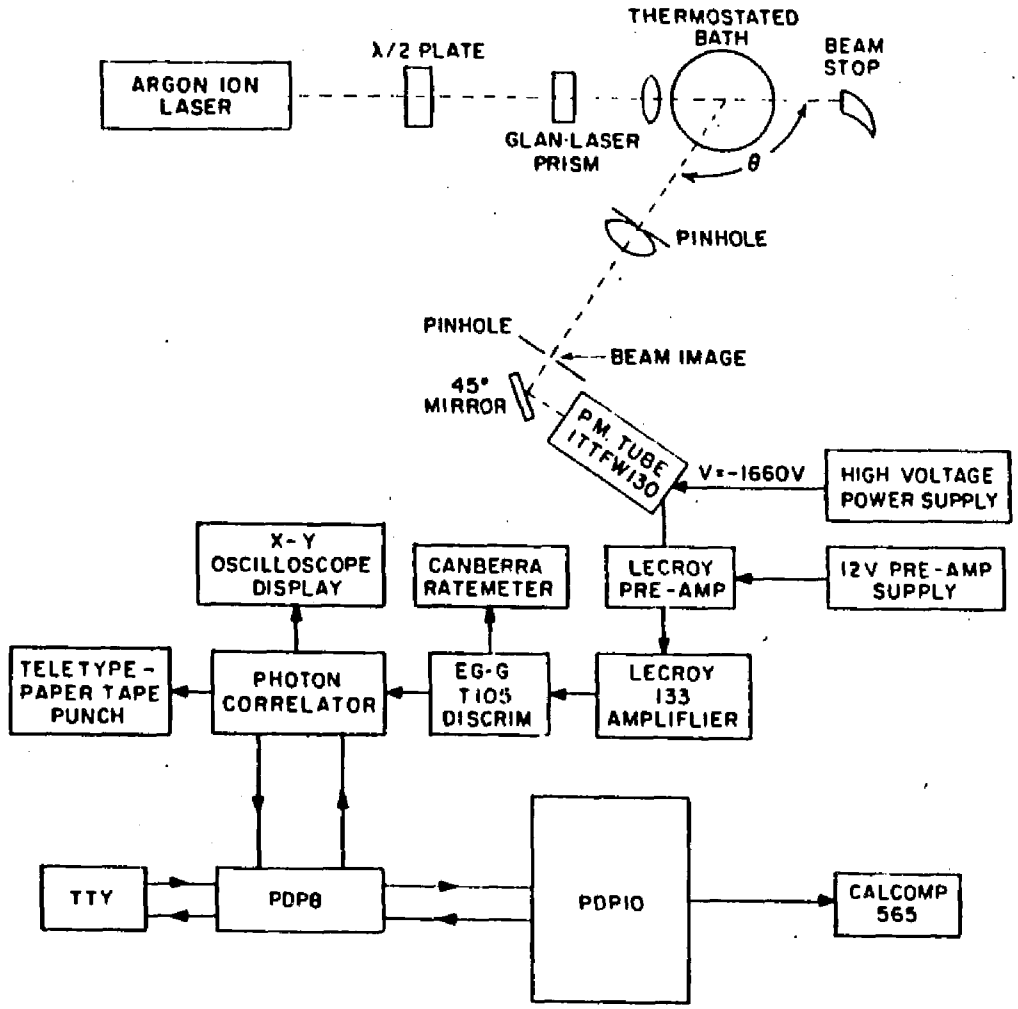

FIGURE 3.2 Block diagram of the apparatus used for the photon correlation spectroscopic measurements.

For particles in Brownian motion, droplet radii are determined from a second order correlation function $g^{(2)}(\tau)$, where τ is the delay time. This function decays exponentially with delay time according to

$$g^{(2)}(\tau)=B(1+e^{-\Gamma\tau}) \tag{3.2}$$

where

B = the base line

Γ = the inverse correlation time

A = a constant between 0 and 1 determined by the system.

Γ is given by $2Dq^2$, where D is the translational diffusion coefficient and q is the scattering vector given by $q = 4\pi n/\lambda \sin(\theta/2)$; n is the refractive index of the solution, θ is the scattering angle and λ is the vacuum wavelength of the incident light. The diffusion coefficient D is then related to the droplet radius R by the Einstein- Stokes expression:

$$D=\frac{kT}{6\pi\eta R} \tag{3.3}$$

where

k = Boltzmann's constant,

η = the viscosity of the microemulsion

T = absolute temperature.

In the case of a polydispersed system, the correlation function does not exhibit simple exponential decay, but is instead a superposition of exponentials. It is then possible to extract the mean decay time Γ_0 and μ_2, the second moment of Γ about Γ_0. By a cumulants analysis technique, the average radius (actually the z-average radius) is found from Γ_0 while the ratio μ_2/Γ_0^2 is an index of polydispersity. For droplets whose size distribution is gaussian with a mean radius of R_0 and standard deviation σ, the fractional width of the

distribution is approximately related to the index of polydispersity by

$$\frac{\sigma}{R_o}=7\frac{\mu_2}{\Gamma^2} \tag{3.4}$$

The correlation function was accumulated in a 60 channel photon autocorrelator and initially displayed on an oscilloscope. The sampling time was adjusted to obtain exponentially decaying correlation functions which were collected by a DEC PDP-8 minicomputer and subsequently analyzed by the technique of multiple linear regression (cumulants analysis) on a VAX 11/780 mainframe computer. The light scattering apparatus was calibrated with a standard, monodisperse sample of polystyrene.

3.2.5. SURFACE TENSION MEASUREMENTS

Surface tension measurements of sodium cetyl sulfate and dodecyldimethylamine oxide solutions were determined with a Rosano Tensiometer (Arenberg-Sage), equipped with a sandblasted platinum blade. A stock 1×10^{-2} M solution of DDAO:SCS in a 3.7:1 molar ratio was prepared. From the stock solution, subsequent dilutions were made. The surface tension of each solution was determined after the systems were allowed to equilibrate for 2 days at 25°C. A plot of the surface tension vs log c can be seen in Fig. 3.3. All glassware was thoroughly cleaned with a freshly prepared potassium dichromate/sulfuric acid solution and rinsed with distilled water.

3.2.6. INTERFACIAL TENSION MEASUREMENTS

The interfacial tension γ_i as a function of the logarithm of the concentration was determined for systems prepared with an aqueous 3.7:1 DDAO:sodium cetyl sulfate mixture and n-octane at 25°C, see Fig. 3.4.

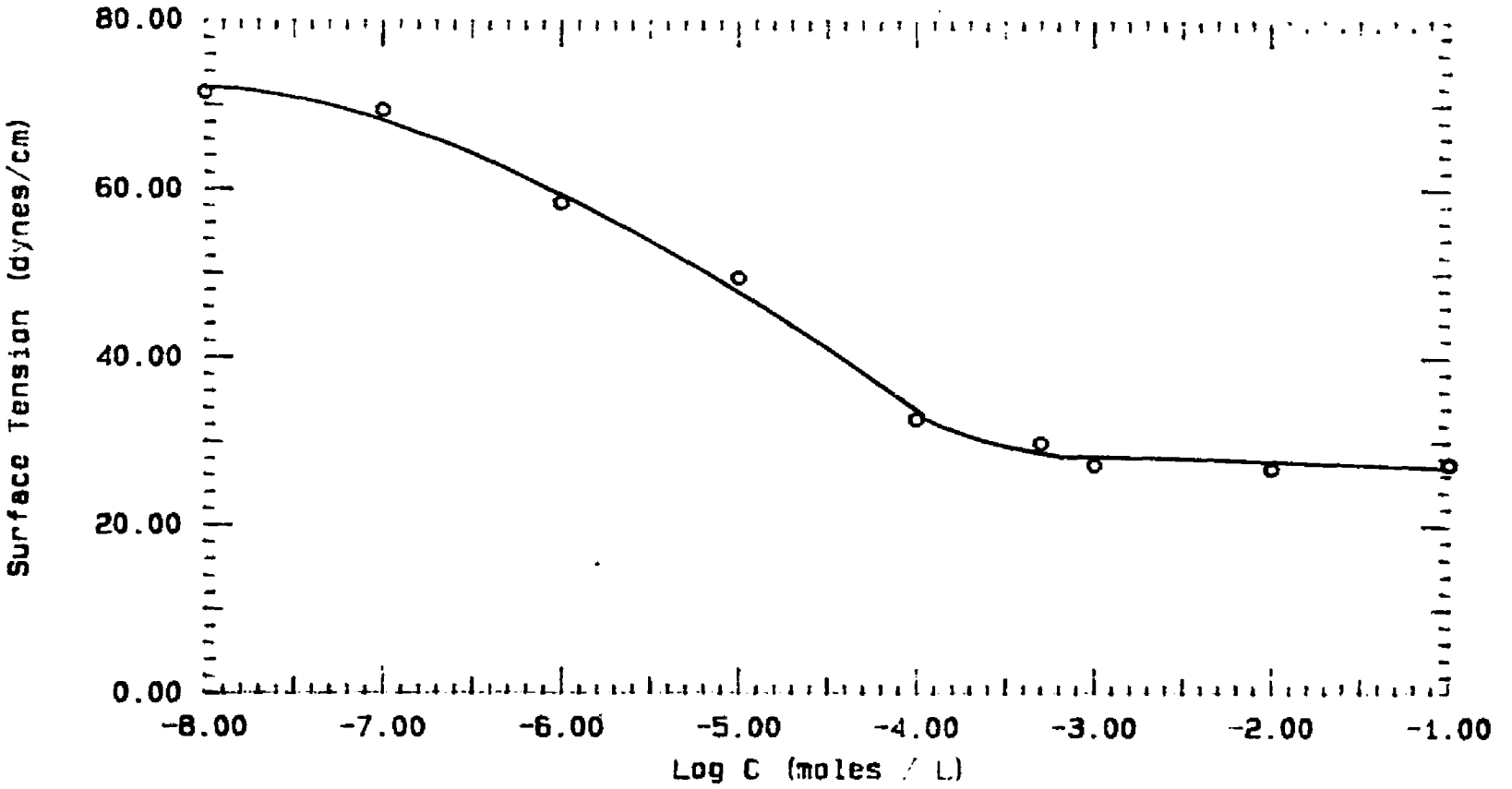

FIGURE 3.3 Surface tension vs Log C for a 3.7:1 DDAO:SCS solution at various concentrations at 25°C.

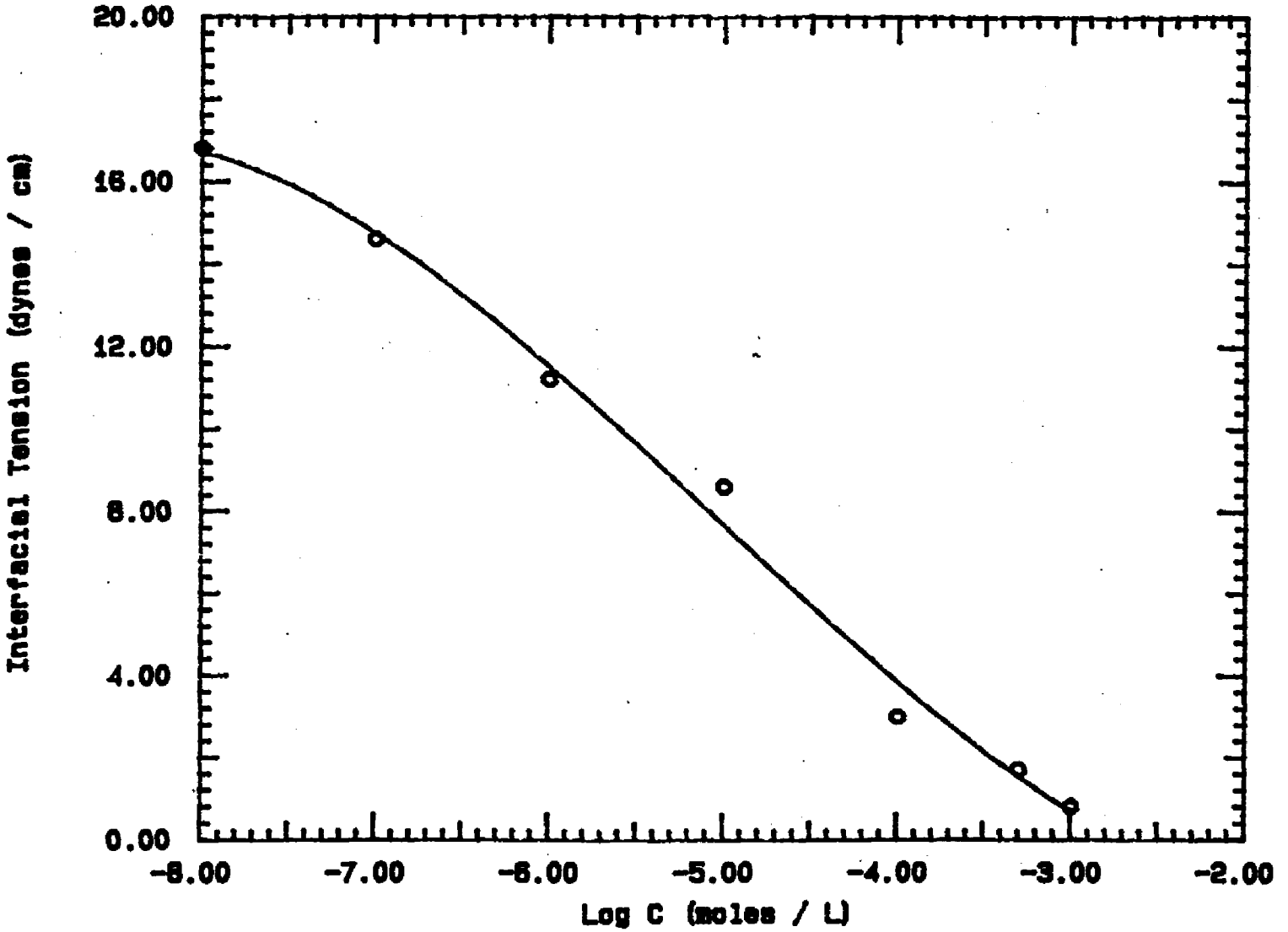

FIGURE 3.4 Interfacial tension vs Log C for a 3.7:1 DDAO:SCS solution at various concentrations containing 20 cc n-octane at 25°C.

The systems were prepared by mixing 70 cc of the aqueous mixture and 20 cc n-octane in 100 cc pyrex dishes. A teflon blade attached to a microforce transducer-amplifier (Sandborn, Model 311 A) was submerged in the lower aqueous phase and slowly raised into the upper oil phase using a mechanical elevating stand. The signal from the transducer amplifier was plotted by a calibrated strip-chart recorder (Sergent-Welch Corporation). For systems with interfacial tension values significantly low, the spinning drop method (25) was used to determine γ_i. Appendix B shows the program used.

3.2.7. PRESSURE - AREA MEASUREMENTS

From the interfacial tension values obtained,the pressure Π vs area per molecule σ was determined using the Gibbs equation. For a binary mixture of two different surfactant components, the Gibbs equation may be written as

$$d\,\Pi = \Gamma_1 d\,\mu_1 + \Gamma_2 d\,\mu_2 = \Gamma_1 RT\, d\ln c_1 + \Gamma_2 RT\, d\ln c_2 \qquad (3.5)$$

where $d\,\Pi$ is the change in the surface pressure of the solution, Γ_i is the absorption density of the surfactant component i in the mixed film, $d\mu_i$ is the change in chemical potential of component i in the system, R is the gas constant, T is the absolute temperature, and c_i is the concentration of composition i of surfactant in the aqueous solution. When the aqueous solution is fixed (i.e., $c_1 = \alpha c$ and $c_2 = (1 - \alpha)\, c$ with c being the total surfactant concentration in solution) Eq. 3.5 can be written as

$$\Gamma = \frac{-1}{2.303RT}\frac{\partial \gamma_i}{\partial \log c} \qquad (3.6)$$

The value of σ is given by $1/\Gamma$. The minimum value of σ was determined by plotting Π vs σ for a 3.7:1 DDAO:SCS, n-octane mixture. These results are shown in Fig. 3.5. This plot actually represents the area occupied by

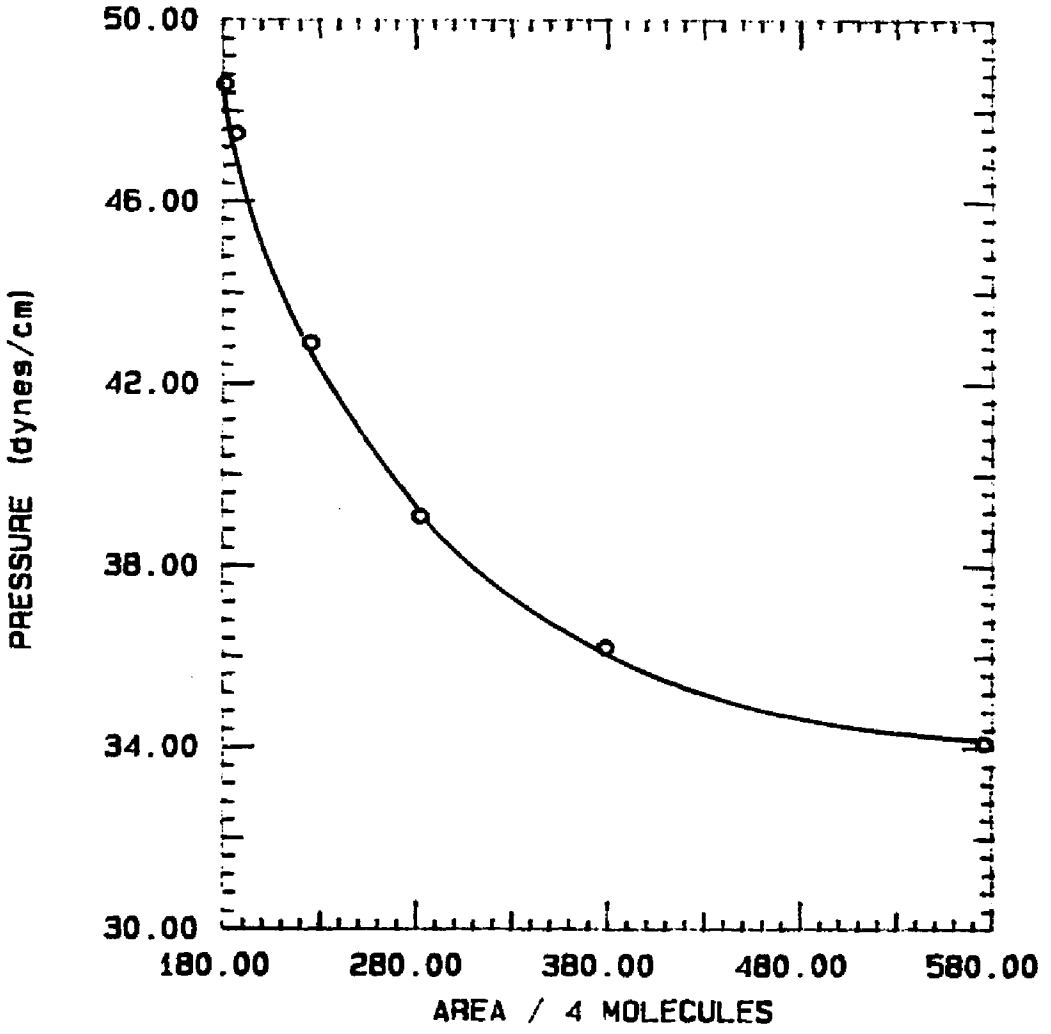

FIGURE 3.5 Pressure vs area curve for a 3.7:1 DDAO:SCS solution at 25°C.

approximately four molecules, (i.e., three SCS and one DDAO). The minimum value of σ was found to be 45$\mathring{A}^2$ per molecule. This value is in agreement with monolayer and duplex film measurements of octadecyl sulfate and octadimethylamine oxide (12).

3.3. THEORY

3.3.1. BENDING ENERGY AND MICROEMULSION STRUCTURE

In order to understand the interactions responsible for the phase behavior observed in microemulsion systems, we have used a phenomenological theory suggested by Safran (20) based on a model of interacting globules. This model assumes that for an oil, water and surfactant system, all the surfactant is at the oil/water interface (i.e., the interface is completely saturated with surfactant). This assumption is based on the low solubility of oil in water and the surfactant in either pure oil or water. For such a system the energetics are governed by the energy of the surfactant layer at the oil/water interface. In addition, the surfactant layer is assumed incompressible compared with its resistance to orientational distortions (bending of the surfactant sheath) while keeping the area per surfactant molecule constant.

The total free energy for such a system can be expressed as

$$F_T = nF_B - TS_M + F_{AT} \tag{3.7}$$

where nF_B is the total bending energy of all the globules of the system, S_M is the free energy due to the entropy of dispersion and F_{AT} is the free energy due to the interaction of the droplets.

It is well known that for a given amount of surfactant, the total surface area is constant. The surface free energy term corresponding to the creation of this interface will be assumed irrelevant, since it is a constant depending on the

amount of surfactant used in the initial preparation of the microemulsion. The energy of the system is then related to the curvature of the interface and the total bending energy is related to the sum of the curvature or bending energies of all the individual droplets composing the system. The microemulsion in the dilute limit can then be viewed as a collection of non-interacting globules of oil-in-water. The bending energy per droplet is given by

$$F_B = \frac{K}{2}\int \left| \frac{1}{R_1}+\frac{1}{R_2}-\frac{2}{\rho_0} \right|^2 dS + \frac{K'}{2}\int \left| \frac{1}{R_1}-\frac{1}{R_2} \right|^2 dS \qquad (3.8)$$

where the integral is over the surface of the globule. R_1 and R_2 are the local radii of curvature, ρ_0 is the spontaneous radius of curvature which represents the tendency of the interface to bend either to the water side ($\rho_0 > 0$) or towards the oil side ($\rho_0 < 0$) of the interface. The bending is determined by the packing and geometry of the surfactant molecules at the interface. K and K' are the elastic and saddle-splay constants related to the rigidity of the interfacial film. The first term in Eq. 3.8 represents the bending energy of a general interface with spontaneous radius of curvature ρ_0. The second term represents the energy required to distort the surface to a saddle shape. To minimize F_B the saddle-splay term favors structures with equal radii of curvature, for example spheres and lamellae instead of cylinders or ellipsoids.

The total curvature energy of the system is then given as the sum of F_B over all the globules. It is important to mention that since the number of globules is not constant the system will choose the size, shape and number of globules that will minimize its free energy. It is assumed that for a microemulsion system, the curvature energy is minimized by the formation of monodispersed spherical droplets of radius ρ_0. As explained by Sarfan (20), the total surface area of all the globules is fixed by the incompressibility of the surfactant molecules at the oil/water interface. In addition, the total volume of

all the globules is fixed by the incompressibility of the internal water or oil phase. Therefore for an arbitrary concentration of oil, water and surfactant the system cannot produce a monodispersed set of globules of radius ρ_0. What determines the optimal size of the globules is the competition between the tendency of the system to form globules of radius ρ_0 (minimizing the bending energy) and the necessity to use all the oil, water and surfactant molecules available to the system. Therefore only specific component concentrations can produce optimal droplet radii. It should also be mentioned that for a dilute microemulsion system, a term expressing the entropy of dispersion should be added to the total curvature energy expression. Since the number of droplets is not a constant, both the curvature energy and entropy of dispersion must be considered when minimizing the free energy. Incorporating a term which expresses the entropy of dispersion has been reported to show that small structures are favored over larger ones when microemulsions are formed.

The droplet internal bending energy per unit volume is

$$F_B = nF_G = \frac{6KX}{\rho^3}(1-\rho/\rho_0)^2 \qquad (3.9)$$

where X is the volume fraction of the spheres in the microemulsion and n the number of globules per unit volume. Equation 3.9 shows that as the globules grow in size, the bending energy is reduced. Addition of internal phase results in the excess water being phase separated out as to maintain an optimal bending energy.

When $\rho=\rho_0$, the bending energy is at a minimum, the globules have their optimal radius of curvature and the droplets are spherical. Upon addition of added internal phase, the droplet radius increases. The radius cannot grow beyond ρ_0. Addition of excess internal phase results in the excess internal phase being phase separated out. This separation has been called "emulsification

failure instability". It results in a phase separation of spherical droplets of radius $\rho=\rho_0$ coexisting with a bulk phase of excess oil or water (the internal phase).

3.3.2. PHASE SEPARATION AND DROPLET INTERACTION

While a complete understanding of the curvature energy is useful for explaining droplet size and shape, an understanding of droplet interactions can lead to a physical description applicable to phase separation in microemulsion systems. The main ideas and development of this theory are due to Safran (20). For simplicity, we will assume that the microemulsion globules are spherical. The hard-core interactions of spheres can be accounted for by the entropy of mixing for hard spheres

$$S_M = n_0[\phi(\log\phi - 1)4\phi^2 + 5\phi^3 + \ldots] \tag{3.10}$$

where $n_0 = 4\phi\rho^3/3$. The attractive interaction between globules can be written as

$$F_{AT} = -\frac{1}{2}k_b T A(\rho,T)x^2 \tag{3.11}$$

where k_b is the Boltzmann constant and T the absolute temperature. The virial coefficient $A(\rho,T)$ is

$$A(\rho,T) = n_o \int [\exp^{-u(r,\rho)/kT} - 1]d^3r \tag{3.12}$$

which explicitly depends on the drop-drop interaction $U(r,\rho)$ given by

$$U(r,\rho) = \frac{-A}{6}\left|\frac{2\rho^2}{r^2-4\rho 2} + \frac{2\rho^2}{r^2} + \log(1-\frac{4\rho^2}{r^2})\right| \tag{3.13}$$

where A is the Hamaker constant and r is the distance of separation between

the droplets. For $r \gg 2\rho$, Eq. 3.13 reduces to

$$U(r,\rho) = -16\,\frac{A}{9}(\rho / r) \qquad (3.14)$$

Because of the drop size-dependence of the virial coefficient, as the volume fraction of droplets is varied the strength of the interactions between the droplets is also varied. Thermodynamically, the competition between the entropy of mixing and the attractive interactions between the droplets permits a collective "liquid/gas" phase separation to occur whereby the system separates from a single isotropic phase into two coexisting phases of spheres dispersed in the same continuous phase. This transition is achieved by varying the radius ρ of the droplets. Safran (20) has shown that when the radius attains a critical value ρ_c such that the virial coefficient $A(\rho_c, T) \sim 21$, the interactions are strong enough so that the microemulsion can separate into a "liquid" (high number density of droplets) and "gas" (low number density of droplets) phases. The density of the two coexisting phases are determined solely by the entropy and interaction terms.

The radius ρ can not exceed the natural bending radius ρ_0, since at that point single-particle emulsification-failure instability occurs. If $\rho_0 > \rho_c$, the liquid/gas collective instability occurs followed by emulsification-failure. As more internal phase is added, the system phase separates out the excess internal phase from the two coexisting microemulsion phases (i.e., the liquid and the gas phase), resulting in three phases coexisting in equilibrium. The three phases are two microemulsion phases in equilibrium with an excess internal phase.

In accordance with the above description on the energitics of microemulsion systems, a model involving the total free energy of formation per droplet G_T, has been derived which can be used to describe microemulsion formation. This expression accounts for three energy terms ; 1) the solvation between the

dispersed oil phase and the hydrocarbon tails of the surfactant molecules, 2) the work required to expand the interface, and 3) the interfacial bending energy of the surfactant sheath surrounnding each dispersed phase droplet. This equation may be expressed by

$$G_T = -\frac{4}{3}\pi r^3 G_S + 4\pi r^2 \left[\gamma + \frac{K}{2}\left[\frac{1}{r} - \frac{1}{r_0}\right]^2\right] \qquad (3.15)$$

The first term of Eq. 3.15 represents the solvation between the oil and the hydrocarbon tails of the surfactant molecules, where G_S is the energy of solvation in ergs/cc. This term is negative since it represents a favorable interaction. In most cases, the dispersed oil phase and the hydrocarbon tails of the surfactant molecules will be quite soluble in one another and therefore require very little energy to go into solution. The value of this solvation term G_S, was estimated based on the free energy of mixing ΔG_M, between octane and dodecane given by

$$\Delta G_M = R\,T\,X_1 \ln \phi_1 + R\,T\,X_2 \ln \phi_2 \qquad (3.16)$$

where ϕ_1 and ϕ_2 are volume fractions. If it is assumed that $X_1 = X_2$ and $\phi_1 = \phi_2 = 0.5$, then $\Delta G_M = 1.7x^7$ ergs/mole. This calculation assumes that the microemulsion is an athermal solution i.e., $\Delta H_v = 0$. This situation occurs when the components (i.e., oil and surfactant tails) of the system are similar in chemical nature but different in molecular size. From this assumption G_S was found to be $2x10^7$ ergs/cc. The second term of Eq. 3.15 represents the amount of work required to expand the interface, where γ is the microemulsion interfacial tension in ergs/cm^2. This value has been determined for the three phase microemulsion systems SDS / toluene / 1-butanol / saline (27) and found to be between 10^{-4} - 10^{-1} dyne/cm. The last term of Eq. 3.15 represents the flexibility of the interfacial surfactani sheath where K is the flexibility constant

in ergs and r_o is the natural radius of curvature (determined by the geometry of the surfactant molecules and their association with the oil phase and the cosurfactant). This term becomes an important consideration when the interfacial tension is almost zero. For simplicity we have neglected in this model any terms which account for the interactions between the microemulsion droplets, realizing that a much more accurate free energy description should account for such interactions as : 1) the surfactant head/head repulsion and 2) effects due to the entropy of dispersion during microemulsion formation which have previously been investigated by Ruckenstein (26).

Figure 3.6 shows the change in G_T vs. r for various values of K. In all cases, r_o = 90 A and γ = 0.1 ergs/cm^2. To a first approximation it is assumed that the interfacial tension is independent of r. That is as the droplets increase in size the interfacial tension remains constant. It is observed that when K is approximately 10^{-10} ergs, the free energy starts out positive and decreases to a minimum value for r = 90 to 180 A. For r > 180 A, G_T increases as the droplet radius increases. When K is on the order of 10^{-11} ergs, the value of G_T decreases continuously and no minimum is observed as r is increased. These results suggest that for droplets to form, K > 10^{-11} ergs, suggesting that a low interfacial tension is not solely responsible for microemulsion formation. In addition to a low γ, the interfacial rigidity must be high enough in order to spontaneously curve the interface and form microdroplets. When K $\sim$ 10^{-10} ergs, the interfacial rigidity is high enough to produce a minimum value in the total free energy curve required for spontaneous dispersion and droplet formation.

3.4. RESULTS

In this section, the main emphasis will be on the vapor pressure of O/W

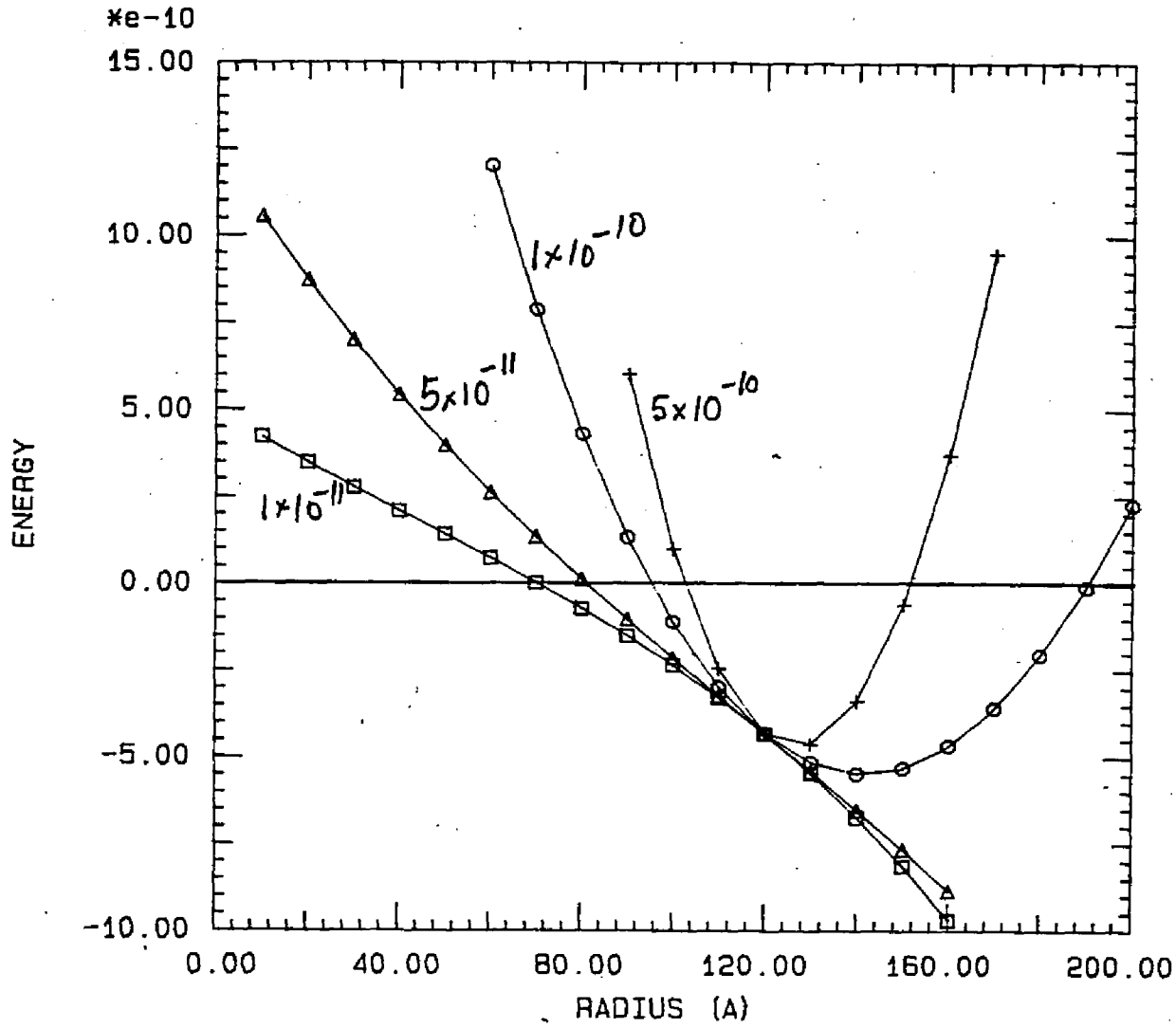

FIGURE 3.6 Change in total free energy vs. radius during microemulsion formation for various values of interfacial flexibility (K).

microemulsions. Using vapor pressure analysis, microemulsion droplet molecular weight and size will be determined. It also will be demonstrated that as the dispersed phase volume is increased, emulsification - failure instability occurs as predicted by Safran (20).

3.4.1. ln P vs 1/T

The vapor pressure of each microemulsion shown in Table 3.1, was determined from Eq. 3.1, by plotting ln p vs 1000x1/T. From the slope of the line ($-\Delta H_v/R$), the heats of vaporization were determined. The intercept at 1000x1/T = 0 yields a value of $\Delta H_v/RT_o$. Thus from the slope and intercept, both ΔH and T_o can be evaluated. For water at 30°C, excellent correlation (98.5%) was obtained between the experimental value of ΔH = 45.3 kJ / mole and the literature value of 46.0 kJ / mole (Handbook of Chemistry and Physics, Weast, 57th Edition, CRC Press). Fig. 3.7 shows a typical plot for a system 5 microemulsion (1 gm SDS / H_2O / 3.7 DDAO) containing 1 cc of n-octane. In all cases, a straight line was obtained with excellent correlation (>0.99). The same procedure was repeated for all the systems investigated containing various amounts of oil.

3.4.2. Vapor Pressure vs Volume of Oil at Various Temperatures

The vapor pressure vs various volumes of n-octane was determined for system 5 (1 gm SDS / 20 cc saline / n-octane / 3.7 gm DDAO) between the temperatures 15 - 40 °C, as shown in Fig. 3.8. It is evident that at each temperature, two distinct regions are present depending on the volume of n-octane used in the initial preparation of the microemulsion. Upon the addition of 0.25 cc of n-octane at 30 °C, the vapor pressure decreases to 25.4 mm Hg (from 32.4 mm Hg for the zero ml oil system) and remains low up to the addition of 1.1 cc

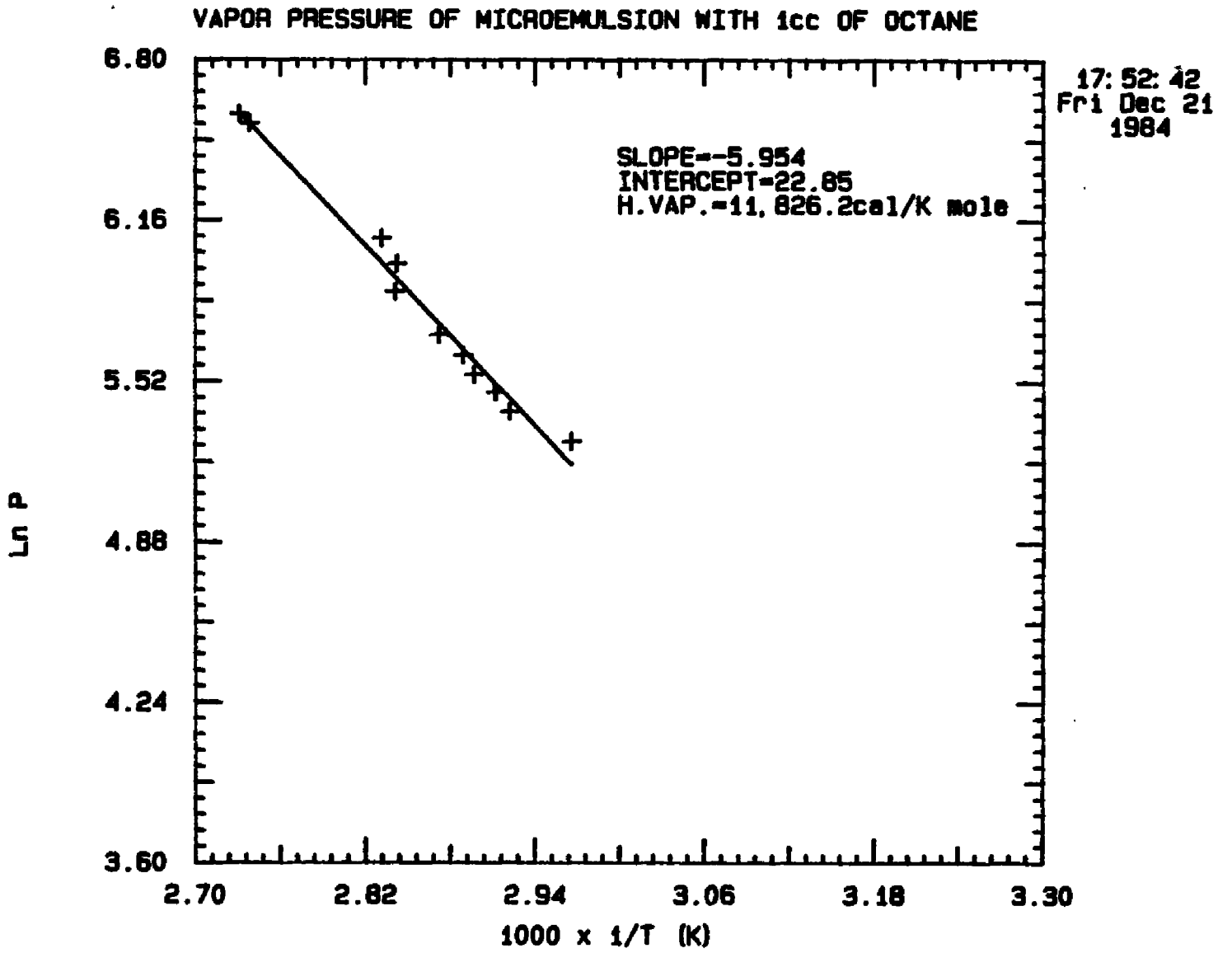

FIGURE 3.7 Plot of the Ln P vs 1000/T for a microemulsion containing 1 gm SCS/20 cc saline/1 cc n-octane and 3.7 cc DDAO.

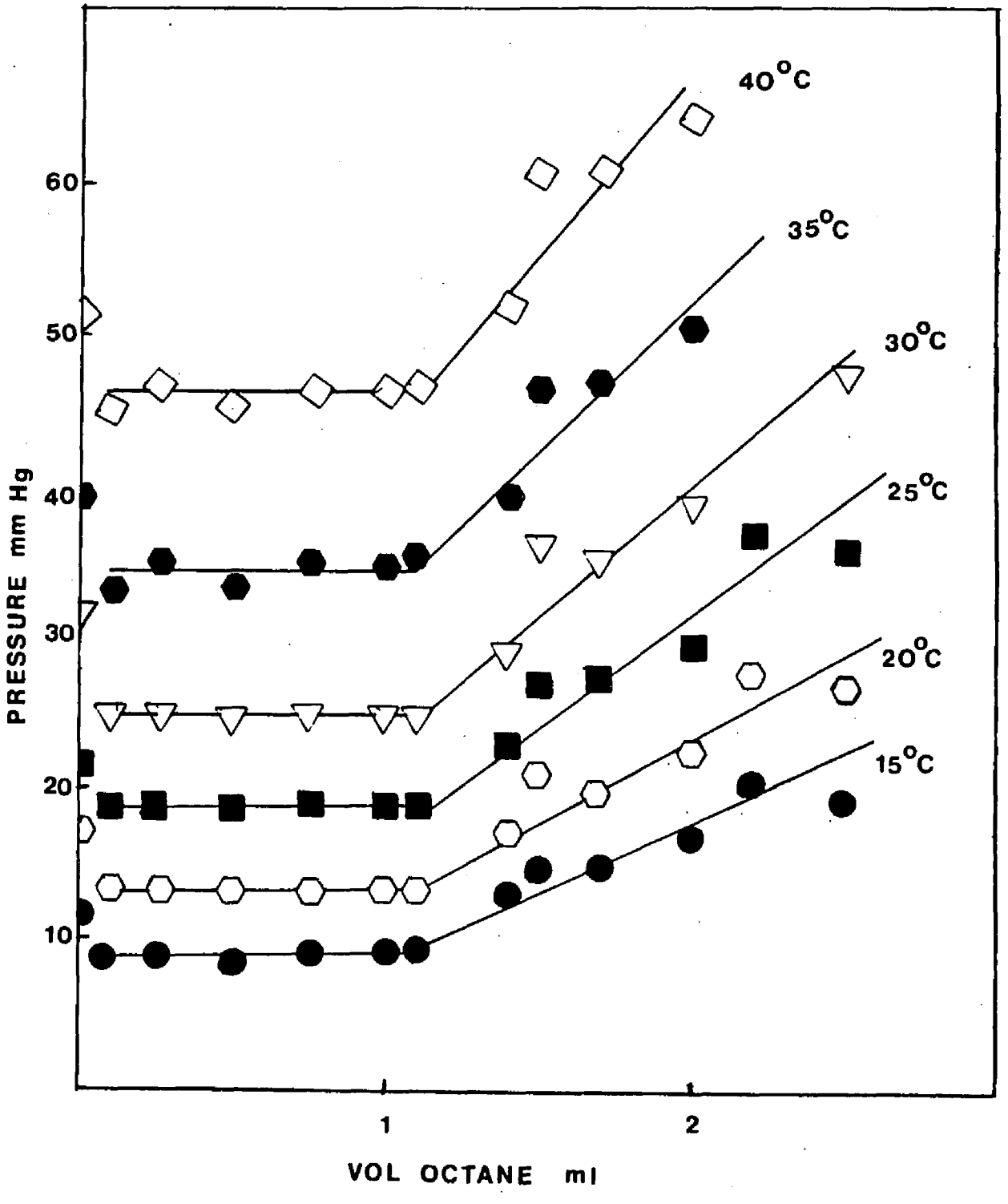

FIGURE 3.8 Change in vapor pressure vs volume n-octane for a microemulsion prepared with 1 gm SCS/20 cc saline/3.7 cc DDAO and various volumes of n-octane between 15-40°C.

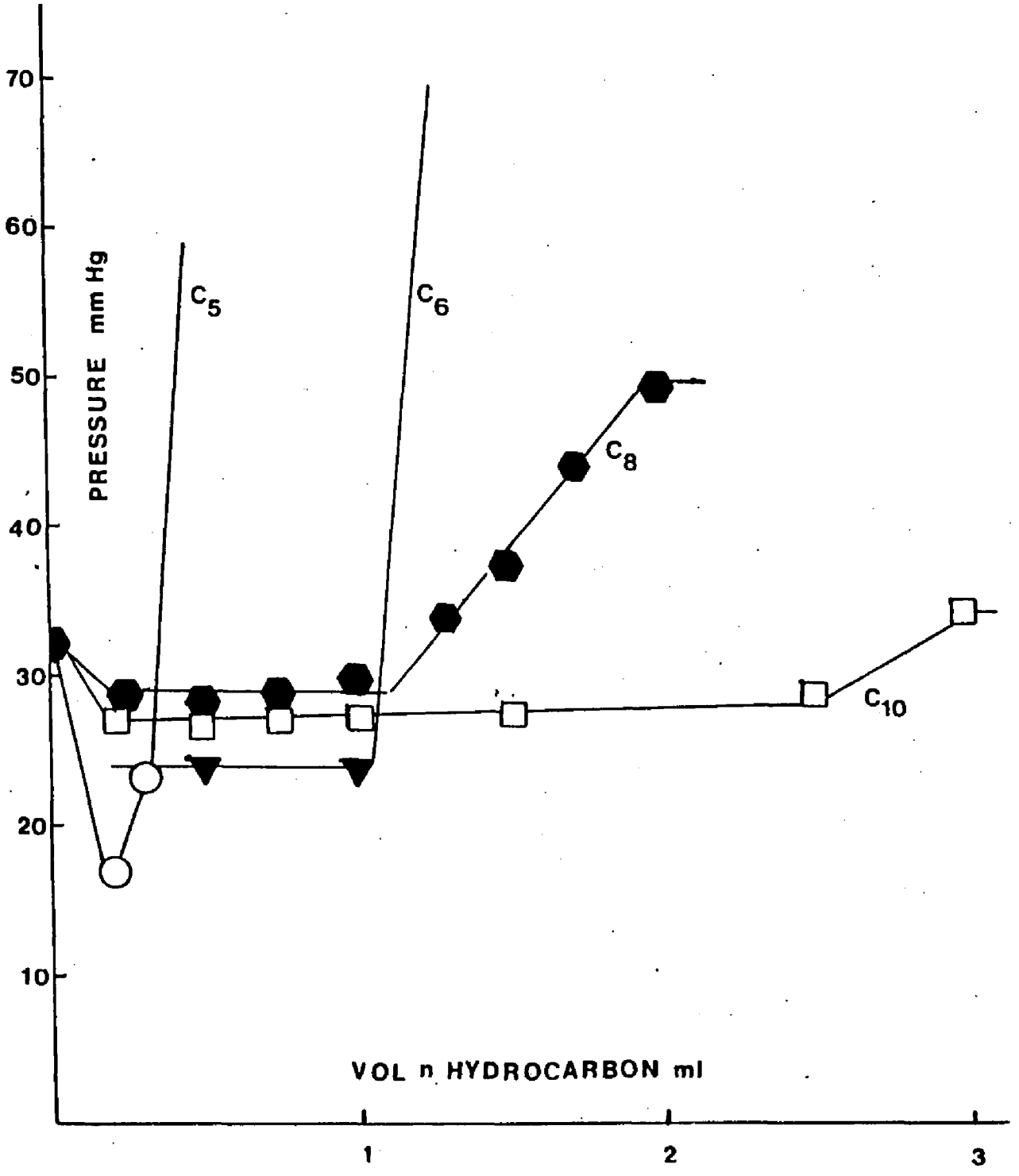

FIGURE 3.9 Vapor pressure of four o/w microemulsions prepared with 1 gm SDS / 20 cc H_2O / various volumes of C_5, C_6, C_8, C_{10} and DDAO at 30°C.

of octane (25.6 mm Hg). Between 1.1 and 2.2 cc of n-octane, a steady increase in the vapor pressure is observed. Beyond 2.2 cc of n-octane, a two phase system is formed and the vapor pressure reaches a maximum value of 51 mm Hg, the sum of the individual components (i.e., n-octane 19 mm Hg and saline 32 mm Hg) of the system.

3.4.3. Vapor Pressure vs Volume of n-Pentane, n-Hexane, n-Decane and two n-Octane Microemulsion Systems

Figure 3.9 shows a plot of the vapor pressure determined at 30°C vs various volumes of oil for microemulsions prepared with n-pentane, n-hexane, n-octane and n-decane (see systems 1-4, Table 3.1). A basic characteristic observed for all the systems investigated is a significant lowering of the vapor pressure upon the addition of small volumes of oil.

Microemulsions prepared with n-pentane show an initial lowering of the vapor pressure (16.5 mm Hg), then a sharp increase for volumes greater than 0.3 cc. Microemulsions prepared with n-hexane show a similar vapor pressure lowering. For the n-hexane microemulsion systems, an initial lowering in the vapor pressure is observed; however, the vapor pressure remains low until the added volume of n-hexane exceeds 1 cc. Beyond this volume, a sharp increase in the vapor pressure is observed. Microemulsions prepared with n-octane and n-decane also show a significant lowering in the vapor pressure when oil is added. It is interesting to note that, as the hydrocarbon chain length increases, the minimum observed in the vapor pressure curve is also increased over a larger oil volume.

For a microemulsion prepared with 1 gm SDS/20 cc water/12 cc DDAO and various volumes of n-octane, the viscosity was determined at 22°C. It was observed that a maximum in viscosity was achieved when the microemulsion

TABLE 3.3						
OCTANE (cc)	15 (°C)	20 (°C)	25 (°C)	30 (°C)	35 (°C)	40 (°C)
0.1	8.25×10^5	6.85×10^5	5.77×10^5	4.95×10^5	4.4×10^5	3.99×10^5
0.25	7.79×10^5	6.79×10^5	6.17×10^5	5.9×10^5	6.13×10^5	7.26×10^5
0.50	7.39×10^5	6.34×10^5	5.53×10^5	4.99×10^5	4.72×10^5	4.71×10^5
0.75	7.98×10^5	7.05×10^5	6.4×10^5	6.14×10^5	6.34×10^5	7.48×10^5
1.0	8.18×10^5	7.15×10^5	6.41×10^5	6.03×10^5	6.06×10^5	6.74×10^5
1.10	8.49×10^5	7.36×10^5	6.6×10^5	6.29×10^5	6.39×10^5	7.29×10^5
1.25	1.45×10^6	1.33×10^6	1.52×10^6	1.77×10^6	2.86×10^6	
1.40	6.6×10^6	6.29×10^6	6.78×10^6	1.98×10^7		

TABLE 3.3 Calculated values of the G.M.W. per mole droplet for a microemulsion containing 20 cc of 5% NaCl + 0.01N NaOH / 1 gm SCS / 3.7 gm DDAO and various volumes of n-octane between 15-40°C.

TABLE 3.4		
OCTANE (cc)	radius_{VP}	radius_{PCS}
0.1	85.4	80.8
0.25	93.2	76.8
0.5	85.8	85.6
0.75	95.1	80.5
1.0	94.3	94.4
1.1	96.3	115.0
1.25	161.5	198.0
1.4	540.2	958.0

TABLE 3.4 Calculated radius values for microemulsions prepared with various volumes of n-octane assuming $\sigma = 45$ Å^2 per molecule.

contained 0.125 cc of n-octane. Upon increasing the volume of n-octane to 0.5 cc, the viscosity decreased and remained at a minimum value of 19 cps.

3.4.4. Molecular Weight Determinations

For microemulsions containing various volumes of n-octane, the droplet molecular weight was determined from the lowering of the vapor pressure (for system 5, Table 3.1). The experimental vapor pressure values determined between 15-40°C are shown in Table 3.2. Using the van't Hoff equation

$$M. = RT\frac{C}{\pi} \tag{3.17}$$

where;

M. = gram molecular weight

R = gas constant

T = temperature (°K)

C = solution concentration (gm/L)

$\pi = p_o - p$

the M. per droplet in the microemulsion was determined from the difference in vapor pressure between the solution containing no oil (p_o), and the microemulsion containing various volumes of n-octane (p).

For example, at 30°C, a system prepared with 0.5 cc of n-octane where π = 6.04 mm Hg, C = 159.7 gm/L and T = 303.15 °K, the M. = 4.99×10^5 grams/mole. Table 3.3 shows the values of the G.M.W.'s per droplet for microemulsions containing 0.1 - 1.4 cc of n-octane. Although some scattering is observed in Table 3.3, it is evident that as the volume of n-octane is increased, the apparent G.M.W. per droplet also increases.

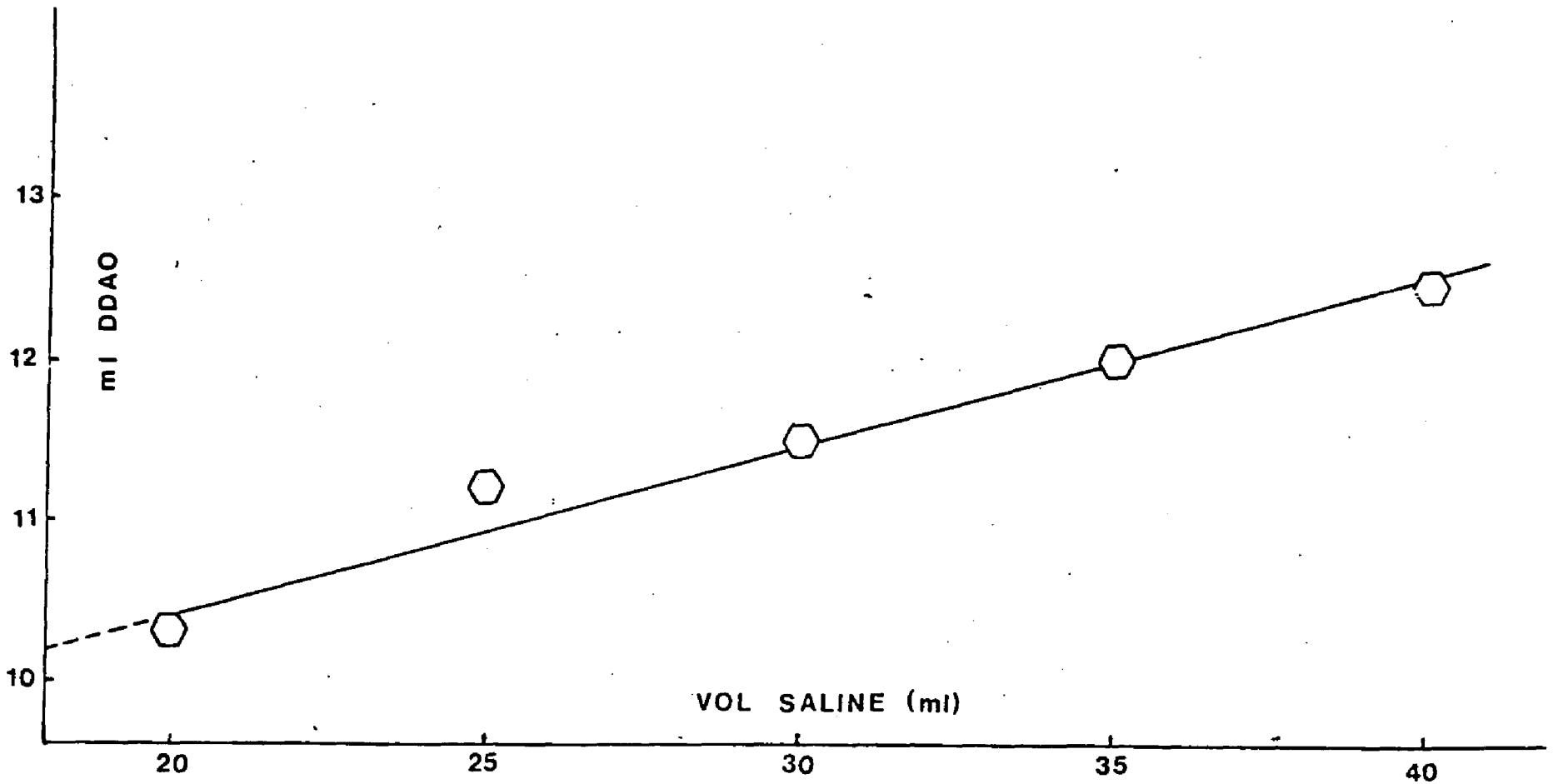

FIGURE 3.10 Minimum volume of DDAO vs volume of saline required to titrate an emulsion prepared with 1 gm SCS/1 cc n-octane and various volumes of saline to clarity at 25°C.

3.4.5. Radii Determinations

From the values of the average G.M.W. per droplet, droplet radii were determined by considering that the ratio of the G.M.W. divided by S.W., (the average weight of associated surfactant and cosurfactant at the droplet interface) gives the number of surfactant molecules at the droplet surface. For spherical droplets, of surface area $4\pi r^2$

$$\frac{G.M.W}{S.W.} = 4\pi\frac{r^2}{\sigma} \tag{3.18}$$

and

$$r = \left| \frac{G.M.W.}{S.W.} \times \frac{\sigma}{4\pi} \right|^{\frac{1}{2}} \tag{3 19}$$

where σ is the average cross-sectional area per surfactant molecule, droplet radii values were determined assuming $\sigma = 45\mathring{A}^2$ per molecule. If it is assumed that all the surfactant absorbs at the droplet interface then the ratio of surfactant / cosurfactant at the interface can be determined by the titration technique (1,10). This is done by plotting the volume of DDAO vs the volume of saline, shown in Fig. 3.10. This plot represents the minimum volume of DDAO required to titrate to clarity a system 5 emulsion. From the extrapolated intercept value, the ratio of DDAO:SCS was found to be 3.7:1 and the average S.W. of associated surfactant / cosurfactant at the droplet interface is 243.1 gm / mole.

Table 3.4 shows the droplet radius determined from vapor pressure analysis assuming $\sigma = 45\mathring{A}^2$ / molecule for increasing volumes of n-octane. Also shown in Table 3.4 are the radii values determined by photon correlation spectroscopy. Droplet radii determined by vapor pressure measurements were found to be in agreement with those found using PCS with the exception of the system prepared with 1.4 cc of n-octane, where a high polydispersity was

TABLE 3.2						
OCTANE (cc)	15 (°C)	20 (°C)	25 (°C)	30 (°C)	35 (°C)	40 (°C)
No oil	12.7	17.1	22.9	30.3	39.8	51.8
0.10	9.4	13.1	18.0	24.6	33.2	44.4
0.25	9.1	12.9	18.2	25.4	34.9	47.6
0.50	8.8	12.5	17.5	24.3	33.3	45.2
0.75	9.0	12.9	18.2	25.3	34.9	47.6
1.00	9.0	12.9	18.1	25.1	34.5	46.9
1.10	9.1	18.2	18.2	25.3	34.7	47.3
1.25	10.6	14.8	20.8	28.5	38.7	51.9
1.40	12.2	16.7	22.4	29.9	39.6	52.0
1.50	15.5	20.8	27.5	36.1	47.1	60.3
1.7	14.6	19.8	26.5	35.2	46.3	60.3
2.0	16.5	22.14	29.5	38.9	50.8	65.8
2.2	20.1	27.7	37.8	51.0	68.1	90.1
2.2	24.3	31.9	41.7	53.8	69.0	87.8
2.5	19.9	26.6	35.3	46.4	60.4	77.9
2.5	17.9	24.3	32.6	43.3	56.9	74.2
3.0	17.8	24.0	32.1	42.2	55.8	72.6
4.0	19.7	26.7	35.9	47.6	62.7	81.8
5.0	23.1	30.9	41.1	53.8	70.4	90.9

TABLE 3.2 Vapor pressure for a microemulsion prepared with 20 ml 5% NaCl + 0.01N NaOH / 1 gm SCS / DDAO and various volumes of n-octane between 15-40°C.

found.

An alternate method to calculate the droplet radius in a W/O microemulsion has been suggested by Weatherford (14). Based on the Kelvin equation

$$\frac{p}{p^o} = e^{\frac{-4\gamma_c V_c}{RTd_c}} \tag{3.20}$$

where

γ = the surface tension of pure water

V_c = the molar volume of water (cm^3 / mole)

p = the measured vapor pressure over the microemulsion

p^o = the vapor pressure of the continuous phase

the inner aqueous core diameter can be determined by

$$d_c = \frac{4.81\gamma_c V_c}{RT \ln \frac{p^o}{p}} \tag{3.21}$$

Using Eq. 3.21 and substituting the values of n-octane for γ, V_c, p^o and p, the inner oil core radius was determined. The value was found to be 110 A, also in agreement with the two previous values shown in Table 3.4. It should be noted that the value of 110 A does not take into account the polar heads of the surfactants, which account for approximately 10 A.

3.4.6. Activation Energy

It is well established that with very few exceptions, the rate of a reaction increases (often very sharply) with temperature. The relationship between the reaction rate and temperature was first proposed by Arrhenius:

$$K = A\, e^{-E_a / RT} \tag{3.22}$$

where

K = the reaction rate constant

A = the frequency factor

R = gas constant

T = the absolute temperature

E_a = the activation energy (kJ / mole).

It is apparent that by determining the value of K at several temperatures, the plot of $\ln K$ vs. 1/T will yield the activation energy from the slope of the curve and the frequency factor from the value of the intercept. The constant A may be ignored unless the temperature is high.

For the five o/w microemulsion systems investigated the activation energy values were determined by plotting the change in vapor pressure as a function of the dispersed phase volume between 15 - 40°C. It is apparent from Fig. 3.8 that the slope of the vapor pressure curve increases with temperature. This increase is due to droplets breaking in solution as described by Weatherford (14). Therefore, as the temperature is increased, the rate of breaking also increases so that, $K=(\partial P/\partial V)_T$. From the value of the slope of the line at different temperatures, the activation energy corresponding to the amount of energy required to break the surfactant sheath was determined using

$$\ln\frac{K_2}{K_1}=\frac{E_a}{R}\left|\frac{1}{T_1}-\frac{1}{T_2}\right| \qquad (3.23)$$

where

K_1 and K_2 are the slope values at temperatures T_1 and T_2

Activation energy values based on viscosity measurements were independently determined for pure n-pentane, n-hexane and n-octane. These values were

then compared to microemulsion activation energy values determined from Eq. 3.23 for systems containing the corresponding oils. It was found that a large difference exists between the two measured values. This difference may be related to the strength of the surfactant sheath surrounding the droplets.

3.5. DISCUSSION

3.5.1. PERCOLATION IN MICROEMULSION SYSTEMS

The concept of a percolation transition between droplets has been used to describe electric conductivity in disordered microemulsion systems. In systems containing random distributions of particles, the percolation transition signifies the first emergence of an infinite cluster of droplets at some critical volume of dispersed phase ϕ_d. If the particles are conducting and the background matrix is insulating, no conductivity will be observed for $\phi < \phi_d$. At ϕ_d, there will be a continuous transition to the conducting state. For microemulsion systems, this transition is measured through the ionic conductivity. Recent measurements of the conductivity of microemulsions have suggested the existence of a percolation threshold as a function of the volume of the dispersed phase, temperature and globule size (21,22). This transition has been shown to occur near the "liquid-gas" phase separation region (20). Some studies have attributed this transition to the onset of a bicontinuous phase (23). Recent scattering experiments on AOT w/o microemulsions have shown that there is no change in the particle size and shape as the critical point for phase separation is approached. These results suggest that conductivity measurements can be interpreted to occur at the percolation threshold and resemble the interaction between clusters of droplets.

The vapor pressure results shown in Fig. 3.8 indicate that microemulsions prepared with various volumes of n-octane in the dispersed phase exhibit two

distinct regions of transparency. These two regions are separated by a sharp transition in the vapor pressure of the system. Upon the addition of n-octane, the vapor pressure decreases, typical of a colloidal or high molecular weight polymer solution. Within this region, the droplet structure is that of encapsulated spherical droplets surrounded by a surfactant sheath dispersed throughout the continuous phase. Upon increasing the volume of n-octane, the vapor pressure increases. This increase is attributed to: 1) the droplets increasing in size as a result of increasing the dispersed phase volume and 2) a dynamic equilibrium existing between the breaking and reforming of the droplets in solution. As suggested by Weatherford (14), a dynamic equilibrium is established whereby a mass transfer of oil occurs from the droplet hydrocarbon core, through the annular surfactant layer to the continuous medium, and into the vapor phase. Hydrocarbon vapor in turn, is adsorbed by exposed transitory flat surfaces of hydrocarbon core liquid released by collapsed microemulsion droplets, which subsequently reform into submerged droplets, thereby completing the dynamic cycle.

The results of Fig. 3.8 can also be interpreted by considering that when the droplets contain a small volume of n-octane, the hydrocarbon is strongly associated with the tails of the surfactant molecules. This interaction results in a highly structured core and prevents hydrocarbon vapor from being present in the vapor phase. Alternatively, as the volume of hydrocarbon is increased, the situation within the droplet core is quite different. Increasing the volume of n-octane results in a core showing characteristics of bulk hydrocarbon. The hydrocarbon vapor is free to enter the vapor phase resulting in an increase in the measured vapor pressure. Similar behavior has been shown to exist for AOT/isooctane/water microemulsions systems as the water content was varied (20).

The aggregation and merging processes of droplets in w/o microemulsions have been investigated by Cazabat (16). For systems of low water concentration, isolated noninteracting droplets were found. At higher water concentrations, droplet interactions were found to be repulsive, where the collisions are short lived and no overlap occurred between colliding droplet interfaces. However, if the interactions are attractive, the duration of collisions were found to increase and transient droplet clusters were formed. The probability of such transient merging in ternary systems has been shown to be low (~ 10^{-3} per collision). For quaternary systems the merging probability between droplets is quite high (~ 1) indicating that the interactions between droplet cores play an important role in these systems.

It is well known that surfactants in solution can form a variety of structures ranging from spherical micelles to lamellar structures. During the preparation of the microemulsion systems investigated in this study, viscosity changes were observed for systems containing relatively small volumes of n-octane. Viscosity values as high as 180 cps were noted for a microemulsion containing 0.125 cc of n-octane. The viscosity progressively decreased and remained at 19 cps for systems prepared with more than 0.5 cc of n-octane. The increase in viscosity can best be explained by the formation of lamellar structures composed of associated SDS/DDAO present throughout the continuous phase. The formation of these structures is responsible for an overall increase in the system viscosity along with the binding of bulk water. As the volume of n-octane is increased, it was found that the viscosity decreased. This effect results from the resolution of the lamellar structures into droplets dispersed throughout the continuous phase. The formation of the lamellar structures and the formation of a large number of droplets in solution contributes to the initial decrease observed in the vapor pressure. Once the system is

completely resolved into droplets, it behaves as an ordinary colloidal dispersion, exhibiting a decreased vapor pressure.

3.5.2. ACTIVATION ENERGY BASED ON VAPOR PRESSURE MEASUREMENTS

The effect of temperature on the slope of the curve of vapor pressure vs. volume of n-octane is demonstrated in Fig. 3.9. It is observed that for systems containing greater than 1.1 cc of n-octane, the slope increases as the temperature is increased. The increased value of the slope is related to the breaking and reforming of the surfactant sheath surrounding the droplets. The slope can be interpreted as a change in pressure with respect to the radius $(\partial P / \partial r)_T$. In a recent publication (15) it was demonstrated from sedimentation experiments that a fixed amount of surfactant will cover only a constant total interfacial area. Within this constraint, a change in the dispersed phase volume will cause the droplets to swell, shrink or change in number. Consequently, when the volume of n-octane increases, the radius increases while the number of droplets decrease. Since $(\partial P / \partial r)_T$ was found to increase with temperature this change must therefore be related to the strength of the sheath around each droplet. The activation energy determined from Fig. 3.9 using Eq. 3.23 was found to be 35.2 kJ / mole. This value is significantly higher than activation energy values determined for pure n-octane obtained through viscosity measurements by plotting $\ln \eta$ vs. 1/T. The activation energy value calculated for pure n-octane was found to be 8.8 kJ / mole. Activation energy values for pure n-pentane and n-hexane have also been determined from viscosity measurements and found to be 6.3 and 7.5 kJ/mole respectively. When these hydrocarbons are microemulsified with water, SDS and DDAO, the activation energy values were found in both cases to be 20.9 kJ/mole. These results clearly demonstrate that when hydrocarbon oils are encapsulated by a

surfactant sheath, more energy is required in order for the hydrocarbon to penetrate the sheath. The difference between the pure component activation energy and those for the microemulsion systems must therefore reflect both the strength and rigidity of the interfacial sheath.

3.5.3. HEAT OF VAPORIZATION

Depending on the volume of oil used in the dispersed phase, different droplet structures are present. These two regions are clearly demonstrated in Fig. 3.11 which shows the heat of vaporization ΔH_v as a function of the volume of n-octane in the dispersed phase. The observed discontinuity in the slope undoubtedly reflects the differences in the physical structure between the droplets present within the encapsulated and dynamic regions. For systems containing less than 1.1 cc of n-octane, ΔH_v increases. Since droplets within this region are quite stable, more energy is required to vaporize the n-octane. Systems containing greater volumes of n-octane show a decrease in ΔH_v since the droplets within this region are in a dynamic equilibrium and less stable. Thermodynamically, one would expect that since the droplet structures are quite different, the free energy of formation ΔG_f, corresponding to microemulsions in the encapsulated region, should be significantly different than in the dynamic region. Interestingly enough, the ΔG_f values were found to be 17.0 kJ / K mole for a microemulsion prepared with 0.5 cc and 18.3 kJ / K mole for a microemulsion containing 1.4 cc of n-octane. These results demonstrate that the ΔG_f values are independent of the dispersed phase volume. Nevertheless, based on vapor pressure analysis the structures are very different.

3.5.4. INTERFACIAL FLEXIBILITY

De Gennes and Taupin (17) have described microemulsions based on struc-

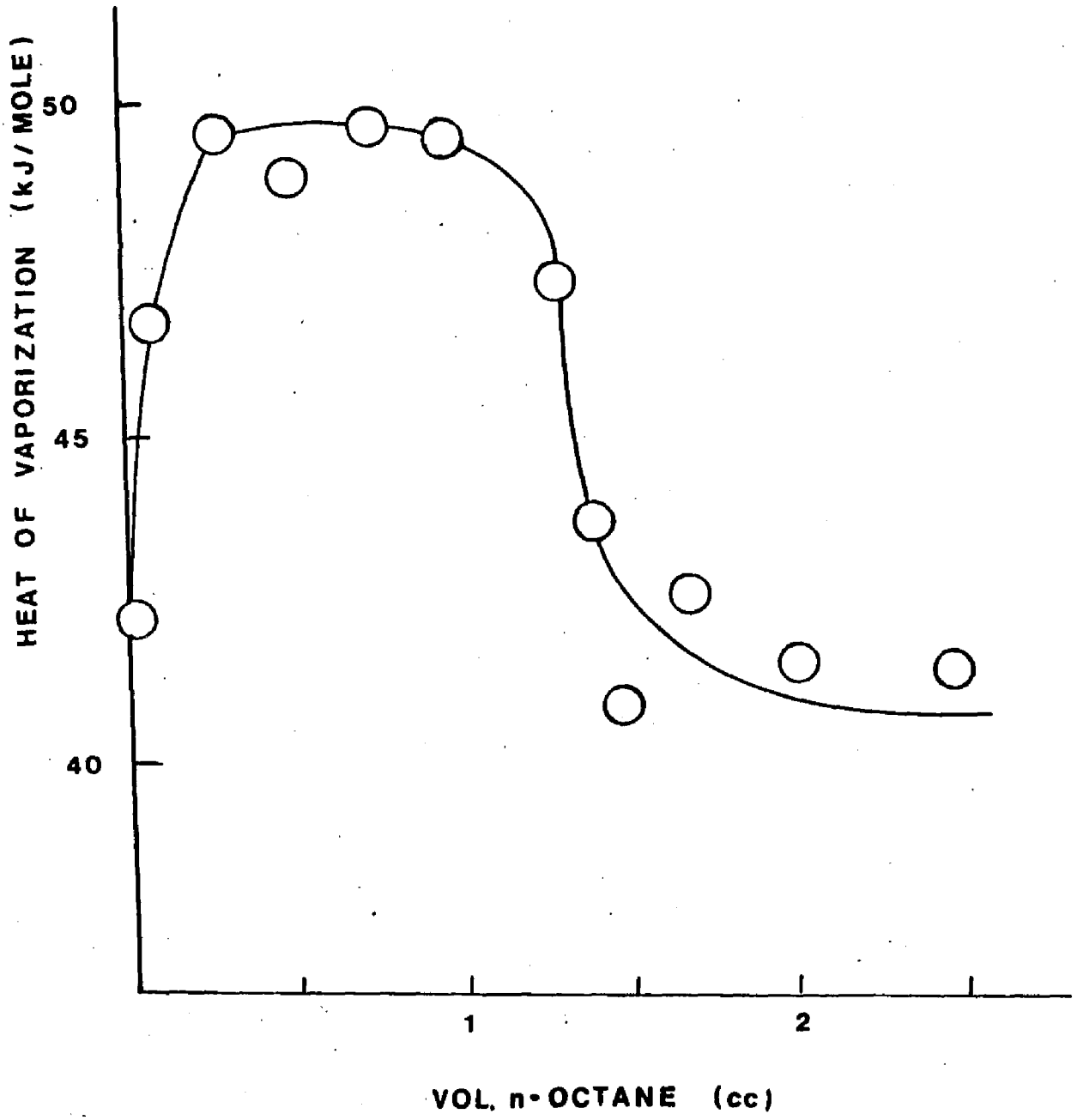

FIGURE 3.11 Heat of vaporization vs volume of n-octane for a microemulsion prepared with 1 gm SCS / 20 cc saline / 3.7 cc DDAO and various volumes of n-octane at 30°C.

tural models which divide the micromemulsion into consecutive cubes of linear length ξ randomly filled with either oil or water. The model also takes into account the film flexibility and rigidity of the interfacial film. Safran (18) has determined that a more complete description of microemulsions can be obtained by introducing a term which takes into account the curvature energy of the surfactant layer. Recently, di Meglio has determined the rigidity constant K for a lamellar phase system prepared with sodium dodecyl sulfate (SDS) / cyclohexane / water and 1-pentanol close to the isotropic microemulsion region using the spin labelling technique (19). The systems investigated were prepared at 1) a constant swelling ratio (oil/water ratio) while staying at the linear border of the lamellar phase and 2) by varying the concentration of 1-pentanol at a fixed swelling ratio. The results obtained indicate that as the concentration of 1-pentanol was increased, the amplitude of the undulations at the interface also increased, resulting in a decrease of the rigidity of the interfacial film.

Rosano (27) has reported that if one plots the overall change in interfacial tension γ of the upper and lower phases for the three phase system SDS/toluene/1-butanol/saline, γ is at a minimum within the three phase region. In order to produce the finest dispersion γ should be as low as possible, but when γ is to low separation rapidly occurs. A low value of γ is necessary for dispersion but does not produce interfacial curvature. Since γ must regain a low positive value for any degree of microdroplet stability, the interfacial ridigity must be higher than for lamellar phase systems where $K = 10^{-14}$ ergs has been reported (19).

For the systems investigated by vapor pressure analysis, the structure of the interfacial film in the encapsulated and dynamic region of Fig. 3.9 has been determined. It was found that the ratio of DDAO:SCS varied as the dispersed

phase volume increased. A microemulsion prepared with 0.5 cc of n-octane was found to contain a 1.1:1 DDAO:SCS ratio while a 5:1 ratio of DDAO:SCS was found for a system containing 1.4cc of n-octane. For each system the entropy of mixing ΔS_m was determined from

$$\Delta S_m = -N_A\ R\ X_A\ \ln X_A - N_B\ R\ X_B\ \ln X_b \qquad (3.24)$$

where

N_A and N_B are the total number of moles of surfactant and cosurfactant

X_A and X_B are the mole fractions of surfactant and cosurfactant

The ΔS_m value in the encapsulated region was found to be 6.0 J / K while in the dynamic region the value of ΔS_m is 8.8 J / K. These values strongly suggest the idea that a major role of the cosurfactant is to induce disorder at the interface. From these results it was concluded that as the interfacial film became more flexible the probability of droplet merging increased.

Droplet stability and its effect on vapor pressure can also be explained by considering results based on sedimentation measurements (15) for o/w microemulsions. It has been shown that for a given amount of surfactant, the total interfacial area remains constant, regardless of the amount of oil present. When the volume of oil exceeds the capacity of the surfactant to stabilize it, the droplets increase in size. Therefore, a critical amount of surfactant is required to form a stable microemulsion. For the system investigated, it seems reasonable that stable encapsulated droplets are formed when the volume of oil is small since there is a sufficient amount of surfactant molecules present in order to form a stable interfacial film around each droplet. When the volume of oil exceeds the amount of surfactant present, the interfacial film is weakened and the droplets become less stable and can merge. In reference to the results presented here, this effect is shown by the increased vapor pressure as the

volume of oil is increased.

4. REFERENCES

1 Rosano, H.L., Cavallo, J.L., and Lyons, G. Presented at the 5th International Conference on Surface and Colloid Science, Potsdam, New York, June 25 - 28, 1985.

2 Hoar, T.P., Schulman, J.H., Nature, (London) 152, 102, (1943).

3 Shinoda, K., Prog. Coll. & Polymer Sci. 68, 1, (1983).

4 Damazewki, l., and Mackay, R., J. Coll. Interface Sci. 97, 160, (1984).

5 Biais, J., Botherel, P., Clin, B., and Lalanne, P., J. Coll. Interface Sci. 80, 136, (1981).

6 Biais, J., Botherel, P., Clin, B.,and Lalanne, P., J. Sci. Technol. 2, 67, (1981).

7 Biais, J., Obderg, L., and Stenius, P., J. Coll. Interface Sci. 86, 350, (1982).

8 Prigogine, I., and Defay, R., "Thermodynamique Chimique." Desoer Ed. Liege, (1950).

9 Adamson, A.W., "Physical Chemistry of Surfaces," 3rd ed. Interscience, New York, (1976).

10 Rosano, H.L., J. Cosmetic Chem., 25, 609, (1974).

11 Graciaa, A, These Doct. es Sci., University de Pau, (1978).

12 Chang, D.L., and Rosano, H.L., Submitted for publication.

13 Hwang, J.S and Cummins, H.Z., J. Chem. Phys. 77, 616, (1982).

14 Weatherford, W.D. To Be Published.

15 Rosano, H.L., Lan, T., Weiss, A., Gerbacia, W.E.F. and Whittam, J.H., J. Coll. Interface Sci. 72, 233, (1979).

16 Cazabat, A.M., Chatenay, D., Guering, P., Urbach, W., Langevin, D., and Meunier, J., To Be Published.

17 De Gennes, P.G. and Taupin, C., J. Phys. Chem. 86, 2294, (1982).

18 Safran, S.A., Turkevich, L.A., Phys. Rev. Lett. 50, 1930, (1983).

19 di Meglio, J. M., Dvolaitzky, M., Leger, L., Ober, R., Paz, L., and Taupin, C., Presented at the 5th International Conference on Surface and Colloid Science, Potsdam, New York, June 25 - 28, 1985.

20 Safran, S.A., Turkevich, L.A., Surfactants in Solution", eds. K. Mittal and B. Lindman, Plenum Press, N.Y. 1984.

21 Huang, J.S., Kim, M.W. To be published.

22 Eicke, H.F., Kubick, R., Hasse, R., Zschakke, I., Surfactants in Solution, K.L. Mittal and B. Lindman, eds. Plenum Press, N.Y. 1533, (1984).

23 Chatenay, D., Urbach, W., Cazabat, A.M., Langevin, D., Phys. Rev. Letts., 20, 2253, (1985).

24 Safran, S.A., Webman, I., Grest, G.S., Phys. Rev. A 32, 506, (1985).

25 Jon, D., Ph.D Thesis, City University Of New York, (1986).

26 Ruckenstein, E., and Krishnan, R., J. Coll. Interface Sci. 76, 188, (1980).

27 Rosano, H.L., Jon, D., Whittam, J.H., J. Am. Oil Chem. Soc. 59, 360, (1982).

CHAPTER 4

THE EFFECT OF POLYMERS ON THE VAPOR PRESSURE OF O/W MICROEMULSION SYSTEMS

4.1. INTRODUCTION

In the previous chapter, it was demonstrated based on vapor pressure analysis that o/w microemulsions clearly exhibit two distinct regions of transparency depending on the volume of hydrocarbon in the dispersed phase. For low volumes of hydrocarbon, encapsulated noninteracting droplets are formed in solution, while for higher volumes of hydrocarbon, a dynamic merging equilibrium exists whereby the droplets are continuously breaking and reforming.

The need to understand the stability of colloidal dispersions has been the central motivating factor in the study and development of colloidal science. The concept of stability in this context is generally understood to mean kinetic stability, i.e., stability imposed by a strong repulsive barrier acting against contact between the suspended particles (1).

London-van der Waals dispersion forces are at the origin of the tendency of colloidal systems to coagulate and aggregate. The sources of repulsive forces needed to stabilize the dispersion against these attractive forces are usually of two types;

1) coulombic repulsion due to electric charges on the particle surface, i.e., electrostatic interactions between the ionic double layers surrounding the

particles

2) static repulsion introduced by large molecules or polymers adsorbed on the particle surface.

In this chapter, the effect of dissolved polymers in the continuous phase of o/w microemulsions will be investigated in order to demonstrate the effect these large molecules have on the droplet interactions. Both anionic and cationic polymers will be investigated. It is hypothesized that polymers added to the continuous phase of microemulsion systems may reinforce the encapsulated droplets or prevent the droplets to some extent from merging. If the presence of polymers in the aqueous phase can alter the droplet interactions, this effect should be demonstrated by vapor pressure analysis.

4.2. EXPERIMENTAL

4.2.1. CHEMICALS

Polymer JR-400, a quaternary water-soluble cationic nitrogen-substituted cellulose ether, (Union Carbide Corp.) and sodium carboxymethlycellulose (CMC), a low viscosity anionic water soluble polymer, 99.5% purity (approx. Mol. Wt. 90,000), (Hercules Inc.) were used. The hydrocarbon, surfactant and cosurfactant used were previously described.

4.2.2. PREPARATION OF POLYMER MICROEMULSION SYSTEMS

In a water-jacketed beaker maintained at 25°C, initial emulsions were prepared containing 15 cc of water, 1 gm. SDS and various volumes of n-octane. These emulsions were titrated to clarity (92% T @ 520 nm.) with DDAO. To these transparent systems 5 cc of a 0.1% JR-400 or 0.1% CMC polymer solution was added. At the concentration of polymer used, no viscosity changes were observed. In all cases the systems remained transparent upon addition of

polymer. The microemulsions were then throughly stirred for 15 minutes to ensure complete mixing.

4.3. RESULTS

4.3.1. MICROEMULSIONS INVESTIGATED

Figure 4.1 shows the vapor pressure of an o/w microemulsion for various volumes of n-octane in the presence and absence of polymer dissolved in the aqueous phase. Curve A represents the vapor pressure behavior of a microemulsion prepared with 1 gm. SDS / 20 cc water / 3.7 gm DDAO and various volumes of n-octane. As previously discussed the vapor pressure decreases upon addition of n-octane. The structure of the droplets within this region is thought to be that of encapsulated droplets surrounded by a surfactant/cosurfactant sheath. Increasing the volume of n-octane results in the existence of a dynamic equilibrium of merging droplets and an increase in vapor pressure. The vapor pressure increases until separation of oil and water occurs, i.e., a two-phase system is formed.

Curve B demonstrates the vapor pressure behavior of a microemulsion prepared with 1 gm. SDS / 15 cc water + 5 cc of 0.1 % Polymer JR-400 / 2.4 gm DDAO and increasing amounts of n-octane. It is observed that upon addition of 0.25 cc n-octane the vapor pressure decreases to approximately 24 mm Hg and remains low up to the addition of 0.5 cc. When the volume of n-octane exceeds 0.5 cc, a sharp increase in vapor pressure results. For a microemulsion prepared with 0.8 cc n-octane, a maximum vapor pressure of 41 mm Hg is reached. The vapor pressure was found to remain high up to the addition of 1.3 cc.

Curve C represents the vapor pressure of a microemulsion prepared with 1 gm. SDS / 15 cc water + 5 cc of 0.1 % CMC / 3.7 gm DDAO and various

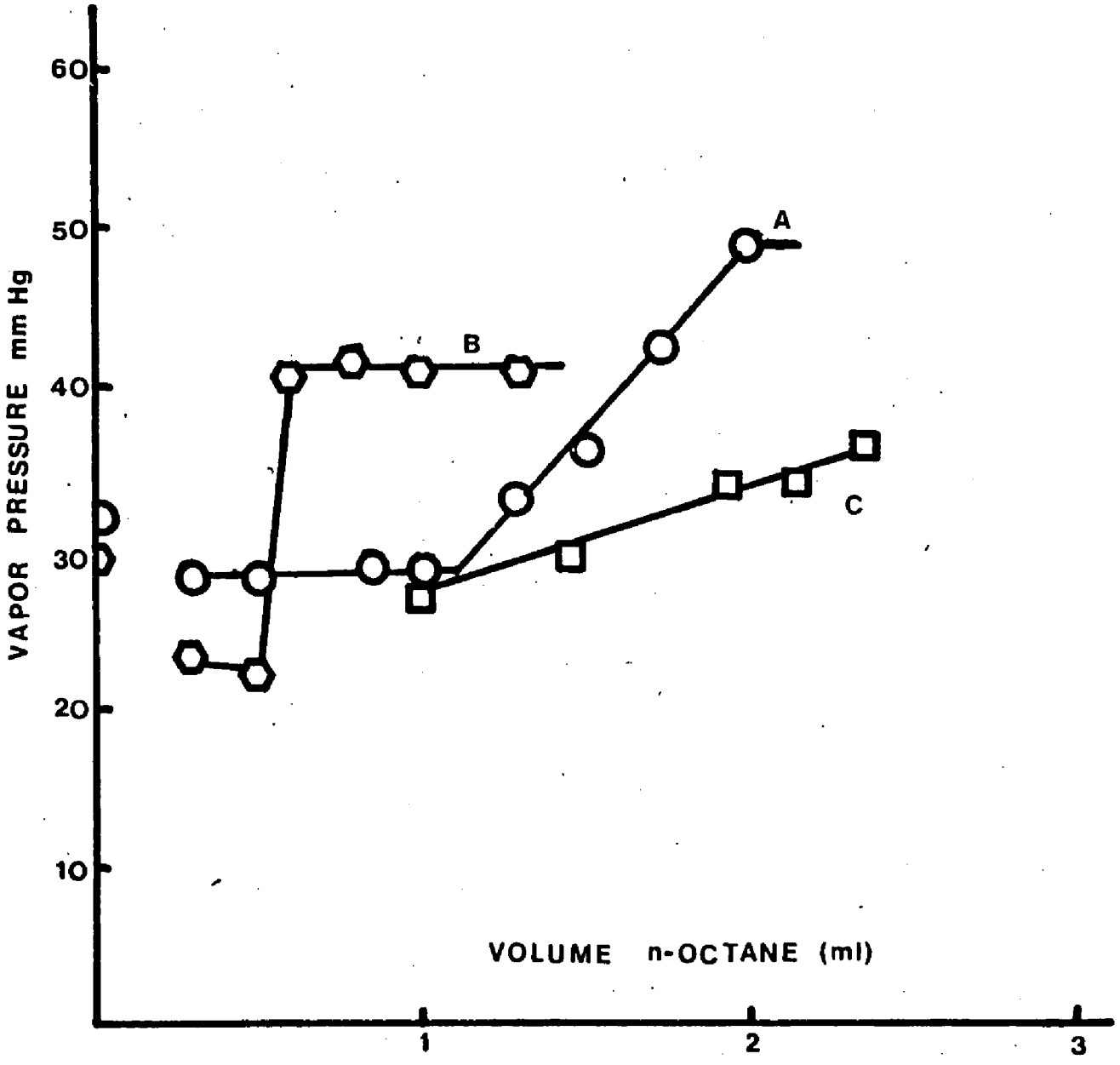

FIGURE 4.1 Change in vapor pressure vs volume of n-octane for a microemulsion prepared with water / 1 gm SDS / n-octane and DDAO (curve A) containing Polymer JR (curve B) or CMC (curve C) in the continuous phase.

volumes of n-octane. It is observed that when CMC is added to microemulsions containing large volumes of n-octane, the vapor pressure is reduced compared to microemulsions prepared in a pure aqueous phase. For 1 cc of n-octane, it can be seen that the vapor pressure is approximately equal to that of a microemulsion prepared in pure water. Increasing the volume of n-octane does not result in a sharp vapor pressure increase. It is interesting to note that phase separation was observed for microemulsions prepared in pure water containing 2 cc of n-octane, but was not seen for microemulsions containing CMC. These results clearly demonstrate that the droplet interactions in microemulsion systems can be strongly influenced by the addition of polymers. The influence can in some cases result in stabilization or destabilization of the microemulsion.

4.4. DISCUSSION

The results shown in Figure 4.1 demonstrate that cationic or anionic polymers added to the continuous phase of o/w microemulsion systems can significantly influence drop-drop interactions over a wide range of oil volumes. Surface tension measurements on solutions of Polymer JR in water, show that the polymer is weak surface active. At a level of 0.1%, the polymer was found to reduce the surface tension of pure water by ca. 4 dyn/cm (2). This small reduction of the surface tension of water suggests that the polymer is very active in the bulk phase.

Using surface tension data, Goddard (2) has demonstrated that addition of Polymer JR caused a marked decrease in the surface tension of SDS surfactant solutions at low concentrations. It was suggested that in certain cases, complexes would form between cationic polymers and anionic surfactants. This interaction would modify the polymer and render it more surface active by adsorption of surfactant "head-head" onto cationic sites along the polymer

chain. Modification of the polymer was demonstrated by an increase in the overall viscosity of the system.

4.4.1. MICROEMULSION INTERACTION WITH POLYMER JR

Addition of Polymer JR introduced to the continuous phase of an o/w microemulsion prepared with water / SDS / n-octane and DDAO seems to have a destabilizing effect on the microemulsion droplets. For relatively small volumes of n-octane, the vapor pressure was found to sharply increase leading to a breakdown of the microemulsion and eventual phase separation. It was thought that addition of a cationic polymer to a microemulsion prepared with an anionic surfactant, the polymer would "wrap-around" the microemulsion droplets and enhance their stability over larger volumes of n-octane. Contrary to the expected results, destabilization of the microemulsion occurred. These results are in agreement with the formation of complexes formed between the cationic polymers and SDS. Adsorption of SDS onto the cationic sites along the polymer chain reduces the amount of surfactant at the o/w interface. The complexation between Polymer JR and SDS reduces the droplet stability.

4.4.2. MICROEMULSION INTERACTION WITH CMC

Microemulsion systems prepared with CMC in the aqueous phase are shown to exhibit a stabilizing effect when compared to microemulsions prepared in a pure water continuous phase or a continuous phase containing Polymer JR. Figure 4.1 shows that when CMC is added to the continuous phase of a microemulsion containing large volumes of n-octane, the vapor pressure is lower than for microemulsions prepared in a pure water phase. Since there is no association between the surfactant and the anionic polymer, there is no depletion of the surfactant at the o/w interface. In addition, since both surfactant

and polymer are anionic, they produce a repulsive interaction. This interaction aids in keeping the surfactant at the o/w interface while enhancing the droplet stability.

The interaction between hydroxyethylcellulose and SDS using surface tension measurements has been investigated by Goddard (2). Surface tension measurements clearly show that there is little or no association between hydroxyethylcellulose and SDS in the bulk phase. These results are based on the fact that when hydroxyethylcellulose is added to an SDS solution, no appreciable surface tension lowering occurs. This suggests that microemulsions containing CMC in the aqueous phase contain only unassociated CMC. Free CMC in the bulk phase should therefore exhibit a repulsive interaction between other CMC molecules and the anionic surfactant heads of the microemulsion droplets. This effect should interfere with microemulsion droplet merging resulting in stable microdroplets over larger volumes of hydrocarbon. Figures 4.2 and 4.3 show the interaction between microdroplets in the presence of cationic or anionic polymers.

4.4.3. THE EFFECT OF POLYMERS AND ACTIVATION ENERGY

If CMC added to microemulsions stabilizes the droplets, the activation energy required to break the surfactant sheath surrounding the droplets should be slightly higher than in the absence of CMC.

The activation energy for microemulsions prepared with CMC in the dispersed phase was determined from Eq. 3.20 between 15-40°C. The results clearly demonstrate that in the presence of CMC, microemulsion droplets are significantly stabilized as shown by the vapor pressure curve in Fig. 4.1. The activation energy was found to be 35.4 kJ/mole. This value clearly demonstrates a stabilizing effect over microemulsions prepared in pure water, where

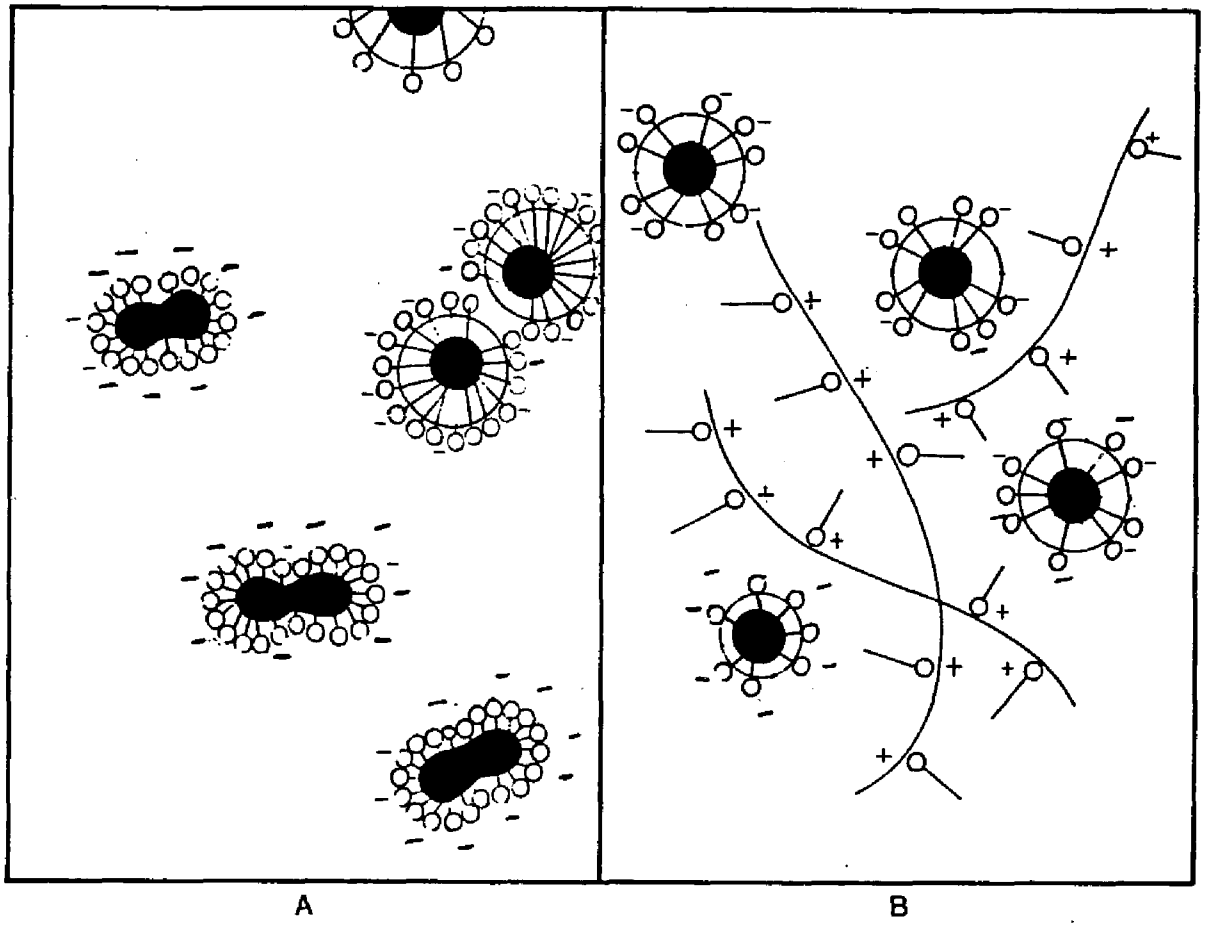

FIGURE 4.2 Microdroplet behavior in solution A) water continuous phase, B) water + Polymer JR.

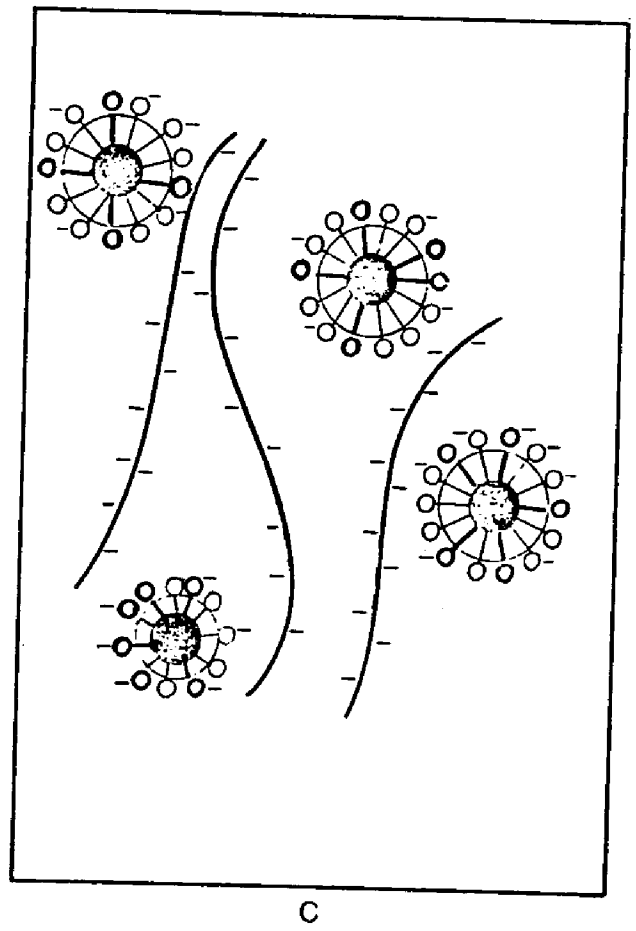

FIGURE 4.3 Microdroplet behavior in a water + CMC solution.

the activation energy was found to be 31.5 kJ/mole. Due to surfactant/polymer association, activation energy values for microemulsions prepared in the presence of Polymer JR were not obtained since these systems rapidly separated.

Activation energy barriers to coalescences between two stabilized w/o microemulsion droplets have been determined (3). As two droplets approach each other, the interfacial film surrounding each of the drops begin to mix. As the monolayers mix, solvent is dispersed from the interfacial layers, causing an increase in free energy as the film becomes locally more concentrated in surfactant and cosurfactant. When such a change in composition increases the free energy, the drops will be stabilized against coalescences. Systems where the dispersed phase volume was increased from 1.0 to 1.44 ml while keeping the droplet radius at 25 A and a constant amount of surfactant caused an energy change of 2kT. Systems with the smaller dispersed phase volume were found to have the higher energy barriers aganist coalescence since the concentration of surface active components at the interface is higher.

These results demonstrate that microemulsion systems can be made inherently unstable under certain conditions. In the presence of anionic polymers, droplet interactions are reduced while a high concentration of surfactant remains at the droplet interface.

4.5. REFERENCES

1 Hirtzel, C.S., Rajagopalan, R., Chem. Eng. Commun. Science Publishers, Inc. 33, 301, (1985).

2 Goddard, E.D., Phillips, T., and Hannan, R.B., J. Soc. Cosmet. Chem., 26, 461, (1975).

3 Gerbacia, W.E.F., Rosano, H.L., "Colloid and Interface Science", M. Kerker, Academic Press, New York, Vol. II, 245, (1976).

CHAPTER 5

CONCLUSION

Transparent ternary, quaternary and polyphasic systems have all been called microemulsions. There is disagreement as to whether these systems are thermodynamically stable or not. For the quaternary systems (oil / water / surfactant / cosurfactant) investigated in this study, it is concluded that microemulsions are thermodynamically stable systems. However, the order of preparation has been shown to play a major role in their formation. It was also shown that microemulsion formation is a spontaneous process. This was demonstrated by showing that the free energy of transforming an emulsion into a microemulsion is a small negative value. Since this value is small, the driving force for these processes is also small and seems to indicate why a specific order must be followed when preparing these transparent systems. These results indicate that when the correct order of mixing is followed, the activation energy barrier these systems must overcome during their formation is significantly lowered. Microemulsion formation cannot simply be accounted for by thermodynamic properties alone. Although all the free energy values were found to be negative, both positive and negative values were found for the enthalpy while one negative entropy value was obtained. These results indicate that other effects should be considered to explain microemulsion formation.

Viscosity and phase volume measurements indicate that microemulsions are formed by the resolution of filament structures into microdroplets. The microemulsion equilibrium phase diagram obtained was found to be similar to a simple phase diagram showing the surfactant behavior in an oil/water system. It was concluded that transparent systems of the oil-in-water type should be classified more appropriately as swollen micellar solutions.

The term microemulsion seems to be an unfortunate term to describe these transparent systems. The word microemulsion can only designate a transparent emulsion. It is well known that significant differences exist between these two types of systems. The formation of a microemulsion does not depend on the amount of surfactant or mechanical work put into the system as is the case for emulsions. In 1943 Hoar and Schulman called these transparent solutions of the w/o type oleopathic hydro-micellar solutions. In the case of o/w systems the term hydropathic oleo-micellar solution was used. In view of the results presented in this thesis, it is felt that these terms are more appropriate to describe transparent systems.

The vapor pressure measurements of o/w microemulsion systems suggest that two distinct regions of transparency exist depending on the dispersed phase volume. It has been shown that for small volumes of hydrocarbon, stable encapsulated droplets exist in equilibrium with the continuous phase. The size of these droplets was determined by vapor pressure analysis and found to be in good agreement with that obtained using photon correlation spectroscopy. For larger volumes of hydrocarbon, a dynamic equilibrium has been shown to exist, resulting in a mass transfer of hydrocarbon, caused by droplets breaking and reforming in solution. This fact also suggests that there are two types of microemulsion systems.

For a given o/w microemulsion formulation, it was found that as the volume of oil was increased two situations occur : 1) individual droplets are formed up to a given volume of oil and 2) for larger volumes of oil, a transition region occurs where droplets merge and/or reform simultaneously, resulting in a bicontinuous system or phase separation. The heat of vaporization was found to increase up to the volume of octane corresponding to the beginning of droplet merging. This increase suggests that the octane/surfactant tails form rela-

tively strong associations. In the region where droplet merging exists, the activation energy corresponding to the amount of energy required to disperse octane in the vapor phase was found to be 35.2 kJ/mole vs. 8.8 kJ/mole for pure octane determined through viscosity measurements. This result supports the idea of a structured oil/surfactant sheath surrounding the droplets. The heat of vaporization within this region was found to decrease, suggesting that less energy is required to vaporize the core hydrocarbon due to droplet merging.

The free energy model proposed for microemulsion formation involves three energy terms : 1) the energy of solvation between the oil and the surfactant tails, 2) the energy required to expand the interface and 3) a term which accounts for the interfacial flexibility. This model demonstrates that in order for microdroplet formation to occur, the interfacial rigidity must be higher than the rigidity of lamellar phase systems in order for interfacial curvature to form microdroplets.

Studies on three phase SDS/toluene/1-butanol/saline microemulsion systems have indicated that the interfacial tension is a minimum within the three-phase bicontinuous region. As the two phase (o/w or w/o) microemulsion region is approached, it was shown that the interfacial tension increased to a small positive value resulting in microdroplet formation and stability. The systems which have been investigated indicate that as the dispersed phase volume is increased : 1) the droplet interfacial flexibiltiy increases and 2) the interfacial tension decreases. These results suggest that as the interfacial flexibility is increased, attractive interactions between the microdroplets result in the formation of merging droplet clusters leading to a bicontinuous structure as the dispersed phase volume is increased.

APPENDIX A

Computer Program To Determine The Thermodymamic Values of Microemulsion Formation

```
c  This is a program to determine delta G, delta S, and delta H
c  through a linear least square fitting of
c  two variables. The input is as follows, a file named
c  thermo is created and the first line of the file must be
c  the density, the molecular weight of the cosurfactant and the
c  molecular weight of the surfactant. The second and following
c  lines are the x and y values used to determine the linear fitting
c  and the temperature of the experiment. The program will reorder and
c  output the values in a ascending order according to the
c  temperature.
      dimension x(200),y(200),t(200),sigmam(20),sigmab(20)
      dimension xxi(200),yi(200),tj(200),tp(20)
      dimension xi(20),xb(20),slope(20),b(20),delG(20),tt(20)
      character*10 thermo
      data t/200*0.0/,sigmam/20*0.0/,sigmab/20*0.0
      data slope/20*0.0/,b/20*0.0/
      kk=0
      nn=0
      jj=0
      nnk=100
      nnj=20
4     write(6,750)
750   format(/' write the name of the data file: ',$)
      read(5,710)thermo
710   format(a10)
      if(thermo.ne.'          ')goto 5
      write(6,740)
740   format(' file name is a blank')
      goto 4
5     open(1,file=thermo)
      open(2,file='john')
      write(6,510)
      write(2,510)
510   format(/' write the density, mw of cos, and mw of surfac. '/)
      read(1,*,err=70)den,amw,x2
      write(6,550)den,amw,x2
      write(2,550)den,amw,x2
550   format(4x,f7.3,5x,f8.1,6x,f7.1/)
      write(6,500)
      write(2,500)
```

```
500     format(' write the values of x, y, and temperature '//)
        do 10 i=1,100
        read(1,*,end=14,err=70)x(i),y(i),t(i)
        kk=kk+1
10      continue
14      call sort(x,y,t,nnk,kk,xxi,yi,tj,tp,nnj)
        do 720    i=1,kk
        write(6,540)i,x(i),y(i),t(i)
        write(2,540)i,x(i),y(i),t(i)
540     format(5x,i5,4x,f6.2,6x,f7.2,7x,f8.1)
720     continue
        ki=1
        close(1)
15      jj=jj+1
        if(t(jj).ne.t(jj+1))goto 25
        goto 15
25      nn=nn+1
        call linear(ki,jj,nnk,x,y,slope(nn),b(nn),sigmam(nn),sigmab(nn))
        xb(nn)=slope(nn)*den/amw*18
        xi(nn)=b(nn)*den/amw
        xd=xi(nn)+1/x2
        xi(nn)=xi(nn)/xd
        delG(nn)=-8.314*(273.15+t(jj))*alog(xi(nn)/xb(nn))
        delG(nn)=delG(nn)/1000.
        tt(nn)=t(jj)
        ki=jj+1
        if(t(jj+1).eq.0.0)goto50
        goto15
50      call linear(1,nn,nnj,tt,delG,entrpy,bint,sm,sb)
        Temp=30.0
        delG30=Temp*entrpy+bint
        entrp=-entrpy
        delH30=delG30+(Temp+273.15)*entrp
        write(6,560)
        write(2,560)
560     format(////)
        write(6,520)
        write(2,520)
520     format(/6x,' T (oC)    slope    intercept     xb          xi
     1  deltaG (kJ)  ')
        do 60 i=1,nn
        write(6,530)i,tt(i),slope(i),b(i),xb(i),xi(i),delG(i)
60      write(2,530)i,tt(i),slope(i),b(i),xb(i),xi(i),delG(i)
530     format(/ 2x,i3,2x,f5.1,3x,1pe10.3,2x,e10.3,2x,e10.3,2x,e10.3,
     12x,e10.3,2x,e10.3)
        write(6,600)
        write(2,600)
```

```
600       format(///5x,' delta G ',4x,' = ',5x,'delta H ',4x,' -',5x,
     1'(T + 273.15)',3x,'*',4x,'delta S ')
          write(6,700)
          write(2,700)
700       format(7x' (kJ) ',14x,' (kJ)',17x,'(oC)',12x,'(kJ/ K)')
          write(6,610)delG30,delH30,Temp,entrp
          write(2,610)delG30,delH30,Temp,entrp
610       format(/4x,1pe10.3,11x,e10.3,13x,0pf5.2,10x,1pe10.3,//)
          write(6,590)
          write(2,590)
590       format(///9x,'  STD slope',4x,'STD intercept')
          do 40 i=1,nn
          write(6,640)i,sigmam(i),sigmab(i)
          write(2,640)i,sigmam(i),sigmab(i)
640       format(/,3x,i3,4x,1pe10.3,5x,e10.3)
40        continue
          write(6,650)
          write(2,650)
650       format(//,4x,'entropy',5x,'intercept',4x'STD entropy',5x,'STD
     1 intercept')
          write(6,660)entrp,bint,sm,sb
          write(2,660)entrp,bint,sm,sb
660       format(/,2x,1pe10.3,3x,e10.3,4x,e10.3,5x,e10.3)
          write(6,670)
670       format(//'   lpr john ')
          close(2)
          stop
70        write(6,570)
570       format('  there is an error in the input data')
          close(2)
          stop
          end
c &&&&&&&&&&&&&&&&&& &&&&&&&&&
          subroutine linear(in,kn,indx,x,y,slope,b,sigmam,sigmab)
          dimension x(indx),y(indx)
          kk=kn-in+1
          sumxy=0.0
          sumx=0.0
          sumy=0.0
          sumx2=0.0
          do 20 i=in,kn
          sumxy=sumxy+x(i)*y(i)
          sumx=sumx+x(i)
          sumy=sumy+y(i)
          sumx2=sumx2+x(i)*x(i)
20        continue
          slope=kk*sumxy-sumx*sumy
```

```
      d=kk*sumx2-sumx*sumx
          if(d.eq.0.0)then
          write(6,40)
          write(2,40)
40        format(/' value of the slope is undefined, denominator is 0')
          return
          end if
          slope=slope/d
          b=sumy*sumx2-sumx*sumxy
          b=b/d
          sigmay=0
          do 30 i=in,kn
          sigmay=sigmay+(y(i)-slope*x(i)-b)**2
30        continue
          if(kk.le.2)then
          write(6,50)kk
          write(2,50)kk
50        format(/' Number of points are ',i3,', STD cannot be calculated')
          return
          end if
          sigmay=sigmay/(kk-2)
          sigmam=kk*sigmay/d
          sigmab=sigmay*sumx2/d
          sigmam=sqrt(sigmam)
          sigmab=sqrt(sigmab)
          return
          end
          subroutine sort(x,y,t,index,n,xi,yi,tj,ti,np)
          dimension x(index),y(index),t(index)
          dimension xi(index),yi(index),tj(index),ti(np)
          knn=1
          kl=0
          do 20 j=1,n
          tmin=min1(tmin,t(j))
          tmax=max1(tmax,t(j))
          xi(j)=x(j)
          yi(j)=y(j)
          tj(j)=t(j)
20        continue
          ti(1)=tmin
          tdum=1.0e10
          do 30 i=2,np
          do 40 j=1,n
          if(tj(j).gt.ti(i-1).and.tj(j).lt.tdum)tdum=tj(j)
40        continue
          ti(i)=tdum
          knn=knn+1
```

```
      if(tdum.eq.tmax)goto 80
          tdum=10e10
30        continue
80        do 50       i=1,knn
          do 60  j=1,n
          if(tj(j).ne.ti(i))goto 60
          kl=kl+1
          x(kl)=xi(j)
          y(kl)=yi(j)
          t(kl)=tj(j)
60        continue
50        continue
          return
          end
```

APPENDIX B

Computer Program To Determine The Interfacial Tension Values Using the Spinning Drop Method

```
      character*80 name
      dimension diameter(50),period(50),tension(50)
      k=0
      write(0,100)
      read(5,90)name
 90   format(a80)
      write(0,101)
      read(5,*)temp,rindx
      write(0,102)
      read(5,*)denup,denlr
      write(0,103)
 100  format('  write the name of the solution ')
 101  format('  write the temperature and lower phase refractive index ')
 102  format('  write the upper phase and lower phase density ')
 103  format('  write the diameter of the drop and the period (end with 0)
')
 110  k=k+1
      read(5,*,end=120)diameter(k),period(k)
      if(diameter(k).le.0.0)goto 120
      goto 110
 120  k=k-1
      difden=abs(denlr-denup)
      do 121 i=1,k
      radius=diameter(i)/(100*2*rindx)
      omega=2*3.1415927*1000/period(i)
 121  tension(i)=difden*(omega**2)*(radius**3)/4
      write(6,130)name
 130  format(/,/,6x,a80)
      write(6,140)temp,rindx
 140  format(/,4x'temperature= ',f7.2,5x,'refractive index= ',f8.5)
      write(6,150)denup,denlr
 150  format(/,4x'upper phase density= ',f7.5,5x,'lower phase density= '
     & ,f7.5)
      write(6,160)
 160  format(/,t7'tension (dynes/cm)',6x,'diameter (cm/100)',4x,'period
     &(msec/rev)',/)
      do 200 i=1,k
      write(6,170)tension(i),diameter(i),period(i)
 170  format(t7,1pe13.6,18x,0pf6.3,9x,1pe12.5)
 200  continue
```

```
      call average(k,tension)
          stop
          end
c  ###################################
c
          subroutine average(n,y)
          dimension y(n)
          average4value=0.0
          std4deviation=0.0
          do 122 k=1,n
122       average4value=average4value+y(k)
          average4value=average4value/n
          do 123 k=1,n
          sqind4deviation= (y(k) - average4value)**2
          std4deviation= std4deviation + sqind4deviation
123       continue
          std4deviation= sqrt(std4deviation / (n-1))
          write(6,250)average4value,std4deviation
250       format(/,6x,'average= ',1pe12.5,6x,'standard deviation= +/-'
         &e12.5,/,/)
          return
          end
c &&&&&&&&&&&&&&&&&&&&&&&&&&&&&&&&&&&&&&&&&&&&&
c
c title name                              NCS + OCTANE 10-3M
c temperature, lower phase refractive index  23 1.33
c  densito of lower and upper phase          .7 1.0
c  diameter of the drop and period (cycle)   12.378 17.47
c                idem                      12.272 17.49
c     to end the file code                    0 0
```